# COMPUTATIONAL INVESTIGATION OF URBAN HEAT ISLAND MITIGATION SCENARIOS IN EDUCATIONAL BUILDINGS

A THESIS SUBMITTED TO
THE GRADUATE SCHOOL OF NATURAL AND APPLIED SCIENCES
OF
MIDDLE EAST TECHNICAL UNIVERSITY

BY

GÜLİN YAZICIOĞLU

IN PARTIAL FULFILLMENT OF THE REQUIREMENTS
FOR
THE DEGREE OF MASTER OF ARCHITECTURE
IN
ARCHITECTURE

JANUARY 2023

Approval of the thesis:

**COMPUTATIONAL INVESTIGATION OF URBAN HEAT ISLAND MITIGATION SCENARIOS IN EDUCATIONAL BUILDINGS**

submitted by **GÜLİN YAZICIOĞLU** in partial fulfillment of the requirements for the degree of **Master of Science** i**n Architecture, Middle East Technical University** by,

Prof. Dr. Halil Kalıpçılar
Dean, Graduate School of **Natural and Applied Sciences** _____

Prof. Dr. F. Cana Bilsel
Head of the Department, **Architecture** _____

Assoc. Prof. Dr. İpek Gürsel Dino
Supervisor, **Architecture, METU** _____

Assoc. Prof. Dr. Çağla Meral Akgül
Co-Supervisor, **Civil Engineering, METU** _____

**Examining Committee Members:**

Assoc. Prof. Dr. Funda Baş Bütüner
Architecture, METU _____

Assoc. Prof. Dr. İpek Gürsel Dino
Architecture, METU _____

Assoc. Prof. Dr. Çağla Meral Akgül
Civil Engineering, METU _____

Assist. Prof. Dr. Güzide Atasoy Özcan
Civil Engineering, METU _____

Assist. Prof. Dr. Gizem Deniz Güneri Söğüt
Architecture, Atılım University _____

Date: 11.01.2023

**I hereby declare that all information in this document has been obtained and presented in accordance with academic rules and ethical conduct. I also declare that, as required by these rules and conduct, I have fully cited and referenced all material and results that are not original to this work.**

Name Last name : Gülin Yazıcıoğlu

Signature :

# ABSTRACT

## COMPUTATIONAL INVESTIGATION OF URBAN HEAT ISLAND MITIGATION SCENARIOS IN EDUCATIONAL BUILDINGS

Yazıcıoğlu, Gülin
Master of Architecture, Architecture
Supervisor: Assoc. Prof. Dr. İpek Gürsel Dino
Co-Supervisor: Assoc. Prof. Dr. Çağla Meral Akgül

January 2023, 156 pages

Recent years have witnessed rapid urbanization due to an increase in population in cities. This will lead to the replacement of natural landscapes with impervious surfaces, and the acceleration of anthropogenic activities, which will increase waste heat. As a result of this, there is a temperature difference between the city centers and their suburbs, which is commonly referred to as an Urban Heat Island (UHI). As a result of the UHI phenomenon, many negative effects are associated with it, such as increased energy consumption, discomfort both indoors and outside, as well as health problems related to it. Compared to other types of buildings, educational buildings are distinguished by their large size, high density of people, and number of unique challenges. Although several studies have been conducted on UHI effects, there has not yet been a comprehensive analysis of UHI effects on educational buildings. This thesis describes a method for generating modified weather files based on UHI for various mitigation scenarios. The six scenarios developed include Cool Pavement (CP), Cool Facade (CF), Green (GR), Cool Pavement-Green (CPGR), and Cool Facade-Green (CFGR), as well as a combination of all these scenarios using ENVI-Met. In this manner, it is possible to examine the impact of each mitigation scenario on outdoor thermal comfort, indoor overheating degrees (IOD), and heating

loads. As a result, CP is the most reasonable scenario for mitigating UHI effect as well as decreasing heating loads whereas CFGR is better for decreasing indoor overheated air temperature. In addition, GR scenario performs better for achieving reduced perceived temperature in summer.

Keywords: ENVI-Met, Building heating load, Mitigation scenarios, Thermal comfort, Urban heat island

# ÖZ

## EĞİTİM BİNALARINDA KENTSEL ISI ADASI HAFİFLETME SENARYOLARININ HESAPLAMALI İNCELENMESİ

Yazıcıoğlu, Gülin
Yüksek Lisans, Mimarlık
Tez Yöneticisi: Doç. Dr. İpek Gürsel Dino
Ortak Tez Yöneticisi: Doç. Dr. Çağla Meral Akgül

Ocak 2023, 156 sayfa

Son yıllarda kentlerdeki nüfus artışına bağlı olarak hızlı kentleşme yaşanmaktadır. Bu durum, doğal peyzajların geçirimsiz yüzeylerle yer değiştirmesine ve atık ısıyı artıracak antropojenik faaliyetlerin hızlanmasına yol açacaktır. Sonuç olarak, şehir merkezleri ile banliyöleri arasında, genellikle Kentsel Isı Adası (KIA) olarak adlandırılan bir sıcaklık farkı vardır. KIA fenomeninin bir sonucu olarak, artan enerji tüketimi, hem içeride hem de dışarıda oluşan termal konforsuzluk ve buna bağlı sağlık sorunları gibi birçok olumsuz etki ilişkilendirilebilmektedir. Diğer bina türleriyle karşılaştırıldığında, eğitim binaları, büyük boyutları ve kullanıcı yoğunluğunun yanı sıra bir takım zorluklarla sahiptir. KIA etkileri üzerine çeşitli çalışmalar yapılmış olmasına rağmen, eğitim binaları üzerindeki KIA etkilerinin kapsamlı bir analizi henüz yapılmamıştır. Bu tez, çeşitli hafifletme senaryoları için kentsel ısı adasına dayalı olarak değiştirilmiş hava durumu dosyaları oluşturmaya yönelik bir yöntemi açıklamaktadır. Altı senaryo, Soğuk Kaldırım (CP), Soğuk Cephe (CF), Yeşil (GR), Soğuk Kaldırım-Yeşil (CPGR) ve Soğuk Cephe-Yeşil (CFGR) ve ayrıca tüm bu senaryoların kombinasyonu ENVI-Met aracı kullanılarak geliştirilmiştir. Bu şekilde, her bir hafifletme senaryosunun dış ortam termal konforu, iç ortam aşırı ısınma dereceleri (IOD) ve ısıtma yükleri üzerindeki etkisini incelemek

mümkündür. Sonuç olarak, CP, UHI etkisini ve ısıtma yüklerini azaltmak için en makul senaryo iken CFGR, iç ortam aşırı ısınan hava sıcaklığını azaltmak için daha iyidir. Ek olarak, GR senaryosu yaz aylarında algılanan sıcaklığın düşürülmesi için daha iyi performans gösterir.

Anahtar Kelimeler: ENVI-Met, Bina ısıtma yükü, Azaltma senaryoları, Termal konfor, Kentsel ısı adası

To my beloved family…

## ACKNOWLEDGMENTS

This research took an incredible amount of effort and support. At this point, I would like to thank many people who have supported me so far on my journey to this dissertation.

My deepest gratitude goes out to my supervisor, Assoc. Prof. Dr. İpek Gürsel Dino for her generous support and inspirational guidance throughout the years. I have been fortunate to be encouraged and challenged ingeniously by her to achieve the best and the most advanced since the beginning of this study. Also, I would like to express very special thanks to my co-supervisor Assoc. Prof. Dr. Çağla Meral Akgül for all guidance and support in the thesis process. My academic life would be enriched by her knowledge and wisdom. Without their guidance, contribution, this research wouldn't have been possible.

I would like to thank my jury members: Assoc. Prof. Dr. Funda Baş Bütüner, Assist. Prof. Dr. Güzide Atasoy Özcan, and Assist. Prof. Dr. Gizem Deniz Güneri Söğüt for providing me kind support to develop my thesis.

As a last, but not least, words cannot express my gratitude for the constant support, love, patience, and understanding I have received from my beloved family, my mother Özlem Yazıcıoğlu, my father Ediz Yazıcıoğlu, and my sister Selin Yazıcıoğlu as well as throughout my entire life. Having them in my life has been a blessing for me, and I owe them a lot. I feel that this is the most appropriate place to express my gratitude to them. They are one of my greatest treasures in life, and this thesis is dedicated to them.

## TABLE OF CONTENTS

## LIST OF TABLES

TABLES

## LIST OF FIGURES

FIGURES

## LIST OF ABBREVIATIONS

ABBREVIATIONS

**2D:** 2 Dimensional

**3D:** 3 Dimensional

**ASHRAE:** American Society of Heating, Refrigerating and Air-Conditioning Engineers

**BL:** Baseline

**BUHI:** Boundary-Level UHI

**CF:** Cool Façade

**CFCPGR:** Cool Façade + Cool Pavement + Green

**CFGR:** Cool Façade + Green

**CLO:** Clothing Insulation Ratio

**$CO_2$:** Carbon Dioxide

**CP:** Cool Pavement

**CPGR:** Cool Pavement + Green

**CUHI:** Canopy-Level UHI

**EPW:** Energy Plus Weather

**GHGs:** Greenhouse Gases

**GR**: Green

**GUHI:** Substrate UHI

**HVAC:** Heating, Ventilating and Air Conditioning

**INX:** Input File

**IOD:** Indoor Overheating Degree

**IPCC:** Intergovernmental Panel on Climate Change

**IWEC:** International Weather for Energy Calculations

**LAI:** Leaf Area Index

**MET:** Metabolic Rate

**MRT:** Mean Radiant Temperature

**PET:** Physiological Equivalent Temperature

**PMV:** Predicted Mean Vote

**PPD:** Predicted Percentage of Dissatisfaction

**PVC:** Polyvinyl Chloride

**RH:** Relative Humidity

**RSL:** Roughness Sublayer

**SHGC:** Solar Heat Gain Coefficient

**SIMX:** Configuration File

**SUHI:** Surface UHI

**UBL:** Urban Boundary Layer

**UCL:** Urban Canopy Layer

**UHI:** Urban Heat Island

**UMEP:** Urban Multi-scale Environmental Predictor

**UTCI:** Universal Thermal Comfort Index

**UWG**: Urban Weather Generator

**VT:** Visible Light Transmitted

## LIST OF SYMBOLS

SYMBOLS

i: Occupied hour

**$N_{occ}$:** Occupied period

**t:** Time step

**Ta:** Air temperature

**$T_{fr,i,z}$:** Free-running indoor operative temperature at the time step (i) in the zone (z)

**$TL_{comf,i,z}$:** Comfort temperature limits at the time step (i) in the zone (z)

**Ts:** Surface temperature

**Va:** Wind velocity

**z:** Different building zones

**Z:** Total number of zones in a building

# CHAPTER 1

# INTRODUCTION

An introduction is presented in the first chapter of the thesis, which includes seven sections: background, problem statement, aims and objectives, research questions, the scope of the thesis, methodology, and thesis structure.

## 1.1 Background

### Challenges in the Construction Sector

There are several challenges facing the construction sector in the areas of economics, the environment, technology, and social factors such as climate change, overpopulation, dense urbanization, natural resource inequalities, and excessive use of resources.

(i) Global Environmental Impact

Several factors contribute to the environmental damage caused by the construction industry, including pollution, waste, and the consumption of raw materials. Decarbonization of the building sector should be associated with manufacturing efficiency, recycling, and circular economies. However, this policy poses a wide open and difficult challenge to the construction sector.

(ii) Greenhouse Gas Emissions and Climate Change

It has been reported by the Intergovernmental Panel on Climate Change (IPCC) that greenhouse gases caused by human activities have had significant effects on climate change as far back as the mid-20th century (IPCC, 2022). Global greenhouse gas emissions increased by 43 percent from 1990 to 2015 (EPA, 2022). Consequently,

overheating, changing precipitation patterns, and extreme weather events such as floods, hurricanes, storms, and sea level rise are expected to become more frequent in the future (IPCC, 2022).

(iii) Energy Consumption in Buildings

Approximately 36% of global energy consumption is attributed to the construction and building sector. It is significant to note that, in spite of attempts to conserve energy by developed countries, there has been an increase in energy demand due to growing floor areas, relatively small reductions in energy intensity, and increased demands for energy services. Furthermore, increasing air temperatures in cities result in the use of more energy in buildings to maintain a comfortable climate during the summer months (M. Santamouris & Vasilakopoulou, 2021).

(iv) Overpopulation and Rapid Urbanization

There has been a continuous increase in the world's population, and it may reach 11 billion by the year 2050 (UN, 2022). Further, the majority of the growing population lives in cities and the number of urban populations is estimated to reach 6.5 billion by 2050. Less developed countries, which are experiencing this rapid urbanization, may have serious challenges in accommodating people and providing infrastructure (Li et al., 2019).

(v) Urban Heat Island Effect

It is a consequence of rapid urbanization that natural landscapes are being replaced with hard surfaces in order to create new settlements for the population. Because of this replacement, the air temperature in the city center is higher than on the outskirts, thereby making the city center warmer. It is also known as the Urban Heat Island (UHI) effect if there is a difference in temperature between an urban area and its surrounding suburbs (Jiang et al., 2014). It is estimated that there can be a temperature difference of up to 10 degrees Celsius; however, the average value is closer to 5 degrees Celsius. There are serious consequences associated with

overheating in city centers, such as health effects, environmental degradation, and energy consumption in buildings.

## 1.2 Problem Statement

*Urban heat island:* As a consequence of urbanization in recent years, Urban Heat Island (UHI) has been extensively observed, which has been identified as one of the most critical problems in cities. Migration into metropolitan areas is accelerated by changes in land use that result in the opening of newly available areas for the construction of upscale buildings (Wang et al., 2007). There are currently 6.6 billion people living in cities, and it is predicted that there will be nearly 5 billion people living in cities by 2030 (Ash et al., 2008). In light of this, the development of concrete surfaces for urban settlements is related to the creation of warmer city centers than rural areas. The primary causes of this increase are the use of heat-absorbing materials, the construction of mass concrete buildings, and the reduction of green space. As cities have become more urbanized, the issue of adding greenery has become more challenging, despite the fact that urban vegetation can mitigate the effect of urban heat islands. Due to the increased temperatures in cities, urban heat islands also contribute to an increase in energy consumption in buildings. There are numerous negative effects associated with this phenomenon, such as higher energy consumption, overheating, and thermal comfort (Luber and McGeehin, 2008; Sanusi et al., 2016; Yuan et al., 2017). There is a direct correlation between urban thermal comfort and outdoor space usage, which is directly affected by the external climate (Huang et al., 2015; Hwang et al., 2011). Moreover, the increasing heat causes considerable heat stress that affects people's efficiency, well-being, and health (Kovats and Hajat, 2008).

*Urban heat island impact on the energy consumption of educational buildings:* As air temperatures rise in city centers, it causes thermal discomfort and health problems in the indoor environment. Due to the insufficiency of passive cooling techniques,

mechanical cooling systems are required to maintain a comfortable indoor climate. The literature review indicates that UHI may result in an increase in cooling energy consumption of 10% to 120% and a decrease in heating energy consumption of 3% to 45% (Li et al., 2019). Aside from their large size, high occupant density, and schedule for energy savings throughout the year, educational buildings present a number of unique challenges among other building typologies (Palme et al., 2020). Even though there are many studies studying UHI's impact on energy consumption, the scope of these studies does not include educational buildings.

*Urban heat island impact on pupils' perception of outdoor temperature*: Aside from physiological characteristics, climate and urban factors affect outdoor thermal comfort. The fact that city centers are approximately five degrees Celsius warmer than the outskirts has a negative impact on thermal comfort (IPCC,2022). The focus of thermal comfort studies is generally on the metabolism, activity, and perception of adults. However, children and adults possess different physical characteristics. Children, for example, have a high surface area to mass ratio which causes heat to be transferred more easily, their metabolic rates are much higher, their skin temperature rises more rapidly during exercise, and they sweat less (Balbus & Malina, 2009; Cheng & Brown, 2020). Essentially, children are more vulnerable than adults. There is a need for more literature to be devoted to thermal comfort studies from the perspective of children.

*Urban heat island impact on indoor overheating degrees:* Due to the fact that the human body has the capability of responding to and adapting to changes in ambient temperature, excessive heat may overcome this capacity. This may lead to health problems. Consequently, urban heat islands increase thermal stress and adversely affect human health. Further, indoor overheating contributes to an increase in cooling load during the summer months. In order to achieve energy efficiency and thermal comfort within an indoor space, it is critical to investigate the impact of UHI on indoor overheating degrees.

Several studies have addressed the concerns mentioned above in the literature; however, there is still a lack of discussion of the impact of UHI on energy consumption, both indoors and outdoors, and mitigation solutions for each aspect of educational buildings.

## 1.3 Aims and Objectives

This thesis is primarily concerned with understanding the impact of urban heat islands on outdoor air temperatures, developing various UHI mitigation scenarios, and evaluating each scenario's impact on pupils' outdoor thermal comfort, indoor overheating degrees, and the heating load of an existing educational facility. Specifically, developing a method that utilizes UHI impact on energy and indoor overheating calculations as well as outdoor thermal comfort. The purpose of this study is to achieve the following objectives:

- By using computational design tools, it will be possible to gain a better understanding of the climate conditions in Ankara corresponding to the urban heat island effect.
- Frameworks for the mitigation of urban heat islands based on the literature review for use in an existing educational building.
- Comparing and quantifying the effectiveness of each mitigation scenario with respect to decreasing the degree of indoor overheating and the heating load while increasing the comfort level of the outdoors.
- A number of recommendations are being developed for existing educational buildings with regard to UHI mitigation, energy efficiency, and thermal performance.

## 1.4 Research Questions

In light of the discussion in the preceding sections, the purpose of this thesis is to address the following primary question:

*What are the most relevant mitigation scenarios for tackling UHI effect, energy efficiency, low overheating degrees and better outdoor thermal comfort?*

The main question requires a thorough examination of several sub-questions, including the following:

- How does UHI affect the microclimate?
- In what ways can the impact of UHI be measured? In order to perform the simulations, which computational tool should be used?
- Why should educational buildings be selected over other types of buildings, such as residential, commercial, or industrial?
- In an existing educational facility, what mitigation strategies are possible?
- To what extent can a method be developed to investigate UHI mitigation scenarios to evaluate the energy performance of educational buildings, pupil perception of outdoor temperatures, and degree of indoor overheating?

## 1.5 The Scope of the Thesis

A great deal of literature has been written about the assessment of the UHI effect. It is therefore necessary to narrow down and limit the thesis in order to ensure the quality and clarity of the research. As listed below, some aspects are excluded from the scope of the thesis:

- A primary school building located in Ankara is selected as the target building typology. The scope of the thesis does not include other types of buildings, including residences, offices, universities, etc.

- A limited number of urban design alternatives are examined in this study in order to mitigate UHI effects. A change has been made to the material of the outside wall layer of the school building, the paved surface material of the playground, and the number of trees in the schoolyard. As for the building envelope materials, they are customized in accordance with a typical school building in Turkey. The inclusion of water elements and soft surface materials has not been considered as an urban design element. Furthermore, the study does not include urban morphology or arrangement.
- There is a focus on indoor overheating degrees, outdoor thermal comfort, and energy consumption at a primary school in this thesis.
- A comparison of different building construction materials is not conducted for the purposes of calculating indoor overheating degrees or energy consumption. There's no change in building materials for each UHI mitigation scenario.
- To determine the energy consumption for each UHI mitigation scenario, only the heating loads are considered. Neither cooling nor lighting are included in this calculation.
- Physiological Equivalent Temperature (PET) is one of the outdoor comfort metrics used to measure outdoor thermal comfort.

## 1.6 Thesis Methodology

Computational analyses are intended to contribute to the literature as part of a systematic methodology. A method is developed for determining the impact of mitigation scenarios for UHI on outdoor thermal comfort, indoor overheating degrees, and the energy consumption of an educational building. In order to achieve this goal, several steps are followed as indicated below:

(i) An in-depth analysis of the literature concerning climate change, UHI and its calculation methods, measurements of thermal comfort both outdoors and indoors, outdoor thermal comfort based on pupil physiological characteristics, indoor overheating degrees, building energy consumption, and mitigation strategies for UHI impacts.

(ii) Preparation of a baseline model representing the site of the case study and its surrounding area. The air temperature data for each classroom is also collected using 16 receptors located in front of the windows.

(iii) In ENVI-Met, six different mitigation scenarios are presented in the context of the case study site.

(iv) A new EnergyPlus weather file is generated for each classroom based on the air temperature data collected from the sensors so that energy simulations and calculations of the indoor overheating degree can be performed.

(v) Energy and indoor comfort simulations are run for each mitigation scenario after generating customized weather files for the classroom.

(vi) A comparison of indoor overheating degrees and energy consumption based on different mitigation scenarios is performed.

(vii) In addition, PET analysis was conducted for the baseline and each mitigation scenario to examine the outdoor thermal comfort of the students in the schoolyard.

A final step in the thesis consists of comparing and discussing five main aspects, including the impact of UHI on air temperature, heating load, indoor overheating, outdoor thermal comfort, and scenarios for mitigation of UHI.

## 1.7 Thesis Structure

As can be seen in Figure 1.1, this thesis consists of five chapters. First chapter presents a brief introduction to the thesis and provides a conceptual background, a statement of the problem, an aim and objectives, a list of research questions, an explanation of the dissertation methodology, and a description of the thesis structure.

Throughout the second chapter, there is a comprehensive literature review of the thesis' main arguments, such as causes and effects of climate change, UHI impacts, indoor overheating degrees, outdoor thermal comfort, the impact of UHI on building energy consumption, mitigation scenarios for UHI, and calculation tools.

A detailed methodology description of the case study can be found in the third chapter. The fourth chapter, the results are compared and discussed. In the final chapter of the thesis, a conclusion is presented, as well as limitations and possible future extensions.

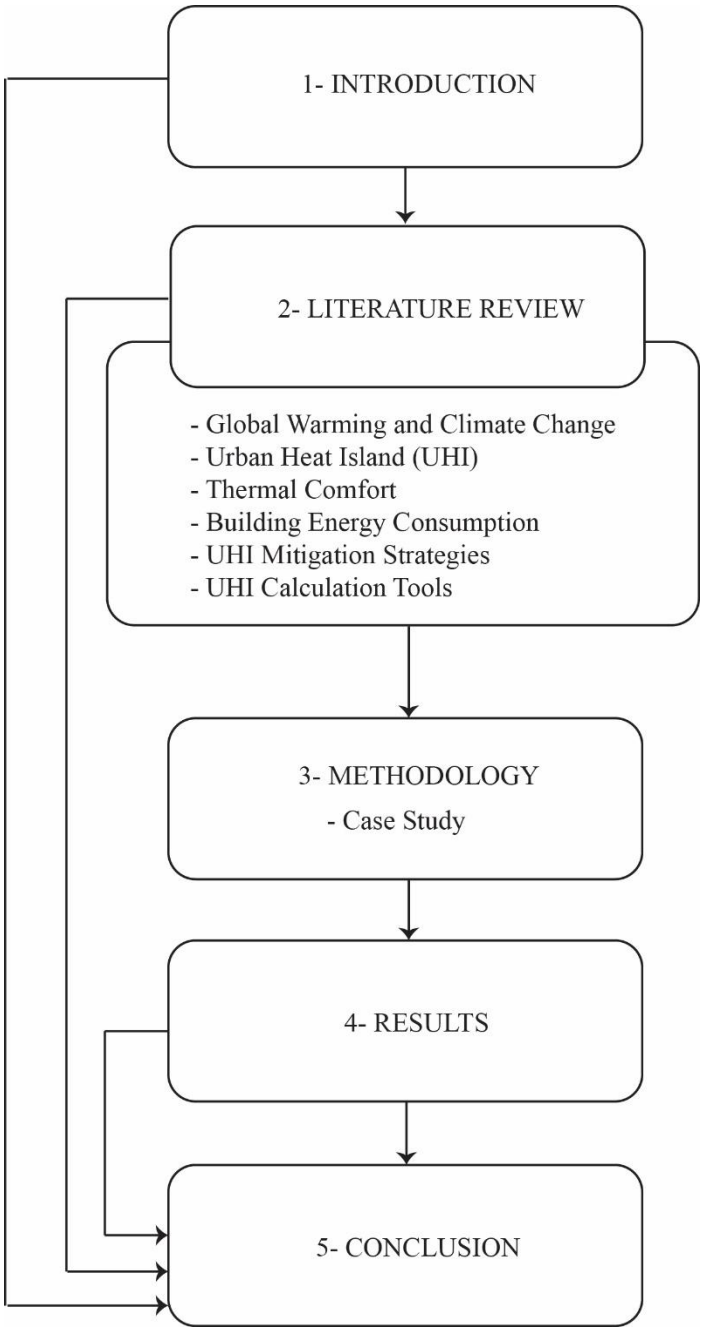


*Figure 1.1.* Thesis structure

# CHAPTER 2

# LITERATURE REVIEW

This chapter presents a comprehensive review of literature related to climate change, urban heat islands (UHI) and their impacts on the built environment, calculation tools for measuring urban heat islands, and thermal comfort models. There are a number of aspects and problems identified by other authors, including comfort requirements in educational buildings and mitigation scenarios for managing UHI in order to reduce indoor overheating degrees and energy consumption.

## 2.1 Global Warming and Climate Change

In the literature, global warming is defined as an increase of 1.5°C in the global surface temperature over the past 150 years (IPCC, 2022). It is widely recognized that climate change is a consequence of global warming. The term is often interchangeable with global warming (Shaftel, n.d.). Figure 2.1 shows that the global average temperature began to rise rapidly after the 1950s, and the trend seems to have continued through the next decade. As a matter of fact, when the historical background is examined, the year 2022 will remain among the top ten warmest years (Rohde, 2022).

As a result of various anthropogenic activities, this anomaly has arisen. Transport, deforestation, building construction, and operation are examples of human-made systems that emit greenhouse gases (GHGs), which contribute to climate change (Younger et al., 2008). In both the natural and built environments, climate change has many adverse effects.

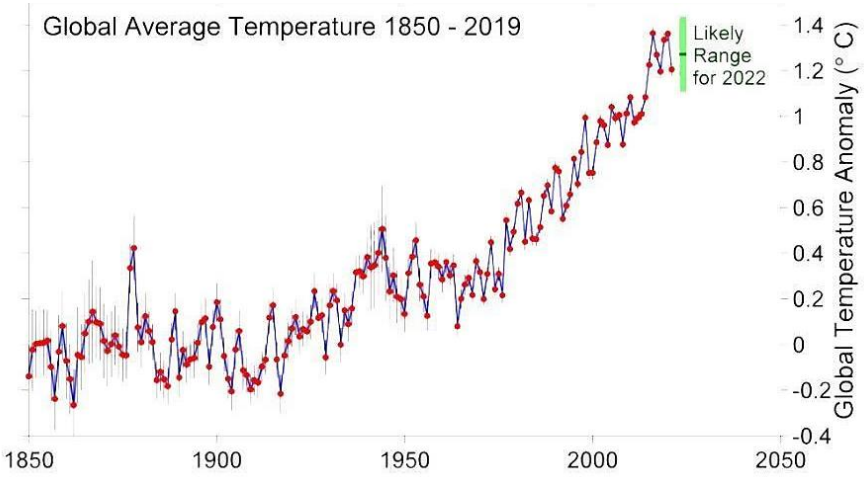


*Figure 2.1.* Global temperature anomaly (Rohde, 2022)

The impacts of climate change also exacerbate serious threats in many countries. There are significant negative impacts on natural systems, food security, biodiversity, health and well-being problems, droughts, floods, and the loss of lives and lands.

### 2.1.1 The Causes and Effects of Climate Change

#### 2.1.1.1 The Causes of Climate Change

The main causes of climate change can be listed under six titles: (i) power generation, (ii) manufacturing, (iii) transportation, (iv) deforestation, (v) food production and (vi) powering buildings.

(i) Power generation

As of today, most electricity is generated through the combustion of coal, oil, or gas, which contributes significantly to global emissions of greenhouse gases. In spite of the availability of clean and renewable energy resources, less than a quarter of the world's electricity comes from these resources (Causes and Effects of Climate Change, n.d.).

(ii) Manufacturing

To produce goods such as cement, iron, steel, electronics, plastics, clothing, etc., the manufacturing industry relies heavily on fossil fuels. As a result of mining, construction, and other industrial processes, harmful gases are released into the atmosphere, which contribute to the cause and effect of climate change (Causes and Effects of Climate Change, n.d.).

(iii) Transportation

There is no doubt that transportation contributes to climate change, but at the same time it is a practical means of commuting. Long distances between homes and work destinations increase the use of vehicles per capita. Compact and mixed-use developments can help reduce distances between destinations, allowing people to get to services easier (Causes and Effects of Climate Change, n.d.).

(iv) Deforestation

Deforestation is the result of agriculture and land use development. There is an estimated loss of 12 million hectares of forest every year. Due to the fact that trees absorb carbon dioxide, when they are cut, this carbon is released back into the atmosphere. Deforestation of forests and other changes in land use are responsible for approximately a quarter of global greenhouse gas emissions (Causes and Effects of Climate Change, n.d.).

(v) Food production

The clearing of forests for agricultural and grazing purposes, the use of energy in farm machinery and fishing vessels, and the use of chemicals in crop growing will result in an increase in carbon dioxide emissions that will result in global climate change (Causes and Effects of Climate Change, n.d.).

(vi) Power for buildings

In the United States, residential and commercial buildings consume over half of all electricity. The demand for energy has been increasing in order to heat, cool, light, and operate electronic devices. This also contributes to a rise in energy-related carbon dioxide emissions (Causes and Effects of Climate Change, n.d.).

#### 2.1.1.2 The Effects of Climate Change

The impact of climate change can be summarized in terms of overheating, thunderstorms, droughts, the rise of the sea level, the loss of species, health risks, and poverty.

(i) Overheating

There has been an increase in air temperature each decade since the 1980s. As a result, heat-related illnesses are prevalent, wildfires are widespread, icebergs are melting in the Arctic Circle, sea levels are rising, and so on. As a result of climate change, high air temperatures make it more difficult to spend time outside (Causes and Effects of Climate Change, n.d.).

(ii) Thunderstorms

Increased air temperatures cause more moisture to evaporate, resulting in heavier rainfall and flooding, causing destructive storms. A storm of this nature could destroy villages, resulting in a large number of deaths and economic losses (Causes and Effects of Climate Change, n.d.).

(iii) Increased drought

Some regions are experiencing water stress as a result of global warming, which exacerbates the availability of water. Therefore, climate change increases the incidence

of agricultural droughts affecting crops and increases the vulnerability of ecosystems (Causes and Effects of Climate Change, n.d.).

(iv) Rising sea level

Most of the heat in the atmosphere is stored in the ocean. Global warming has resulted in a rapid increase in the ocean's temperature over the past two decades. Furthermore, sea levels are rising due to the rapid melting of ice sheets. Oceans also absorb carbon dioxide from the atmosphere. Ocean acidification is caused by the presence of more carbon dioxide in the atmosphere, which puts marine life and coral reefs at risk (Causes and Effects of Climate Change, n.d.).

(v) Loss of species

As a result of climate change, species are disappearing at a rate 1.000 times greater than ever before in human history. In addition, one million species are at risk of extinction in the coming decades (Causes and Effects of Climate Change, n.d.).

(vi) Health risks

Extreme weather events are a result of changing weather patterns, which have a detrimental impact on health, air quality, and food and water security. Environmental factors cause approximately 13 million deaths each year (Causes and Effects of Climate Change, n.d.).

(vii) Poverty

As mentioned earlier, all of the effects of climate change may put and keep people in poverty. Slums are destroyed by floods and lives are lost. Crops and fields are adversely affected by droughts. It can be difficult to work outside during the summer due to the heat. As a result, the population becomes more susceptible to poverty (Causes and Effects of Climate Change, n.d.).

### 2.1.2 Climate Conditions and Climate Change in Turkey

#### 2.1.2.1 Köppen-Geiger Climate Classification Map

Climate classifications based on the Köppen–Geiger system are some of the most widely used methods. It was in 1900 that German botanist-climatologist Wladimir Köppen published the first scheme of the climate map, known as the Köppen-Geiger climate classification map (Beck et al., 2018).

The main climate types are based on patterns of average precipitation, average temperature, and natural vegetation. The Köppen Climate Classification divides the Earth's climate into five main climate groups: (i) A- Tropical, (ii) B-Dry, (iii) C-Temperate, (iv) D-Continental, (v) E- Polar, and there are several sub-groups under them (Beck et al., 2018).

***The climate zones of Turkey***

Located at the crossroads of the Balkans, Caucasus, Middle East, and eastern Mediterranean, Turkey is among the largest countries in the region both in terms of territory and population, and its land area is larger than that of any other European country.

As seen in Figure 2.2, Turkey has mainly three different climate sub-classes, which are Csa (Hot-summer Mediterranean climate), Dsa (Humid continental climate), and Csb (Warm-summer Mediterranean climate). During the warmest months of the year, temperatures in the Mediterranean Sea and the Black Sea region can reach over 22°C, while the coldest months see temperatures between 18°C and -3°C.

Anatolia's mountainous regions are characterized by a Dsa climate. During the coldest months, the air temperature drops below 0°C on average. Despite this, the mean temperature is higher than 10°C for at least four months of the year.

Csb Climate describes the climate of the central Anatolian plateau where a dry summer and a cold winter can be observed throughout the year. Temperatures in its warmest month reach over 22°C, while in its coldest month temperatures range between 18°C and 3°C.

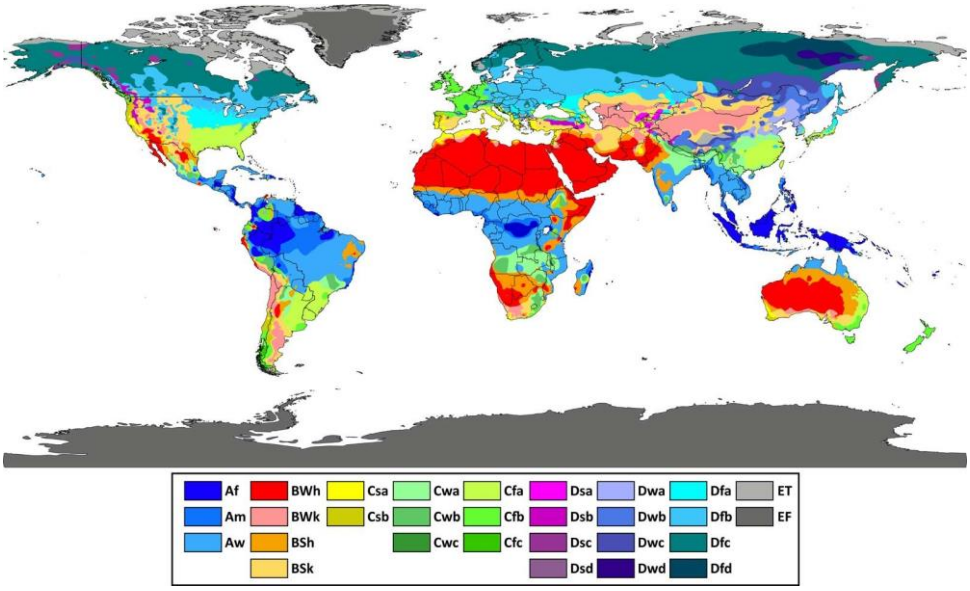


*Figure 2.2* Köppen-Geiger climate classification map (Beck et al., 2018)

#### 2.1.2.2 Future Climate Conditions in Turkey

There are several types of climate patterns in Turkey; however, it is one of the nations that will be most vulnerable to future climate change conditions in the Mediterranean basin. As a result of its location between mid-latitude and subtropical atmospheric circulation regimes, the Mediterranean Basin exhibits large topographic gradients. There has been a rapid increase in Mediterranean atmospheric warming since the 1980s. Compared to the present, the annual and summer warming rates are projected to be 20% and 50% larger, respectively, in the future (IPCC, 2022).

Both the natural and economic impacts of increased temperatures will be more severe in the Mediterranean region. As predicted by the Köppen-Geiger climate classification map, Turkey is likely to experience more hot and dry summers between

2071 and 2100. According to Figure 2.3, the humid continental climate (Dsa) in mountainous regions of Anatolia will be replaced by a hot-summer Mediterranean climate (Csa). Under these circumstances, aggressive interventions should be implemented as soon as possible.

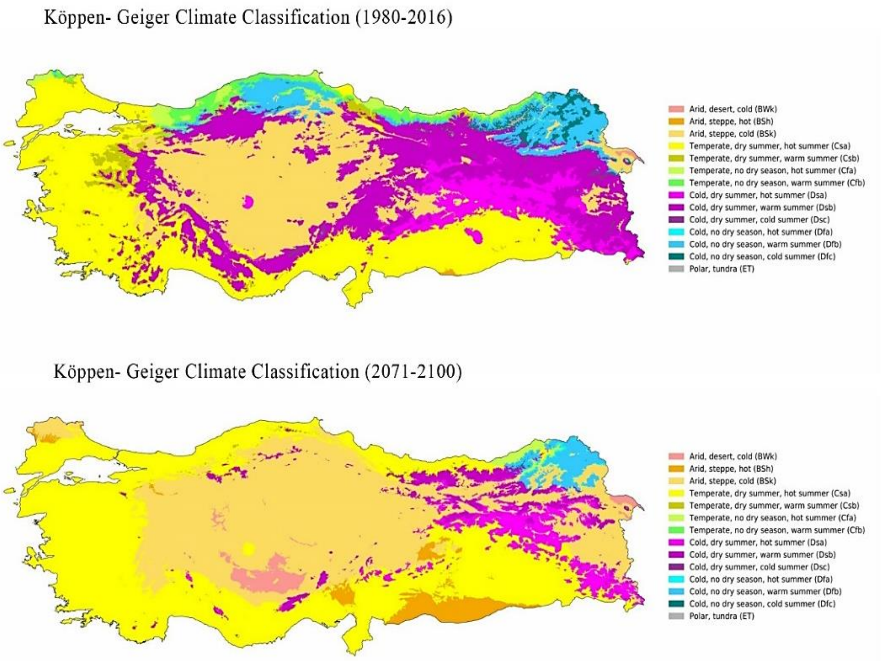


*Figure 2.3* Future climate scenario for Turkey (Beck et al., 2018)

## 2.2 Urban Heat Island (UHI)

The population has grown rapidly in cities in recent years, resulting in widespread urbanization. Therefore, natural landscapes are replaced by hard ground surfaces, anthropogenic activities are accelerated, and waste heat is increased in the atmosphere. Due to this situation, there is a temperature difference between the city centers and their suburbs, which is commonly known as the Urban Heat Island (UHI) effect (Oke, 1988). In addition to the difference in air temperature, other weather factors such as wind, humidity, pressure and soil temperature are also different in urban and rural areas. Due to fluctuations in the atmosphere and ground layer

temperatures, however, cities begin to show different climatic characteristics from their surroundings that result in microclimate zones (Çiçek & Yılmaz, 2013).

UHI includes different scales of analysis depending on time and space to understand the microclimate areas. The UHI effect has mainly three different climate scales: (i) mesoscale, (ii) local scale, and (iii) microscale (Figure 2.4).

As part of the mesoscale, there are various scales, such as the vertical boundary layer between rural and urban areas. The urban boundary layer extends from the urban cover layer to the mixing layer, and its height varies according to the daily cycle. In the atmospheric mixing layer, temperature and specific humidity are approximately constant. As a result of the turbulence created by uneven, hot surfaces during the day, the urban boundary layer (normally more than 1 kilometer) rises during the day and shrinks at night to hundreds of meters.

At the local scale, similar urban areas extend horizontally over several kilometers and rise in height to the roughness sublayer. It is the roughness substrate that is responsible for the majority of the turbulence effects generated by urban surfaces.

The microscale extends several hundred meters horizontally, from street level to the tallest building (urban cover layer). Taking into account these scales, heat islands are classified into three classes, respectively at the urban surface level, at the urban cover level, and at the boundary layer level

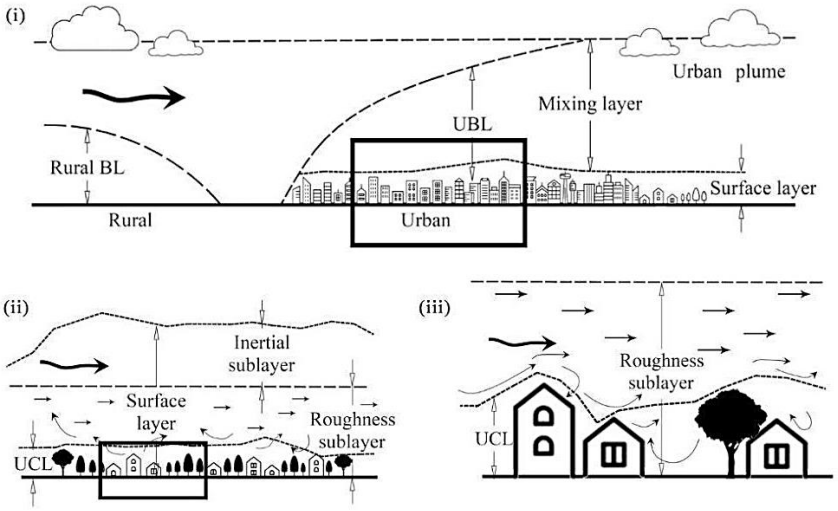


*Figure 2.4.* Different climatic scales for UHI (Costanzo et al., 2021)

### 2.2.1 Types of UHI

UHI can be classified into four major types based on its level. The difference in temperature between a city and a benchmark, which is a rural area, is used to determine each type of UHI.

The first one is the surface UHI (SUHI) where ground floors and building envelopes' materials affect the change in the surface temperature (Ts), which is considered for SUHI. The second is the canopy-level UHI (CUHI). The difference in air temperature (Ta) is calculated based on the temperature of the near-surface air (~ 2 m above the ground). In this thesis, the CUHI is examined. In an urban context, boundary-level UHI (BUHI) is when air temperature changes above all the buildings. The last type of UHI is the substrate UHI (GUHI), which is based on the temperature of the soil beneath the ground surface (Tsub) (Stewart, 2018). Figure 2.5 shows the abbreviations for the urban canopy layer (UCL), roughness sublayer (RSL), and urban boundary layer (UBL).

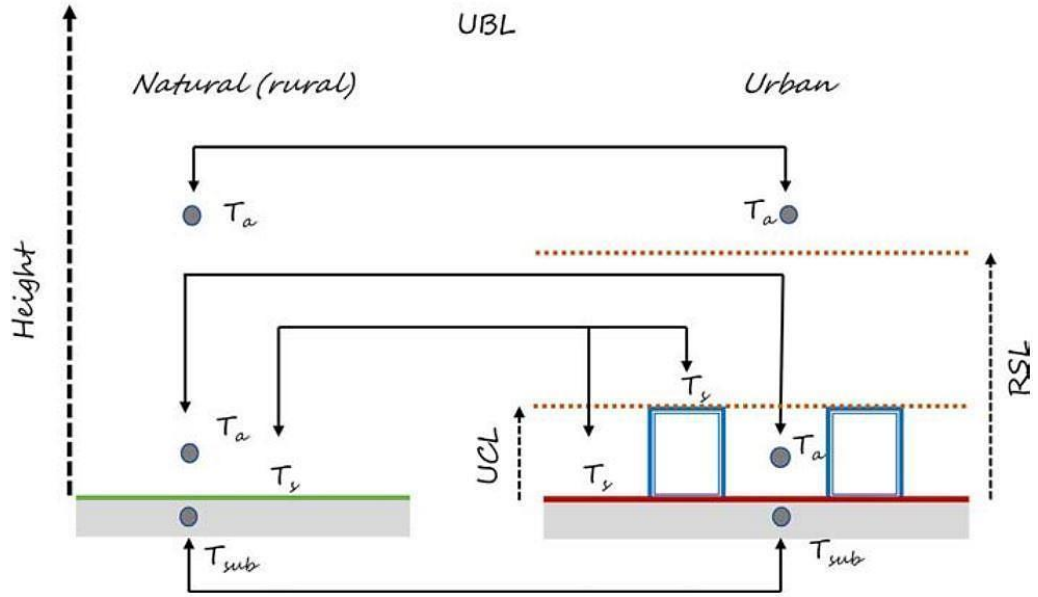


*Figure 2.5.* Types of layers (Stewart, 2018)

### 2.2.2 The Causes of UHI

UHI is caused by more than one reason. These are (i) reduction of green areas, (ii) hard surface material properties, (iii) urban morphology, (iv) anthropogenic heat, and (v) other factors.

(i) Reducing green areas

Vegetation and open spaces that characterize rural areas are generally predominant. In addition to reducing surface temperature by shading, vegetation also lowers air temperature by evapotranspiration (Hove et al., 2011). It is the sum of evaporation from soil surfaces and transpiration from plants that is referred to as evapotranspiration. In this manner, the air is cooled more rapidly. There are more impermeable surfaces in urban areas, which results in reduced evapotranspiration and delayed cooling of the air (Salcedo-Rahola, Baldiri, Van Oppen, Peter, Mulder, 2009).

(ii) Surface material types

In the urban environment, the materials used in buildings and surfaces have a considerable impact on the density of urban heat islands as a result of their radiative and thermal properties. Built surfaces, in general, have a lower albedo than natural surfaces. Measurement of the percentage of solar energy reflected by a surface is known as albedo; it is used to quantify the reflectance of materials. A surface that has a low albedo absorbs more energy from the sun, reflecting less energy back into the environment. Additionally, materials with a high heat capacity are able to store a substantial amount of solar energy. Energy absorbed will be released as heat, thereby increasing surface temperatures and creating an urban heat island (Hove et al., 2011).

(iii) Urban landscape

By definition, urban landscape is the quantitative relationship between building volume and open space, as well as their spatial arrangement (Chatzipoulka et al., 2015). A city consists of a wide variety of surfaces (natural and man-made), most of which are small or have complex geometries. This spatial heterogeneity results in substantial microclimatic variation within short distances. Surface temperatures will be dominated by the thermal and radiative characteristics of the surface, but the near-surface atmosphere will be dominated by a wide variety of surface types. UHI researchers face challenges in describing and organizing heterogeneity in an effective manner (Stewart, 2018).

Each element of the urban landscape has its own climatic effects determined by its individual characteristics and relationship to its neighbors. The urban landscape can be divided into elements which are organized according to scale and structure. Essentially, a facet is a planar element that is made of a consistent material (e.g., glass, asphalt, turf) and has thermal and radiative properties that allow it to be assembled into a street, garden, or building envelope. The geometry of buildings and trees along streets determines the three-dimensional structure of the urban canopy

layer. The formation of blocks and neighborhoods is determined by the arrangement of a number of buildings and open spaces at the local level. For example, the average height of buildings, the proportion of impervious surface (Stewart, 2018).

The geometry of the urban environment plays a significant role in shaping microclimates and urban heat islands. A number of factors are affected by this factor, such as wind flow, energy absorption, and the ability to emit radiation. Materials in dense urban areas are unable to release their heat, which leads to heat storage (Yamamoto, 2005). A sky view factor is used to determine the impact of buildings and other objects on solar radiation. A value between 0 and 1 is assigned to it. The sky view factor is 1 for fully open areas, whereas it is closer to zero for narrow areas. As a result of high-rise buildings that block the transmission of radiation, downtown streets have a near-zero sky view factor. Thus, a city with a low sky view factor will have a higher urban heat island density. Wind and radiation are affected by the geometry of urban areas. Wind speed and wind flow in urban areas are sheltered by many buildings and obstacles. Consequently, air pollution increases while heat transmission is reduced (Kleerekoper et al., 2012).

(iv) Anthropogenic heat

Cities are subject to an increase in heat due to anthropogenic heat. Waste heat is generated by air conditioning, motor transportation, and industrial processes (Salcedo-Rahola, Baldiri, Van Oppen, Peter, Mulder, 2009). Urban heat islands are becoming denser as a result of these activities.

(v) Other factors

Besides the factors listed above, weather conditions and geographical location also contribute to the formation of urban heat islands. In addition to wind, cloudiness is another factor that contributes to the development of heat islands. Low wind velocity and a cloudless period maximize the amount of solar energy reaching urban surfaces, and low wind velocity reduces the amount of radiation that is transported back to the

sky. As a result, the geographic location of a city determines the climate and topography of that city, as well as the density of its urban heat islands.

### 2.2.3 Impacts of UHI

There are some negative consequences associated with the urban heat island. A few of them can be listed as follows: (i) increases in the amount of energy used by buildings for cooling in the summertime due to high air temperature, (ii) the increase in heat stress, which has a great impact on human health, and (iii) the decrease in outdoor thermal comfort.

(i) Effect of urban heat island on building energy consumption

A rise in air temperature has a substantial impact on the amount of energy necessary to heat and cool buildings. High indoor temperatures can cause severe discomfort and health problems, as well as reducing productivity (Skoulika, Fotini; Santamouris, Mattheos; Kolokotsa, n.d.). It is possible to achieve the appropriate indoor comfort level by using passive cooling techniques, however, their overall performance is highly dependent upon the climate and may not be sufficient for all climatic conditions to provide adequate indoor comfort.

Consequently, mechanical cooling is required to reduce indoor temperatures, regulate humidity levels, and provide comfort (Mat Santamouris, 2016). The increase in ambient temperatures caused by climate change is expected to increase the use of mechanical cooling systems. The literature contains several studies that attempt to predict the future consumption of cooling energy in the building sector. There is a study in which three scenarios are developed based on the development of low, average, and high cooling energy use for the year 2050. According to this study, cooling energy consumption in residential and commercial buildings will increase by 75% and 275%, respectively (Mat Santamouris, 2016). These results show that

the urban heat island will have a greater impact on future building energy consumption.

(ii) Heat stress

The human body is capable of responding to a wide range of temperatures. Exposure to excessive heat can overcome the body's resistance, resulting in health problems. Symptoms of heat stress may include redness, cramps, heat exhaustion, and heat stroke, as well as exacerbate medical conditions such as heart disease or lung disease. The urban heat island increases thermal stress and has a negative impact on human health.

(iii) Outdoor thermal comfort

In addition to physiological characteristics, climate and urban factors have a significant impact on outdoor thermal comfort. Thermal comfort can be viewed from three different perspectives. These are the psychological, thermo-physiological, and body temperature balance approaches. Environmental factors, psychological factors (metabolic heat, skin temperature and wetness, the enveloping effect of clothing), as well as psychological factors (wind, relative humidity of the air, solar radiation) all contribute to thermal comfort (Höppe, 2002). Other factors (climate acclimation status, body height/weight ratio, presence of six layers of fat in the skin, age, and gender) also affect thermal comfort. The urban heat island affects the comfort of outdoor activities by causing heat stress.

## 2.3 Thermal Comfort

Various microclimatic parameters and physiological states contribute to thermal comfort (Höppe, 2002). Specifically, there are four different weather parameters, which include air temperature, relative humidity, wind velocity, and mean radiant temperature. As well as the weather inputs, a person's metabolic rate and the insulation ratio of their clothing are also significant factors to consider.

Air temperature (Ta) is significantly important for thermal comfort. This temperature is measured with a dry bulb thermometer, which is why it is also known as dry-bulb air temperature. Furthermore, the temperature of the air and the wind velocity together affect the rate of convective heat dissipation (La Roche, 2016).

Relative humidity (RH) allows evapotranspiration from the skin. It is convenient to cool the body down with a humidity ratio between 30% and 60%. Other than that, either very low relative humidity (less than 30%) or high relative humidity (above 60%) can cause discomfort through difficulties in sweating and skin drying (La Roche, 2016).

Wind velocity (va) is measured in meters per second (m/s) or feet per minute (ft/min). Evaporative cooling is enhanced when the wind velocity is increased (La Roche, 2016). Keeping the hourly mean wind velocity below 5 m/s is defined as being comfortable in accordance with the Dutch wind comfort standard (NEN 8100) (Janssen et al., 2013).

Mean radiant temperature (MRT) indicates the short and longwave radiation exchange of a human body (Gál & Kántor, 2020). In order to measure it, a globe thermometer is used, which responds to the average temperature of the surfaces that surround a particular point with which it will exchange thermal radiation. The view factor is a measurement of the apparent size of each radiating surface in addition to its temperature. Depending on the view factor, the mean radiant temperature varies at different locations (La Roche, 2016).

Metabolic rate (met) is the metric of energy transformation into heat and mechanical work by activities. The total body area is defined in terms of its unit area. On average, an individual has a body surface area of 1.8m2, a metabolic rate of approximately 58.15 W/m2, and a sitting activity of 1 met unit. The level of activity changes depending on the type of exercise such as resting, walking, running, etc. As the activity level increases, the met changes simultaneously. As well as age, gender,

weight, and height, the metabolic rate is also affected by these factors (ASHRAE Standard, 2004).

Clothing insulation ratio (Clo) is the expression of the coverage of the body. A thorough understanding of the transfer of heat from the human body to the surrounding environment is essential. It is typical for Clo to fluctuate between 0 and 1. As an example, 1 clo can be compared to the insulating value of trousers, a T-shirt, a long-sleeved shirt, and a long-sleeve sweater, which cover the majority of the body (La Roche, 2016).

In spite of the fact that thermal comfort depends on different inputs, there are many metrics that can be used to measure it accurately. It is possible to categorize those metrics as outdoor and indoor thermal comfort.

### 2.3.1 Outdoor Thermal Comfort

Thermal comfort is a function of a number of inputs, as previously mentioned. Several metrics are available in the literature to predict "feels like" air temperatures, but this thesis will discuss two of them, Universal Thermal Comfort Index (UTCI) and Physiological Equivalent Temperature (PET).

#### 2.3.1.1 Universal Thermal Comfort Index (UTCI)

As an indicator of thermal comfort, the Universal Thermal Comfort Index (UTCI) integrates meteorological and non-meteorological parameters (Bazejczyk et al., 2013). Meteorological inputs include air temperature (Ta), mean radiant temperature (MRT), wind velocity (va), and relative humidity (RH). A person's thermal perception is influenced by a number of non-meteorological factors, including their metabolic rate and their clothing insulation. UTCI's formula, on the other hand, assumes a 35-year-old male with a clothing insulation rate of 0.90. The weather inputs can be modified by urban geometry and meteorological data.

Based on the results of the calculation, ten different thermal stresses are classified as UTCI values. From +9° C to +26° C shows no thermal stress meaning that the person is in a very comfortable situation. On the other hand, the strong heat stress is observed from +32° C to +38° and strong cold stress between -27 ° C and -13 ° C in a contrast. The detailed range of UTCI is shown in Table 2.1.

Table 2.1. *UTCI range (Błazejczyk et al., 2013)*

| UTCI (°C) | *Stress category* |
|---|---|
| UTCI>46 | Extreme heat stress |
| 38<UTCI<46 | Very strong heat stress |
| 32<UTCI<38 | Strong heat stress |
| 26<UTCI<32 | Moderate heat stress |
| 9<UTCI<26 | No thermal stress |
| 0<UTCI<9 | Slightly cold stress |
| -13<UTCI<0 | Moderate cold stress |
| -27<UTCI<-13 | Strong cold stress |
| -40<UTCI<-27 | Very strong cold stress |
| UTCI<-40 | Extreme cold stress |

#### 2.3.1.2 Physiological Equivalent Temperature (PET)

The Munich energy balance model for individuals (MEMI) is used to determine the physiological equivalent temperature (PET), which is equivalent to the air temperature at which, in a typical indoor environment, the human body is kept in a balanced state with core and skin temperatures that are equivalent to those under the conditions being evaluated (Höppe, 1999; Matzarakis et al., 1999). Using PET, it is

possible to determine how someone perceives the air temperature outside based on how he/she perceives it indoors.

For the PET index, the air temperature, the relative humidity, the wind speed, the mean radiant temperature (MRT), the metabolic rate, as well as personal human characteristics are considered as input variables (Dimitrios Antoniadis et al., 2020). While PET can be applied to both indoor and outdoor environment studies, it has primarily been used to quantify outdoor thermal comfort. Further, it is more accurate at characterizing the thermal bioclimate than UTCI. Table 2.2 provides a summary of PET ranges.

Table 2.2. *PET range (Matzarakis et al., 1999)*

| PET (°C) | *Thermal perception* | *Stress category* |
|---|---|---|
| 4 | Very cold | Extreme cold stress |
| 8 | Cold | Strong cold stress |
| 13 | Cold | Moderate cold stress |
| 18 | Slightly cool | Slightly cold stress |
| 23 | Comfortable | No Thermal stress |
| 29 | Slightly warm | Slightly heat stress |
| 35 | Warm | Moderate heat stress |
| 41 | Hot | Strong heat stress |
| | Very hot | Extreme heat stress |

### 2.3.2 Indoor Thermal Comfort

The calculations of indoor thermal comfort differ from those for outdoor thermal comfort as a result of environmental conditions. A detailed presentation of Predicted Mean Vote (PMV) and Adaptive Thermal Comfort models will be presented in the thesis.

#### 2.3.2.1 Predicted Mean Vote (PMV)

Fanger's thermal comfort model for indoors during the 1960s defined the predicted mean vote (PMV) and predicted percentage of dissatisfaction (PPD). The purpose of Fanger's research at that time was to develop a model that could help heating and air conditioning engineers determine the ideal ambient temperature for the proper indoor climate (Van Hoof, 2008). A model can only be applied to healthy adults; there must be corrections for children and the elderly.

> "The PMV is the average comfort vote predicted by a theoretical index for a group of subjects when subjected to a particular set of environmental conditions. The PMV uses a seven-point thermal scale that runs from cold (-3) to hot (+3) with zero as ideal. Lower or higher values are possible. From the PMV, the PPD can be determined. As PMV moves away from zero in either the positive or negative direction, PPD increases. The maximum number of people that could be dissatisfied with their comfort conditions is 100%. However, as you can never please everybody even under optimum conditions, the minimum PPD number even under optimum comfort conditions is 5%" (La Roche, 2016).

The majority of thermal comfort standards, such as ISO 7730, have adopted Fanger's model. As part of ISO 7730, the following factors are considered when predicting comfort: air temperature (Ta), wind speed (va), the mean radiant temperature (MRT), relative humidity (RH), activity level, and clothing insulation (clo).

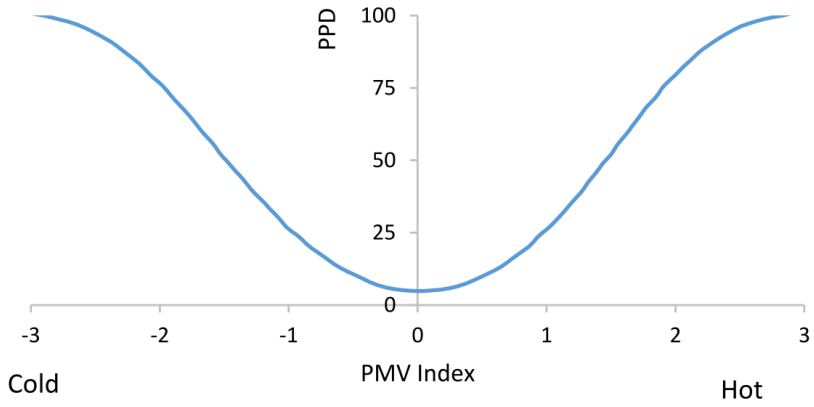


*Figure 2.6.* The relationship between PPD and PMV (Khatoon & Kim, 2020)

#### 2.3.2.2 Adaptive Thermal Comfort Model

According to researchers who have conducted thermal comfort studies in real-life environments, participants' responses differ from the predictions using the PMV model, especially when the rooms do not have mechanical air conditioning systems. In 1976, Humphreys found a statistical relationship between mean dry-bulb temperature and thermal neutrality temperature (Tn), a temperature at which most people are comfortable and do not experience thermal stress. Later, other scientists examined the correlation. Over 20.000 observations from 160 buildings worldwide were examined by De Dear and Brager in 1998. It is found that the PMV model can accurately predict indoor temperatures in buildings that are equipped with HVAC systems. There is, however, no evidence that occupants of buildings that only have natural ventilation are able to tolerate a wider range of temperatures (La Roche, 2016).

.

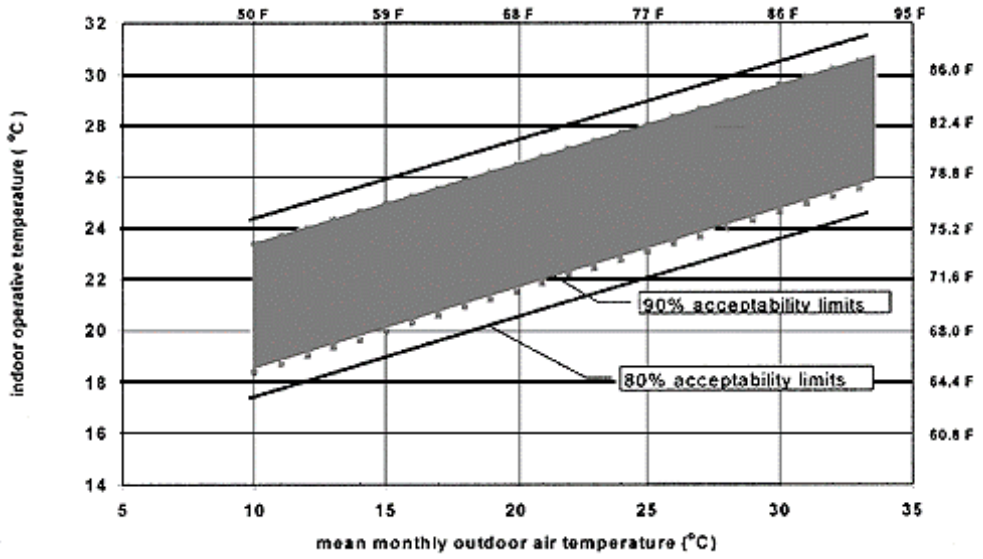


*Figure 2.7.* Acceptable operative temperature ranges (ASHRAE Standard, 2004)

This new finding revised ASHRAE standard 55 crafted by the PMV model. In ASHRAE, the equation is used for calculating comfort temperature:

$Tn = 0.31T_{ave} + 17.8$ ($10°C \leq T_{ave} \leq 33.5°C$)

Tn: neutrality temperature

$T_{ave}$: monthly mean outdoor air temperature (as cited in La Roche, 2016).

There are exceptions to this model, such as naturally ventilated buildings in which occupants have greater control over adjusting their thermal comfort. In this Figure 2.7, the average monthly outdoor air temperature is in the range from 10°C to 33.5°C meanwhile, the indoor operative temperature should be between 18°C and 23°C to stay in comfort inside.

#### 2.3.2.3 Indoor Overheating Degree (IOD)

A Dutch case study introduced the indoor overheating degree (IOD) metric to quantify the sensitivity of indoor temperatures to climate change. IOD considers different thermal comfort limits depending on each zone's thermal adaptation opportunity for the occupants. Furthermore, IOD uses intensity and frequency of indoor overheating to measure the overheating risk (Hamdy et al., 2017). The following equation explains how IOD is calculated where:

$$IOD \equiv \frac{\sum_{z=1}^{Z} \sum_{i=1}^{N_{occ}(z)} \left[ \left( T_{fr,i,z} - TL_{comf,i,z} \right)^{+} \cdot t_{i,z} \right]}{\sum_{z=1}^{Z} \sum_{i=1}^{N_{occ}(z)} t_{i,z}}$$

where:

$T_{fr,i,z}$: the free-running indoor operative temperature at the time step (i) in the zone (z)

$TL_{comf,i,z}$: the comfort temperature limits at the time step (i) in the zone (z)

$N_{occ}$: the occupied period

z: the different building zones

i: the occupied hour counter

t: the time step

Z: the total number of zones in a building

The intensity of indoor overheating is quantified by the temperature difference between the free-running indoor operative temperature (Tfr) and a chosen thermal comfort temperature limit (TLcomf). For the frequency, the intensity of overheating during the occupied period (Nocc) is integrated into the different building zones (z) to present the overall overheating in a building. In calculation, the time step (t) is usually chosen as 1 hour.

### 2.3.3 Thermal Perception of Children

The development of thermal comfort standards is based on the metabolism, activity, and perception of adults. Nevertheless, there are significant physical differences between children and adults that have an impact on comfort. In particular, children have a higher surface area to mass ratio, which causes much heat transfer. In addition, their metabolic rates are higher, their skin temperature rises quickly during exercise, and their sweat rate is lower. Physical disparities affect perceived temperature and make them more vulnerable on warm days (Balbus & Malina, 2009; Cheng & Brown, 2020).

It is surprising that there are not many studies focusing on the perspective of children's thermal comfort in the literature. According to Vanos et al., COMFA (COMfort FormulA) is a new energy budget model intended to assess the thermal comfort of children ages 9-13 exercising in shaded and non-shaded environments under hot air conditions. This model simulates biophysical energy fluxes, which are affected by metabolic heat (activity) and the amount of radiation emitted (Vanos et al., 2017).

Cheng et al. later revised COMFA to include children's physical and physiological characteristics into the model. This model was renamed COMFA-kid and some components were adjusted, such as metabolic heat, convective heat, and evaporative heat exchange. Thus, the prediction had become more accurate and valid to apply to children's thermal perception.

In spite of this, both COMFA and COMFA-kid are steady-state models. They do not calculate dynamic heat exchange over time, but rather estimate values at one point in time (Cheng & Brown, 2020). While further thermal comfort research is needed for children, this fact demonstrates that children perceive heat differently than adults.

#### 2.3.3.1 Thermal Comfort Studies in Schoolyards

The urban schoolyards are primarily public assets where children spend most of their time playing and socializing during the day (Zhang et al., 2017). Therefore, schoolyards can be considered "outdoor classrooms" (Billmore, B., Brooke, J., Booth, R., Funnell, K., & Bubb, 1999). Consequently, the quality of the schoolyards in urban areas plays a significant role in ensuring the safety and health of students.

Nevertheless, schoolyards are not well-designed open spaces; hard surfaces are mostly covered with materials that have high heat capacities such as asphalt, concrete, and brick, which increase the surface temperature and increase the risk of heat stress (Dimitrios Antoniadis et al., 2020). Additionally, due to their height, children are closer to the surface than adults, which can affect their thermal comfort to a greater extent.

In the literature, Moogk Soulis argues that schoolyard heat islands are caused by the absence of trees and the choice of materials in schoolyards (Moogk-Soulis, 2002). One of the main drivers of thermal comfort is the blocking of incoming direction radiation by buildings, trees, and shading structures. As an example, two schoolyards in Greece were studied to determine the impact of trees on perceived temperatures. Trees reduce solar radiation and decrease PET values by as much as 5°C (D. Antoniadis et al., 2016). A study conducted in Korea examined three different types of surface materials. There were three types of turf: natural turf, granite, and artificial turf. Therefore, natural turf has the best thermal comfort performance (Joong-Bin LIM; Jinhang YU; Ju-Yeol LEE; Kyoo-Seock LEE, 2015). A study conducted in Taiwan supports the better performance of natural surface coverage. The study indicates that artificial pavements have a surface temperature of 10°C higher than vegetated surfaces in the summer at noon (Lin et al., 2007). Furthermore, Flax et al. point out that green schoolyards can help create a great environment for children, serve natural resources, and improve health, thermal comfort, and mitigate climate change (Flax et al., 2020).

#### 2.3.3.2 Thermal Comfort Studies in Educational Buildings

A classroom's environment has a significant impact on children's health, well-being, and ability to learn (EPA, 2003). Students' attendance, performance, and productivity get increased when the indoor conditions are comfortable for the occupants in the classroom (Zomorodian et al., 2016). Despite this, students are prone to poor thermal comfort because of their metabolism, as well as their limited ability to adapt to the changing conditions (Katafygiotou & Serghides, 2014). Although they can change their clothes, they cannot freely open or close the windows in the classroom (Corgnati et al., 2009). Furthermore, the uncomfortable indoor conditions result in an increase in energy consumption to meet the desired level of comfort (Zomorodian et al., 2016). Therefore, it is imperative that the indoor thermal comfort of educational facilities plays a significant role in both children's health and energy consumption.

There are a number of programs in educational buildings that interfere with various thermal perceptions in relation to the distinctive characteristics of the classrooms (Teli et al., 2012). A number of parameters were considered in the classification of the previous case studies by Zomorodian et al. (2016), including the climate zone, educational stage, and thermal comfort approach.

The Köppen-Geiger classification divides climate zones into five categories: (i) group A, tropical climates, (ii) group B, semi-arid and arid climates, (iii) group C, temperate climates, (iv) group D, continental climates, and (v) group E, polar and alpine climates. Studies are typically conducted in temperate climates. Table 2.3 indicates the average neutral, lower, and higher comfort temperature limits achieved in each climate zone (Zomorodian et al., 2016).

Table 2.3. *Comfort temperature in each climate zone (Zomorodian et al., 2016, p.899)*

| Climate Zones | Lower Limit (°C) | Neutral (°C) | Higher Limit (°C) |
|---|---|---|---|
| A | 22 | 27.21 | 30.7 |
| B | 19 | 23.08 | 26.6 |
| C | 16 | 21.66 | 30.7 |
| D | 19.9 | 23.58 | 28.3 |

In group A, the lower comfort temperature limit is the highest while in group C, the lower comfort temperature limit is the lowest. The comfortable temperature range in Turkey is between 16°C and 30.7°C, according to the climate category C.

Depending on the children's ages, another parameter is their educational stage. Generally, there are three levels of education, namely (i) the primary level (ages 7-11), (ii) the secondary and high school levels (ages 12-17), and (iii) the university level (ages 18-28). Among educational stages, university studies are carried out most frequently in Asia (31%), while primary schools are studied least in Europe (10%). The Figure 2.8 illustrates the lower and upper comfort limits as well as the neutral comfort temperature at different educational levels (Zomorodian et al., 2016). Due to their metabolic rate and activity level, university students are more tolerant of high temperatures than primary school students.

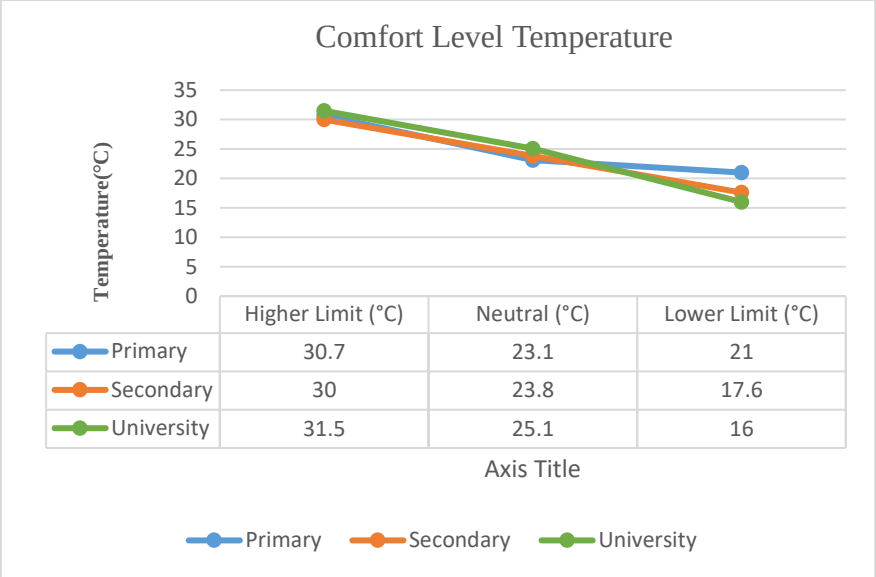


*Figure 2.8.* Comfort level temperature in different educational stage studies (Adapted from Zomorodian et al., 2016)

The last approach focuses on thermal comfort. An adaptive model and a rational model are both types of thermal models. As discussed in another chapter, the rational model is based on Fanger's PMV model. This model is suitable for spaces equipped with air conditioning where the indoor air temperature can be easily controlled. There has been a considerable amount of research on the rational model in the area of thermal comfort for university students in the literature. However, the rational model indicated that only a small portion of the studies had accurate predictions regarding the students' thermal comfort sensation. As a result, the adaptive model would be more appropriate for classrooms since it allows for the flexibility of controlling the indoor climate by opening or closing the windows. The adaptive comfort isn't used much in studies, only 14%. However, it's better at predicting thermal sensation than rational models (Zomorodian et al., 2016).

Thermal comfort conditions in educational buildings represent a challenging issue, and the topic has not been sufficiently addressed, to date. Thus, this issue will be addressed in the context of students between the ages of 7 and 11 as well as the adaptive thermal comfort concept.

## 2.4 Building Energy Consumption

About 40% of the world's energy consumption is attributed to the building sector. Besides heating, cooling, and ventilation, lighting accounts for 11% of the building's total energy consumption, which includes appliances such as refrigerators, kettles, dryers, etc. making up 18%. Miscellaneous, including electronics, makes up 36% of the total building energy consumption (U.S. Department of Energy, 2015). In Figure 2.9, residential buildings account for 22% of the pie chart, followed by non-residential buildings at 18%.

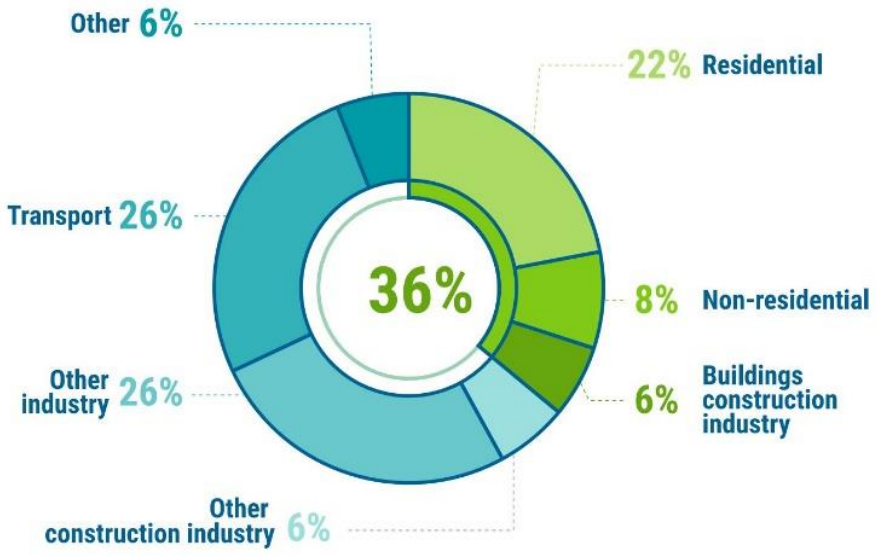


*Figure 2.9*. Buildings and construction's share of global final energy, 2020 (IEA, 2021)

### 2.4.1 Energy Consumption in Educational Buildings

Hospitals, schools, universities, and offices account for about 50% of the energy consumption in non-residential buildings in many countries (Pérez-Lombard et al., 2008). A significant challenge facing educational buildings is their size, their density

of occupants, and their schedule for energy savings throughout the year (Palme et al., 2020). The scope of energy consumption of educational buildings has been examined through several studies conducted under a variety of aspects and geographical regions (Chung & Yeung, 2020).

Using common materials for a classroom, the design variables were changed individually in order to determine the best value for minimum energy consumption in a humid and hot climate zone (Perez & Capeluto, 2009). The following data collection was conducted on 49 school buildings in the Lombardy region of Italy to obtain an understanding of the space heating, occupant behavior, and the mechanical characteristics of these buildings. The survey revealed that different energy retrofit scenarios were developed with different performance goals (Dall'O & Sarto, 2013).

As well, the energy consumption patterns of 8 schools in Portugal were analyzed in order to identify Key Performance Strategies (KPS) to reduce energy consumption by combining user behavior and management policies (Lourenço et al., 2014). In another study, energy management was examined in one school in the United Arab Emirates. An energy management system that is well-structured can result in a 35% reduction in energy use (AlFaris et al., 2016). During a study in South Korea, ten elementary schools were mapped in terms of their energy consumption. The energy saving targets were determined by year, unit area, and per capita (Kim et al., 2012). In Luxembourg, a cluster analysis based on energy sources suggests that passive and low-energy schools are capable of saving up to 70% of energy when compared to standard buildings (Thewes et al., 2014).

### 2.4.2 UHI Impact on Building Energy Consumption

There are a number of factors that affect building energy consumption, such as the outside air temperature, the behavior of the occupants, the indoor climate, the performance of mechanical systems, etc. (Ürge-Vorsatz D et al., 2012). As a result of climate change, rising air temperatures and heat waves have been identified as one

of the most significant drivers of this phenomenon. Increasing cooling demands while decreasing heating demands are some of the effects of overheating in cities on building energy consumption. Based on a literature review, UHI may result in an increase in cooling energy consumption of 10% to 120% and a decrease in heating energy consumption of 3% to 45% (Li et al., 2019).

#### 2.4.2.1 UHI Impact on Building Cooling Load

Studies have shown that urban heat islands have a greater impact on building energy consumption in city centers than in the suburbs. A study by Santamouris et al. found that the building cooling energy consumption slowly decreases from Athens' urban core to the city's periphery (M. Santamouris et al., 2001). City centers in Bahrain have an increased cooling load of 2%-10% when compared to rural sites (Radhi & Sharples, 2013). Another study shows that cooling energy consumption varies between 12% and 46% in Rome's city center in a hot, arid climate (Zinzi & Carnielo, 2017).

Additionally, the effect of UHI on building cooling demand varies depending on the type of building (Li et al., 2019). It was found that the impact of UHI during a hot month on the cooling load of office buildings was greater than that of residential buildings in Hong Kong. On the other hand, residential buildings are more susceptible to damage during mild months (Chan, 2011). Another study in Boston shows UHI affects office building energy consumption more than residential buildings (Street et al., 2013).

#### 2.4.2.2 UHI Impact on Building Heating Load

In contrast to the lack of well-studied effects of UHI on building heating energy consumption, a study of representative global cities indicates that the UHI effect reduces heating energy consumption by 3–45% and increases cooling energy

consumption by 10–120% (Li et al., 2019). In addition, the impact of UHI varies depending on how long the period is, and some studies indicate that an increase in air temperature in the winter decreases heating energy demand (Meng et al., 2020).

## 2.5 UHI Mitigation Strategies

As stated previously, UHI affects the built environment in many ways, including increased air temperature, increased energy consumption in buildings, especially during the summertime, and outdoor discomfort under a broad umbrella of effects. In order to reduce the impact of UHI on cities, a variety of mitigation strategies exist; however, they can be divided into five categories: cool material mitigation strategies, vegetation mitigation strategies, green roof mitigation strategies, water element mitigation strategies, and combined strategies.

### 2.5.1 Cool Material Strategy

By applying reflective materials to buildings as well as the outside of cities, urban heat islands can be reduced. Reflective materials can be applied both to buildings and to the outside of cities. It has been proven in numerous studies that higher surface albedo reduces surface temperature and mitigates UHI. The literature review conducted by Santamouris et al., which included 220 projects, indicated that studies were conducted using cool roofs, cool pavements, or combinations of these two technologies (M. Santamouris et al., 2017).

Cool roofs resulted in a 2.3°C absolute air temperature drop, cool pavements resulted in a 2.5°C absolute air temperature drop. According to another cool material scenario applied in Los Angeles, a hot climate city, an increase of 0.30 in albedo of asphalt and concrete pavements can reduce the temperature by 2.0°C at the pedestrian level in hot summer conditions (Taleghani et al., 2016). The author further estimates that,

given a global increase in the city's albedo, the average reduction in air temperature is 0.3°C per 0.1 increase in albedo (M. Santamouris, 2014).

A significant decrease in the surface temperature was also detected in addition to the change in air temperature. In Toronto, Canada, an albedo value of 0.2 was replaced with a material with a value of 0.4 as a result of a study conducted. As a result, the surface temperature at noon in summer decreased by 7.9°C (Wang et al., 2016).

In spite of the cold climate, the study conducted in Thessaloniki, with a Mediterranean climate, found that the surface temperature of materials with high albedo decreased between 7°C and 9°C (Tsoka, Theodosiou, et al., 2018).

However, some studies report that increasing the solar reflectance of paving does not have a beneficial effect on summer outdoor thermal comfort. Consequently, a person in an urban environment is exposed to a variety of types of radiation that contribute to heating their bodies. Based on the Mean Radiant Temperature (MRT), the net impact on radiant exchange with the body is determined. Therefore, the MRT is an integral part of the calculation of outdoor thermal comfort indexes such as the Physiological Equivalent Temperature (PET). As a result of increased solar reflectance, the MRT may increase. This explains why reflective materials may negatively impact outdoor thermal comfort (Salvati et al., 2022). A cool pavement is more effective for maintaining thermal comfort when it is used under shading.

### 2.5.2 Vegetation Strategy

By shading, respiration, and transpiration, broad-leaved trees play a crucial role in balancing the high air temperature in summer. This is one of the most effective methods of mitigating the impact of urban heat islands. According to a comprehensive literature review (M. Santamouris et al., 2017), the decrease in average air temperature is between 0°C and 3.5°C when the effect is studied in general.

Even though trees reduce the air temperature during the day, their effect changes in the evening. This is due to the fact that sun rays that arrive at the surface during the day with short wavelengths return with long wavelengths at night, which causes the temperature to rise. Because the radiation from the sun disappears at night, only reflections from heated surfaces during the day can be observed in the evening. As a consequence, the radiation trying to reflect becomes trapped beneath the broad-leaved trees in regions with broad leaves, increasing air temperature (Abreu-Harbich et al.).

Another study in the literature shows that cooling air temperature by trees in cool seasons is considerably smaller than hot seasons, and trees can even warming the air up during day time (Meili et al., 2021).

### 2.5.3 Green Roof Strategy

When there is not sufficient space to plant vegetation at ground level, especially in dense cities, the green roof strategy may be an appropriate alternative (Karachaliou et al., 2016). Depending on the vegetation, substrate depth, irrigation complexity, accessibility, and maintenance requirements, green roofs are classified as extensive or intensive. The benefits of these actions include reducing $CO_2$ emissions, mitigating the UHI effect, minimizing energy consumption, increasing biodiversity, etc. (Laloević et al., 2018).

It has been shown that green roofs can reduce air temperatures by between 0°C and 3°C. Furthermore, the cooling potential of the green roof is influenced by the leaf area index (LAI) of the vegetation, irrigation level, and the type of plant (M. Santamouris, 2014). The impact of green roofs on the street level air temperature is almost negligible while building heights increase, even though green roofs are important for cooling the cities (M. Santamouris et al., 2017).

### 2.5.4 Water Element Strategy

As a result of evaporation, water elements are able to cool the surrounding air (Oke, 1988). Furthermore, the water elements have a higher thermal capacity than the surrounding walls and floors, resulting in a lower temperature. Therefore, water bodies heat up later and cool down later, which decreases the outside air temperature. In a study, it was found that air temperature decreased by 2-6 degrees as the water bodies were active (Manteghi et al., 2015).

### 2.5.5 Combined Strategies

As a means of mitigating UHI, greenery, reflective materials, and water elements are the most effective. An extensive literature review conducted by Santamouris examined twenty-five different projects that were found to reduce air temperatures between 0.4°C and 5°C by combining urban greenery with reflective materials. Moreover, when three different strategies, such as reflective materials, greenery, and water elements, are combined, the peak air temperature drops between 1.4°C and 3.1°C (M. Santamouris et al., 2017).

The purpose of this thesis is to compare the cooling effect of cool materials on pavements and façades, and the cooling effect of greenery on schoolyards, and their combinations, in terms of their mitigation of UHI.

## 2.6 UHI Calculation Tools

A number of studies on urban heat islands and microclimates have been conducted using upper scale and satellite images (Duman Yüksel & Yilmaz, 2008), observational data collection (Jeong et al., 2015), and numerical modeling and simulations (Yavaş & Yulmaz, 2019). In the current era, computational tools are available to simulate microclimatic areas that combine a wide range of climate

factors. These are (i) Urban Weather Generator (UWG), (ii) Urban Multi-scale Environmental Predictor (UMEP), (iii) Rayman model, and (iv) ENVI-Met. These are (i) Urban Weather Generator (UWG), (ii) Urban Multi-scale Environmental Predictor (UMEP), (iii) Rayman model, and (iv) ENVI-Met.

### 2.6.1 The Urban Weather Generator (UWG)

The Urban Weather Generator (UWG) has been developed by the Massachusetts Institute of Technology (MIT) for the purpose of analyzing heat island effects (Bueno et al., 2013). Building air temperature and energy consumption can be predicted based on the urban morphology, geometry, and surface materials of the building. UWG calculates the hourly air temperature and humidity of urban areas based on weather data collected at a rural weather station. As a result of the UHI effects, the output file is a modified air temperature file. This model has been validated partially for Singapore, Basel, Toulouse, Rome, and Antofagasta. Those studies indicate that UWG underestimates canyon temperatures in the summer, while producing more realistic results in the winter.

### 2.6.2 Urban Multi-scale Environmental Predictor (UMEP)

In addition to investigating outdoor thermal comfort, wind dispersion, and urban energy consumption, UMEP (Urban Multiscale Environmental Predictor) is an open-source simulation model that allows the evaluation of the effectiveness of possible mitigation actions (Lindberg et al., 2018).

### 2.6.3 Rayman Model

A free radiation flow model, Rayman, was developed at the University of Freiburg which incorporates urban morphology into the modeling. The albedo and mass angle ratios of surrounding surfaces are also taken into account when calculating radiation

fluxes. In urban and regional planning, this method poses the greatest difficulty in quantifying shading from building structures. Radiation fluxes are calculated based on air temperature, relative humidity, cloud cover, and air transparency. This is accomplished by using fish-eye photographs. A drawback of this approach is that it cannot calculate air temperature, air humidity, or set wind velocity (Naboni et al., 2017).

### 2.6.4 ENVI-Met

Bruse and Fleer, who developed ENVI-Met in 1998, calculate the atmosphere's state based on the interaction between buildings, vegetation, hard ground properties, soil, and climatic conditions. Based on the laws of fluid dynamics and thermodynamics, the model simulates the evolution of climate variables throughout the day. Using this model, researchers and designers are able to analyze urban heat islands and outdoor thermal comfort in detail and at high resolution. Several studies using ENVI-Met have been conducted in the literature, all of which can be categorized into four categories: urban geometry, material albedo, vegetation, and water elements as mentioned previously.

# CHAPTER 3

# METHODOLOGY

A primary school building chosen as a case study is used to demonstrate the application of this method in this chapter. Considering the literature, it is found that there is a gap in mitigation strategies for UHI to bridge indoor and outdoor thermal comfort and reduce energy consumption in primary schools.

The novelty of this thesis proposes a method for generating UHI modified weather file for each separate classroom. In other words, this method customizes the UHI effect and allows for investigation of the UHI impact on energy consumption and thermal comfort conditions in classroom specific.

Following are some requirements for structuring the scenarios and analyzing processes:

- Modeling urban microclimate
  - Preparation of 3D model in Rhino
  - Selection of 12 representative days
  - Setting baseline model in ENVI-met by using the 3D model in Rhino
  - Locating receptors in front of the selected classrooms' windows in ENVI-Met
  - Running ENVI-Met baseline model simulation for each representative day
- Shifting weather files in classroom specific
  - Extracting air temperature results from the receptors
  - Generating modified weather file for the baseline by using receptor data for selected representative days in Elements

- UHI mitigation scenarios
  - Simulation of 6 different mitigation scenarios in ENVI-Met
  - Reading the receptor air temperature data for each strategy
  - Generating modified weather file for the scenarios by using receptor data for selected representative days in Elements
- Building energy model
  - Setting energy model by using Honeybee plug-in in Grasshopper
  - Running energy simulation for baseline and 6 mitigation scenarios by using EnergyPlus
- Results
  - Comparison of UHI modified weather file and the station file for the baseline
  - Examining UHI impact on overheating degree
  - Examining UHI impact on heating load
  - Examining UHI impact on outdoor thermal comfort by using PET metric in ENVI-Met Biomet

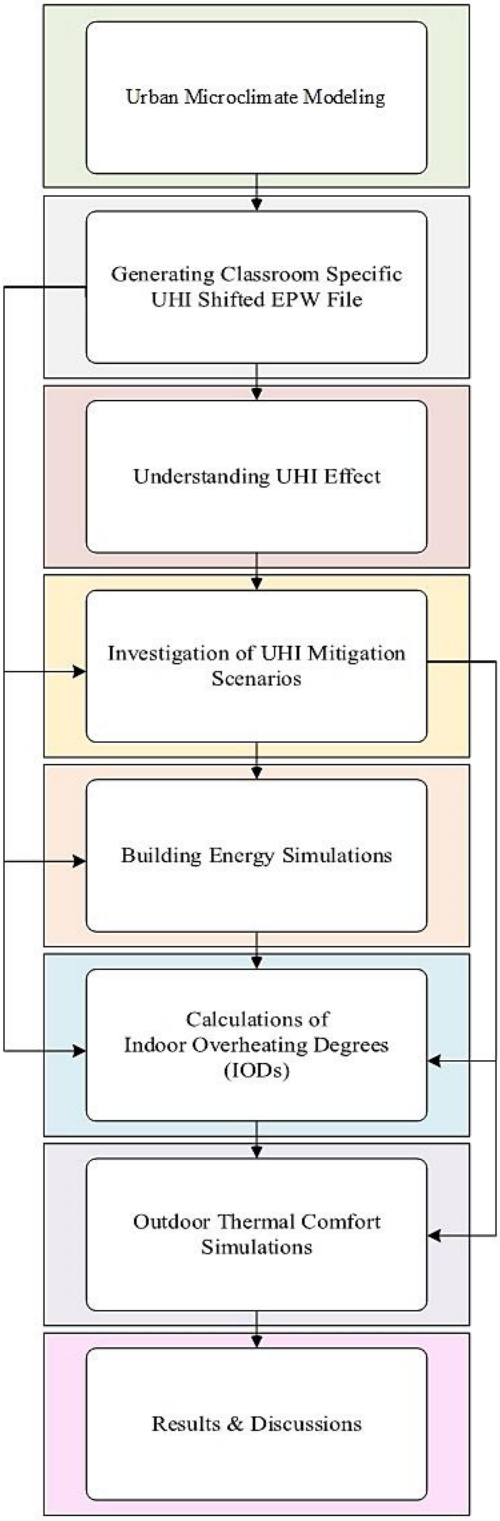


*Figure 3.1.* The workflow of the thesis

## 3.1 Case Description

A literature review was presented in the previous chapter regarding climate change, UHI effect and mitigation strategies, outdoor thermal comfort, indoor overheating degrees, and heating loads of an existing educational building. In this chapter, the reasons for selecting the case study are described and clarified.

The primary school is selected as a case study in terms of being a typical school building regarding its typology, building materials, and mechanical systems in Turkey. A number of factors contribute to the selection of this building, including (i) its orientation, (ii) its surrounding context, (iii) the age range of the occupants, (iv) the variety of construction, (v) its typology, (vi) its schoolyard design, and (vii) the ease of gathering information.

The primary school is in Bahçelievler neighborhood which is rich in vegetation canopy rather than other sites in Ankara. However, the case school has lack of trees, and its playground has hard surface without soft materials that might cause uncomfortable outdoor experience for children. In Figure 3.2, the schoolyard is covered by asphalt, and there are no shading elements or vegetation to block the direct sunlight that causes the heat stress at breaks outside.


*Figure 3.2.* The case school location and street view

The building itself has four levels with a basement however, the east wing of the building is one level lower than the other parts. The building has 53 classrooms, 3 WCs, 1 teacher's room, 1 cafeteria, 1 kitchen, and 4 offices including an administrator room, psychological counselor room, and staff rooms with 3.5meter height. The floor area is 1700 square meters.

The facade is covered with pressed bricks and plaster. The external and internal walls are made up of bricks without insulation. The roof is a pitched roof with a complex shape. It is uninsulated and covered with clay tiles. Windows are double glazed with polyvinyl chloride (PVC) frame.

The mechanical system consists of a gas-fired central heating system without a cooling system and the building is naturally ventilated during the day.

The operation schedule of the school is 5 days a week from the middle of September to the middle of June with one 2-week holiday break at the end of January. However, there is a summer school starting in August. The schedule starts from 08:25 to 15:45 for lessons with six short breaks and one lunch break. The classrooms are occupied by between 12 and 20 students.

## 3.2 Modeling Urban Microclimate

As mentioned in the literature review, there are many urban microclimate modeling tools however, ENVI-Met allows for simulation of more detail as the interaction between surfaces, plants, and air in the built environment. Therefore, ENVI-Met is chosen to conduct urban microclimate modeling to investigate UHI impacts on human comfort and energy consumption.

### 3.2.1 3D Baseline Model

The ENVI-met Grasshopper plug-in for Rhinoceros is used for transferring 3D geometry and material inputs to the ENVI-met workplace. Simulations start with the baseline model which is the current situation of the site area before applying mitigation scenarios. Table 3.1 presents the general frame of the baseline model.

Table 3.1. *The 3D baseline model features*

| | |
|---|---|
| Location | Bahçelievler, Ankara |
| The size of the site area ($m^2$) | 39.345 |
| Building typology | Residential |
| The average building height (m) | 12 |
| Green area ratio (%) | 10 |
| Hard surface area ratio (%) | 90 |
| Dominant hard surface material | Asphalt |
| Building wall material | Brick |

### 3.2.2 Representative Days Selection

Modeling and simulation of urban microclimate are labor-intensive and high in computational cost. Moreover, ENVI-met does not provide annual simulations, it calculates the dynamics of microclimate during a diurnal cycle, which is between 24 and 48 hours.

This limitation makes it difficult to investigate microclimate impact on energy consumption studies that need annual weather data input. Therefore, shifting annual weather data in only representative days for each month rather than 365 days creates more efficiency in a time manner.

A representative day is defined as the day which has the least difference from the average 24-hour long-term observation of the weather station (Tsoka, Tolika, et al., 2018). Instead of simulating the whole year, 12 representative days, one for each month, are selected, and microclimate simulations are conducted on these days in Ankara.

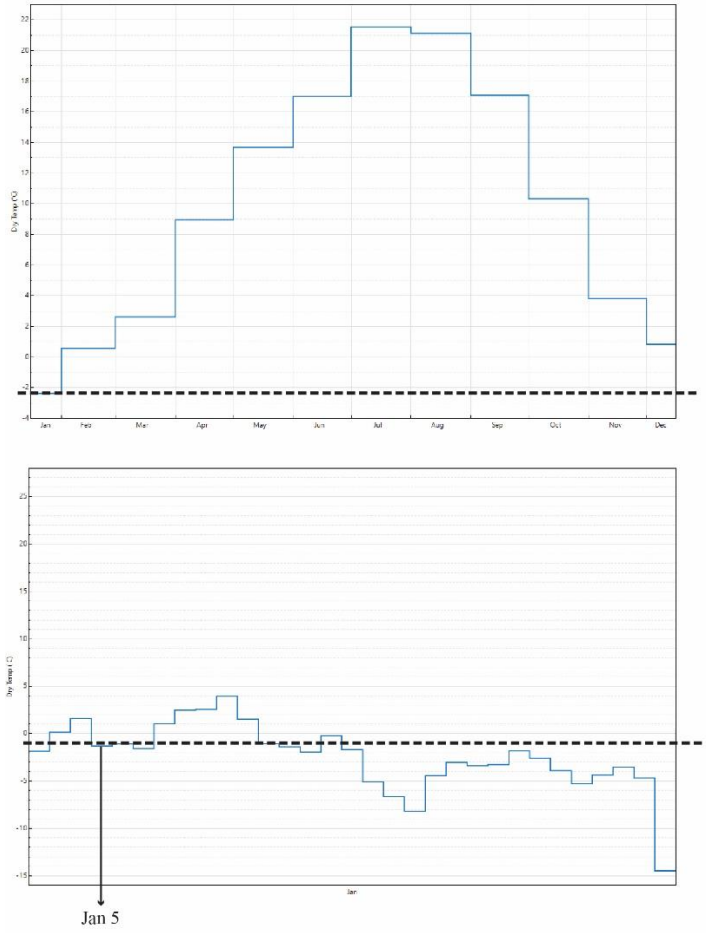


*Figure 3.3.* The case school location and street view

For air temperature data, IWEC Energy Plus Weather (EPW) files with code 171280 from Ankara province are used as a first step. The figure illustrates the -1 °C average for January during a year indicated by the dashed line in figure 3.3. To determine the representative day, -1 °C is placed on a daily air temperature graph and the one which is closest to that level is selected. Ankara representative days are listed in Table 3.2.

Table 3.2. *Representative days for Ankara*

| Month | Representative day |
|---|---|
| January | 5 |
| February | 23 |
| March | 22 |
| April | 5 |
| May | 23 |
| June | 21 |
| July | 31 |
| August | 17 |
| September | 21 |
| October | 9 |
| November | 16 |
| December | 31 |

### 3.2.3 ENVI-Met Simulation Model

To perform ENVI-Met simulation, area input file (INX), database, and configuration file (SIMX) should be provided. Area input file (INX) stores data on the size and resolution of the domain, and spatial features of the grid mesh by using an orthogonal 3D grid (Berghauser Pont et al., 2020).

*Area Input file (INX)*

For creating an INX file, two steps need to be followed. The first step is defining the work area grid that affects the resolution of the results. The selected site area is 215 m x183 m boundary dimensions. Although the higher frequency of the grid gives more accurate outputs, it takes much time for the completion of the simulation. Therefore, the grid mesh is defined as an equidistant grid type for a vertical plane,

and the distance between grid cells is 3m for x-direction and y-direction; 3.5m for z-direction to balance detailed results and the time cost.

As a second step, after the grid was created, the building, hard surface, natural surface material, and vegetation characteristics are determined with the ENVI-met database for the baseline model. The database ensures that descriptive parameters such as thermal conductivity, albedo, and water content, for soil, vegetation, and surface materials can be used to solve equations of the mathematical model (Berghauser Pont et al., 2020).

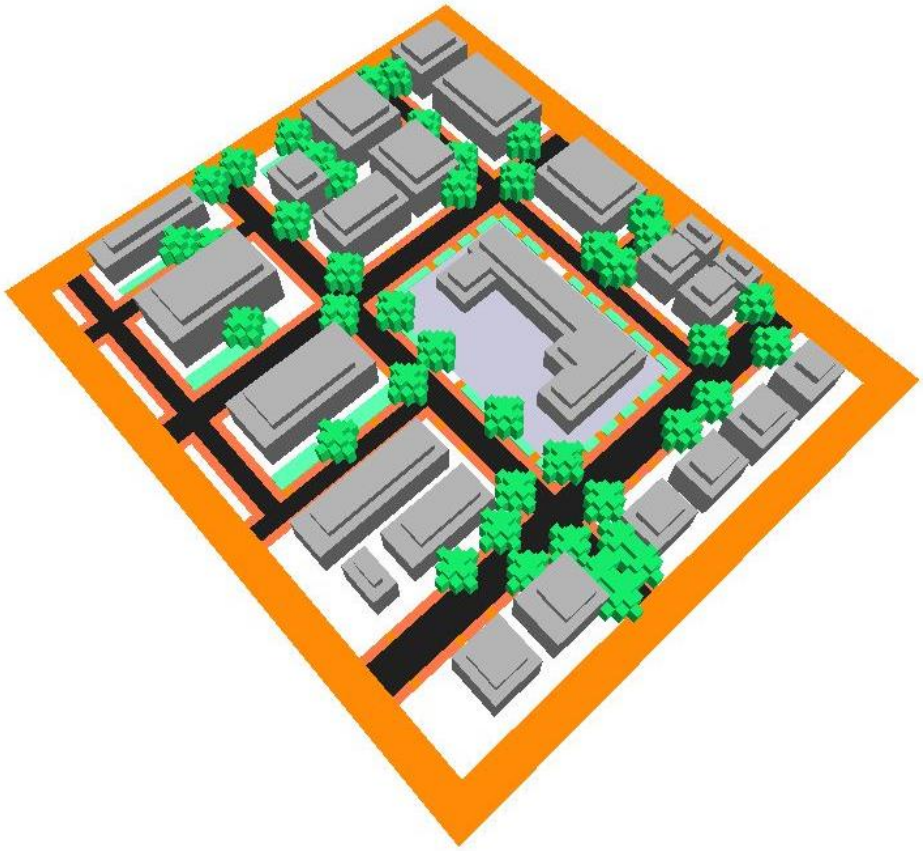

*Figure 3.4.* ENVI-met baseline model

Figure 3.4 shows the baseline model in the ENVI-met workplace. The hard surface material, natural surface material, and vegetation are selected from the ENVI-met default database. For building envelope materials, they are customized based on a

typical school building in Turkey, as a new project database in the ENVI-met. The hard surface material for the context is chosen as asphalt for the road; red stones with 0.3 albedo for the pavements; grey concrete pavement with 0.5 albedo for buildings' parcels; the aged concrete with 0.3 albedo for the schoolyard floor.

The building wall materials have different layers however, the important part is the outside of the envelope for the microclimate modeling. The outside material of the context buildings and the school has plaster with 0.3 albedo. The vegetation is two types in ENVI-met, which are 3D greenery and 2D greenery. In the baseline model, 15-meter-tall spherical deciduous trees, and dense grass are used to project the real conditions of the site area. Moreover, as shown in Table 3.3, trees have a seasonal cycle for their leaves. In the summer, leaf area density reaches its maximum, while in other seasons, it decreases. The details of the INX file inputs can be seen in Appendix A.

Table 3.3. *Seasonal cycle*

| Months | Seasonal scale factor |
|---|---|
| January | 0.20 |
| February | 0.20 |
| March | 0.25 |
| April | 0.50 |
| May | 0.75 |
| June | 1.00 |
| July | 1.00 |
| August | 1.00 |
| September | 0.75 |
| October | 0.50 |
| November | 0.25 |
| December | 0.20 |

*Receptors*

They are located at 1.75 m, 5.25 m, and 8.75 m in front of the selected classrooms' windows. There are 16 selected classrooms facing different directions and levels as seen in Figure 3.5. For instance, classrooms a1, b1, and e1 are on the first floor, and their windows are facing to the north, the east and the west respectively.

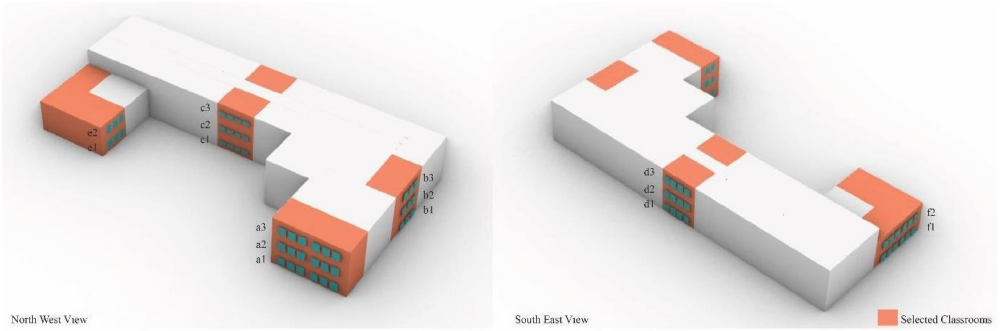


*Figure 3.5.* Selected classrooms

The other classrooms are on the second floor and the third floor facing to west, south and east, too. Table 3.4 summarizes all classrooms and their orientations.

Table 3.4. *Classroom names and orientations*

| Direction | Classroom name |
|---|---|
| North | a1 |
| | a2 |
| | a3 |
| | c1 |
| | c2 |
| | c3 |
| West | b1 |
| | b2 |
| | b3 |
| | e1 |
| | e2 |
| South | d1 |
| | d2 |
| | d3 |
| East | f1 |
| | f2 |

*Configuration File (SIMX)*

To prepare the configuration file (SIMX), the starting time of the simulation and initial weather inputs should be defined. The start date changes regarding selected representative days, and the simulation duration is 24 hours. As a start, IWEC Energy Plus Weather (EPW) file with code 171280 from Ankara province is used for meteorological initial input data. IWEC data files are typical weather files suitable for building energy simulation programs. The average values of air temperature, relative humidity, specific humidity, wind speed, and wind direction data for a selected representative day in this file are used for initial data entries.

The ENVI-Met model offers the so-called forcing method, which allows the definition of daily variations of various meteorological parameters as boundary conditions for a realistic microclimate model (Huttner, 2012). There are two types of forcing: (i) the simple forcing method allows for analyzing only the 1-day variation of air temperature and relative humidity, and (ii) full forcing, the air temperature, and relative humidity, for a longer period. In addition, the change in wind and cloudiness rates can be analyzed.

In this thesis, the simple forcing method is applied to examine only the air temperature change and not to extend the simulation time. Moreover, the building's indoor air temperature is required for simple forcing, which is kept constant at 23°C. Thus, the configuration file (SIMX) stores the simulation settings including weather boundary conditions. The configuration inputs for January 5$^{th}$ that which is one of the representative days can be seen in Table 3.5.

Table 3.5. *Configuration inputs*

| | |
|---|---|
| Simulation start day | 05.01.2018 |
| Simulation start time | 00:00:00 |
| Total simulation hour | 24 |
| Number of the grid (x*y*z) | 80 x 70 x 17 |
| Distance between grid cells (metre) (x, y, z) | 3 x 3 x 3.5 |
| Vertical grid type | Equidistant grid |
| Model rotation | 0 |
| **Initial weather inputs** | |
| Wind speed at 10 meters (m/s) | 0.47 |
| Wind direction | 45 |
| Roughness | 0,5 |
| Initial air temperature (°C) | -1.09 |
| Specific humidity at 2500 meters (gr water/kg air) | 2.80 |
| Relative humidity at 2 meters (%) | 82.25 |
| **Building Indoor Temperature (°C)** | 23 |
| **Forcing type** | Simple forcing |

This process needs to be repeated 12 times for each representative day to collect UHI-modified air temperature data for creating a new weather file for the baseline. One simulation takes approximately 8 hours. The used computer for the simulation has 16GB RAM, i-7 3.60 GHz (8GPU). Thus, a minimum of 96 hours (4 days) is spent for completing only the baseline model.

## 3.3 Creating Classroom Specific UHI Modified Weather File for the Baseline

After the simulations are completed, the air temperature data extracted from the receptors are used for modifying the weather station air temperature data. The main weather data is IWEC Energy Plus Weather (EPW) file, and its air temperature values are replaced with the simulation outputs for each representative day to create a new UHI shifted baseline EPW file of an individual classroom. *Elements* is used for building the new weather file as a tool. It is very practical and enables to change the air temperature data in specific hours in the EPW file and save it as a new one.

## 3.4 UHI Mitigation Strategies

After generating the baseline EPW file, 6 different mitigation scenarios are decided based on the literature review to compare each scenario's impact. The main goal of testing various combinations of interventions is that address the most effective scenario to improve outdoor and indoor thermal comfort while reducing energy consumption.

The scenarios change regarding (i) ground floor albedo, (ii) building façade albedo, and (iii) number of trees as seen in Table 3.6. These interventions are applied to only the educational building's parcel area. The other inputs for surrounding are kept constant as explained in the previous section of the methodology. The only albedo and greenery inputs are changed because they are the most effective interventions according to the literature review.

Table 3.6. *UHI mitigation scenarios*

| Scenarios | Schoolyard floor albedo | School's façade albedo | Number of trees in the schoolyard |
|---|---|---|---|
| Baseline (BL) | 0.3 | 0.3 | 4 |
| Cool Pavement (CP) | 0.8 | 0.3 | 4 |
| Cool Facade (CF) | 0.3 | 0.6 | 4 |
| Green (GR) | 0.3 | 0.3 | 16 |
| Cool Façade + Green (CFGR) | 0.3 | 0.6 | 16 |
| Cool Pavement + Green (CPGR) | 0.8 | 0.3 | 16 |
| Cool Façade + Cool Pavement + Green (CFCPGR) | 0.8 | 0.6 | 16 |

UHI effects are worst in the baseline scenario. The other scenarios gradually improve materials and greenery to determine the appropriate combination of UHI mitigation. Figure 3.6 assigns plaster with 0.3 albedo to the school's façade, and the aged asphalt with 0.3 albedo to the schoolyard ground in the baseline. Moreover, in the other scenarios, the vegetation is the poorest as there are only four deciduous trees on the north side of the schoolyard.

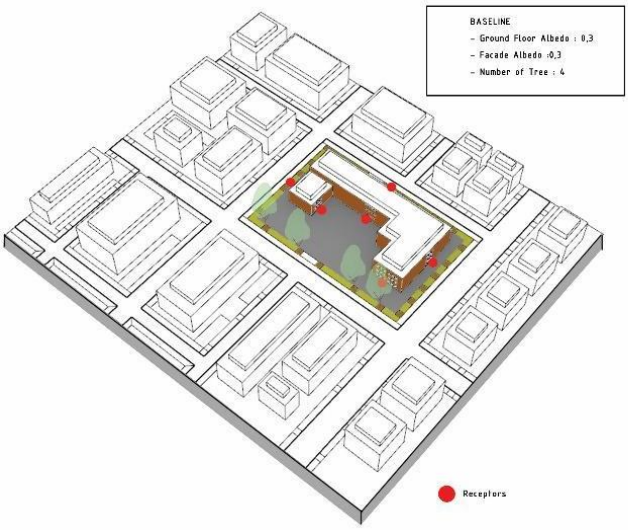


*Figure 3.6.* The Baseline

### 3.4.1 Mitigation Simulations

In the ENVI-met, six mitigation scenarios are simulated 12 times. One simulation takes approximately 8 hours; thus, a minimum of 576 hours (24 days) is spent on the simulations for all mitigation scenarios.

In order to produce scenarios, there are three main interventions: the first is the cool pavement, the second is the cool façade, and the third is the green. The remaining four scenarios are combinations of these three interventions.

*Cool Pavement (CP)*

There are four trees in the Cool Pavement intervention, and the facade albedo is the same as the Baseline; however, the ground floor of the schoolyard is covered with the high albedo material (0.8), also known as light concrete pavement.

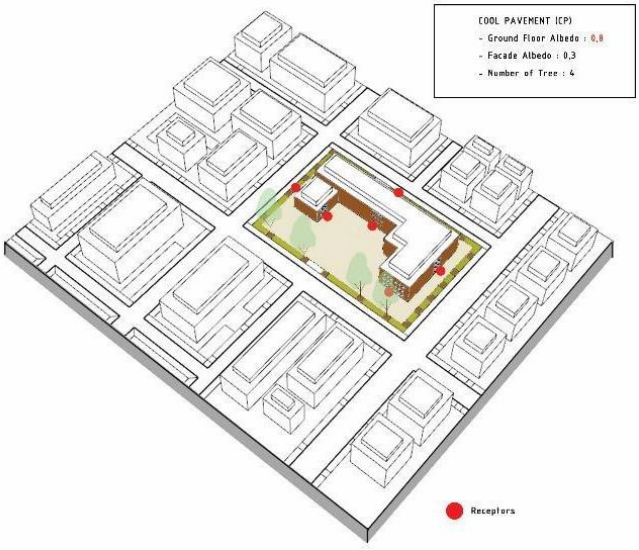


*Figure 3.7.* The Cool Pavement intervention

*Cool Facade (CF)*

In the Cool Facade intervention, the schoolyard floor material and vegetation amount are the same as in the Baseline intervention; however, the light color plaster with 0.6 albedo is replaced with 0.3 albedo plaster.

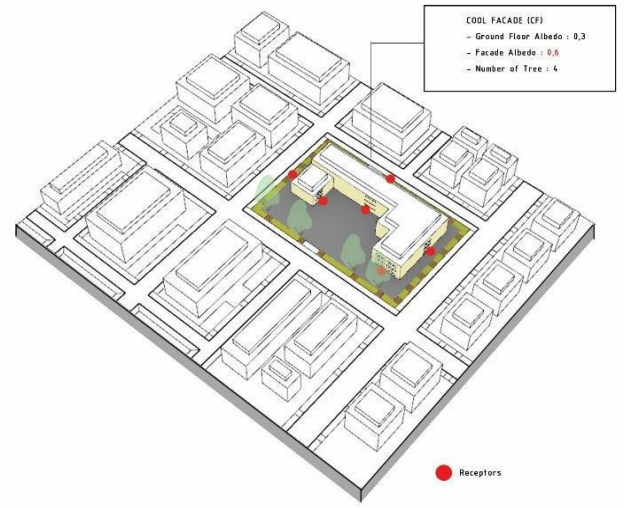


*Figure 3.8*. The Cool Facade intervention

*Green (GR)*

In this scenario, the green intervention involves the planting of more trees. All other parameters are left unchanged in the baseline. The number of trees is multiplied four times by the current amount, resulting in 16 trees planted in four different directions across the schoolyard.

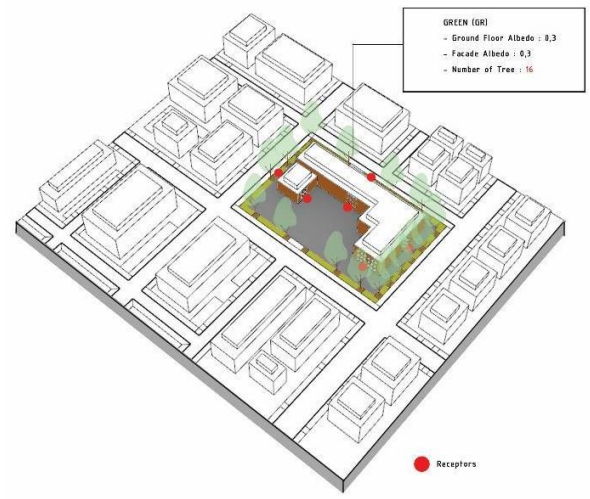


*Figure 3.9*. The Green intervention

*Cool Façade + Green (CFGR)*

In the Cool Facade + Green intervention, the schoolyard floors are made from the same material with 0.3 albedo, while the building facades are made from the material with 0.6 albedo, which ensures that the schoolyard has 4 times more trees.

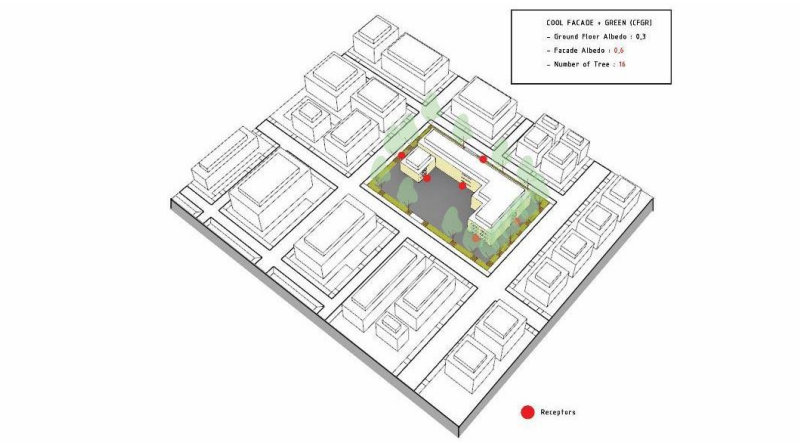


*Figure 3.10.* Cool Façade + Green intervention

*Cool Pavement + Green (CPGR)*

As opposed to the Cool Facade and Green stage, Cool Pavement + Green involves using light materials with an albedo of 0.8 instead of high albedo facade plaster on the schoolyard floor. In addition, the schoolyard is adorned with 16 trees. The facade plaster albedo of the building is the same as in the baseline.

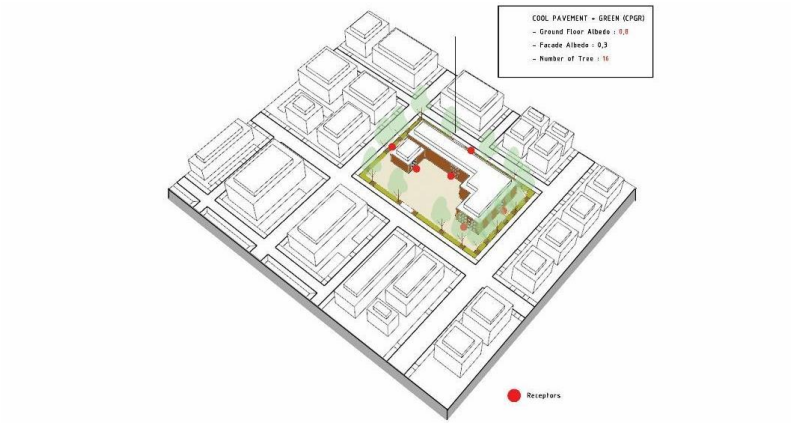


*Figure 3.11.* The Cool Pavement + Green intervention

*Cool Façade + Cool Pavement + Green (CFCPGR)*

There are three different interventions included in the Cool Facade, Cool Pavement, and Green intervention which includes high albedo materials on the facade (0.6) and schoolyard floor (0.8), as well as additional greenery.

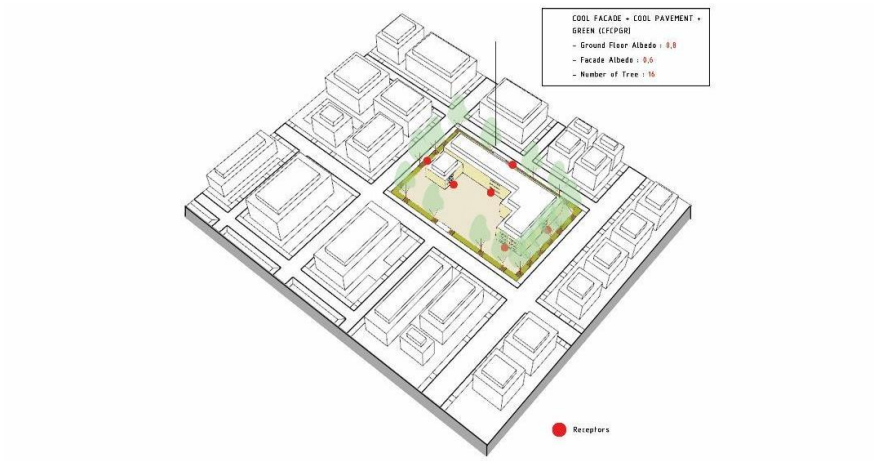


*Figure 3.12*. The Cool Façade + Cool Pavement + Green intervention

### 3.4.2 Generating EPW Files for the Scenarios

Based on the air temperature extracted from the receptors for each scenario, the weather station air temperature data for each scenario is modified to generate a new UHI modified EPW file for every classroom based on the same process followed in the Baseline simulation. The main weather data is IWEC Energy Plus Weather (EPW) file, and its air temperature values are changed by using the Elements tool according to simulation outputs for each representative day. Once these EPW files have been generated, they will be used to run energy simulations.

## 3.5 Building Energy Modeling

To assess the amount of energy consumed by each classroom and the degree to which it overheats indoors, building energy modeling is conducted after creating EPW files

relating to UHI modified scenarios and mitigation scenarios. The energy model is therefore first set with Honeybee plug-ins, then run with EnergyPlus plug-ins for the baseline scenario and six mitigation scenarios.

### 3.5.1 Energyplus Simulation Model

To construct the building energy modeling, Honeybee and Energy Plus plugins are used in Grasshopper. An open-source plugin called Honeybee permits you to assign schedules, ventilation systems, internal loads, and construction materials to individual units within a building's mass, assigning ventilation systems, internal loads, and construction materials to each zone. Additionally, Honeybee provides users with direct access to EnergyPlus, an energy analysis and thermal load simulation engine developed by the U.S. Department of Energy. This application obtains preliminary information regarding weather and location, construction materials, and context geometries from the EPW file. In the future, Honeybee can be used to specify detailed loads, schedules pertaining to occupancy, ventilation, lighting, cooling, and heating. In addition, honeybee assigns these features as default values to the zone program, but EnergyPlus allows the default values to be overwritten (Akköse, 2019).

The energy simulation workflow involves a set of criteria such as weather data, building components, zone program, building loads, zone schedules, heating and cooling set points, zone construction materials, ventilation system, and contextual shading.

*Weather data*

As stated previously, IWEC Energy Plus Weather (EPW) file for Ankara that stores all hourly weather information for all the year. For EnergyPlus simulation of the Baseline, the EPW file is used without any UHI effect however, the other simulation for each mitigation scenario is run by using generated UHI modified EPW.

*Building components*

Rhino is used to generate the 3D geometry of each zone and the wall openings.

*Zone program*

Honeybee has default sets for internal loads and schedules based on the zone program. Therefore, zone program should be assigned to each zone after the geometry is taken from Rhino model.

In this thesis, the zone program is set as primary school classroom as mentioned before. The details about zone areas, wall to window ratio and program can be seen in Appendix B.

*Building Loads*

Building internal loads are defined as equipment load, infiltration rate, lighting density, number of people, ventilation, and recirculated air in the simulation tool. All parameters' values are given based on Honeybee defaults according to the zone program that can be seen in Table 3.7.

Table 3.7. *Building loads*

| | Zone Type |
|---|---|
| Internal Loads | Classroom |
| Equipment Load ($W/m^2$) | 10.97 |
| Infiltration Rate ($m^3/s$- $m^2$) | 0.0002 |
| Lighting Density ($W/ m^2$) | 15.06 |
| Number of people ($ppl/ m^2$) | 0.25 |
| Ventilation ($m^3/s$-person and $m^3/s$-$m^2$) | 0.0006 |
| Recirculated air ($m^3/s$- $m^2$) | 0 |

*Zone Schedules*

Zone schedules include occupancy, occupancy activity, heating set point, cooling set point, lighting, equipment, infiltration, and ventilation schedule. The occupancy

schedule shows the percentage of occupancy of the space. For instance, 75% of the classroom is occupied between 08:00 and 15:00, then the low density, which is 15%, is given until 20:00.

As explained before, the energy simulation was conducted based on the representative days. To ensure that all days are not within the holiday season, the same weekday schedule is assigned to each representative day. Additionally, the lighting and equipment schedules are adjusted in accordance with the occupancy schedules.

Table 3.8. *Zone schedule*

| Hours | Occupancy Schedule | Equipment Schedule | Lighting Schedule |
|---|---|---|---|
| 1 | 0 | 0.35 | 0.1773 |
| 2 | 0 | 0.35 | 0.1773 |
| 3 | 0 | 0.35 | 0.1773 |
| 4 | 0 | 0.35 | 0.1773 |
| 5 | 0 | 0.35 | 0.1773 |
| 6 | 0 | 0.35 | 0.1773 |
| 7 | 0 | 0.35 | 0.9 |
| 8 | 0.75 | 0.95 | 0.9 |
| 9 | 0.75 | 0.95 | 0.9 |
| 10 | 0.75 | 0.95 | 0.9 |
| 11 | 0.75 | 0.95 | 0.9 |
| 12 | 0.75 | 0.95 | 0.9 |
| 13 | 0.75 | 0.95 | 0.9 |
| 14 | 0.75 | 0.95 | 0.9 |
| 15 | 0.75 | 0.95 | 0.9 |
| 16 | 0.15 | 0.95 | 0.9 |
| 17 | 0.15 | 0.35 | 0.9 |
| 18 | 0.15 | 0.35 | 0.9 |
| 19 | 0.15 | 0.35 | 0.9 |
| 20 | 0.15 | 0.35 | 0.9 |
| 21 | 0 | 0.35 | 0.1773 |
| 22 | 0 | 0.35 | 0.1773 |
| 23 | 0 | 0.35 | 0.1773 |
| 24 | 0 | 0.35 | 0.1773 |

*Heating and cooling setpoints*

Setpoint air temperature indicates when the heating and cooling are required. Since there is not air conditioning system in the classrooms, the setpoint for cooling is defined as 100°C indoor air temperature, which means that the cooling system will never be activated. For the heating setpoint, the indoor air temperature is 21°C between 07:00 and 20:00; the other hours have 18°C when the heating starts.

*Zone construction materials*

Although EnergyPlus has default construction material library, it allows the users to make custom construction materials. Thickness, thermal conductivity, specific heat capacity, and density need to be assigned for custom materials. Thermal conductivity is a materials' ability to conduct heat. Specific heat capacity is the amount of heat energy required to raise the temperature of a substance per unit of mass

In order to determine glazing design, it is necessary to define the U-value, solar heat gain coefficient (SHGC), and visible transmittance. Window thermal insulation is determined by its U-value, and the lower the U-value, the better the window's thermal insulation. SHGC measures the transmission of heat from direct sunlight through a window. This range is 0 to 1, with a low SHGC providing effective solar control. The VT is the percentage of visible light transmitted through the glazing whose wavelength range is between 0 and 1 as SHGC (Akköse, 2019). The details for the construction materials can be seen in Table 3.9.

Table 3.9. *Construction and material details of the building (Akköse, 2019)*

| Building Elements | Details | Conductivity (W/mK) | Specific Heat Capacity (J/kgK) | Density (kg/m3) | Reference |
|---|---|---|---|---|---|
| External Wall | 90mm single layer of press-brick | 0.42 | 900 | 2240 | 1 |
| | 240mm single layer of brick | 0.33 | 900 | 600 | 1 |
| | 20-25mm one layer of plaster | 0.51 | 1090 | 1200 | 1 |
| Internal Wall | 190mm single layer of brick | 0.33 | 900 | 650 | 1 |
| | 20-25mm two layers of plaster | 0.51 | 1090 | 1200 | 1 |
| Roof | Gravel | 0.36 | 840 | 1840 | 1 |
| | Separation layer | - | - | - | - |
| | 3mm waterproofing membrane | 0.19 | 780 | 3000 | 1 |
| | 40mm levelling concrete | 0.3 | 840 | 2200 | 1 |
| | 200mm concrete slab | 2.5 | 840 | 2400 | 1 |
| | 20-25mm one layer of plaster | 0.51 | 1090 | 1200 | 1 |
| Floor | 10mm marble tile | 2.8 | 830 | 2680 | 2 |
| | 5mm levelling concrete | 0.41 | 840 | 1200 | 1 |
| | 200mm concrete slab | 2.5 | 840 | 2400 | 1 |
| Ground Floor | 50mm cement finish | 1.4 | 837 | 2000 | 1 |
| | 3mm polyester felt | 0.19 | 1500 | 25 | 1 |
| | 600mm XPS | 0.035 | 1200 | 25 | 1 |
| | 150mm groundwork | 2.5 | 860 | 2400 | 1 |
| | 100mm protective concrete | 1.65 | 860 | 2200 | 1 |
| | Waterproofing | 0.19 | 780 | 3000 | 1 |
| | 100mm blinding concrete | 1.65 | 860 | 2200 | 1 |
| | Gravel | 2 | 840 | 2000 | 1 |
| | | U Value (W/m2K) | Solar Heat Gain Coefficient | Visible Transmittance | |
| Window | 16mm double glazed | 2.7 | 0.80 | 0.8 | 3 |

Table 3.9 (continued)

| | |
|---|---|
| 1 | https://help.iesve.com/ve2021/table_6_thermal_conductivity__specific_heat_capacity_and_density.htm |
| 2 | Rohsenow, W. M., Hartnett, J. P., & Ganic, E. N. (1985). Handbook of heat transfer fundamentals. |
| 3 | https://duzcam.sisecam.com/tr/mimari-camlar/profesyoneller-icin-urun-katalogu/isicam-sistemleri-c-serisi |

*Ventilation system*

In order to simulate indoor thermal comfort and energy efficiency, the ventilation system must be included in the simulation model. All classrooms are equipped with operable windows and natural ventilation systems. Natural airflow is calculated based on the fraction of operable windows and the height of the buildings. The windows are opened as soon as the indoor air temperature reaches the minimum indoor air temperature, which is 23.5°C, as shown in Table 3.10.

Table 3.10. *The natural ventilation parameters*

| | Natural Ventilated Zones |
|---|---|
| Minimum indoor temperature (°C) | 23.5 |
| Maximum indoor temperature (°C) | - |
| Minimum outdoor temperature (°C) | 12 |
| The fraction of operable glazing (%) | 0.3 |
| The fraction of operable glazing height (%) | 100 |

*Contextual shading elements*

As part of the thesis, the shading objects are trees and the building itself, as each room is investigated separately, so contextual shading has a significant impact on building energy and thermal performance. Additionally, due to the fact that the selected tree type is not evergreen, the schedule of leaf growth has been introduced to the model.

### 3.5.2 Energyplus Simulation Model for the Mitigation Scenarios

It is repeated for each mitigation scenario for each classroom with some small changes based on the interventions outlined in Table 3.6. For example, in the cool pavement' energy simulation, the ground floor reflectiveness is 0.8 instead of 0.3 in the baseline simulation. There are 16 classrooms and 6 mitigation scenarios, so the Energyplus simulations are run 96 times. For each mitigation, a new EPW file is generated.

## 3.6 Physiological Equivalent Temperature (PET) Simulations

Several thermal comfort metrics have been discussed in the literature, including physiological equivalent temperatures (PET). Due to its ability to customize metabolic rates for children in a schoolyard environment, the physiological equivalent temperature (PET) method is used to measure outdoor thermal comfort.

### 3.6.1 Simulation Inputs

PET is considered that air temperature, relative humidity, wind speed, mean radiant temperature (MRT), metabolic rate, as well as personal characteristics are input variables for the PET index (Dimitrios Antoniadis et al., 2020). For calculating the metabolic rate, the age, weight, and height of a person must be defined. In this thesis, Table 3.11 shows the differences in inputs between an average adult and a primary school child.

Table 3.11. *Metabolic rate variables*

| Inputs | Adult | Child |
|---|---|---|
| Age | 35 | 10 |
| Weight (kg) | 75 | 35 |
| Height (m) | 1.75 | 1.40 |
| Total metabolic rate ($W/m^2$) | 86.21 | 113.28 |

Physical disparities affect the perception of temperature and make children more vulnerable on hot days, since children have higher metabolic rates, their skin temperature rises quickly when exercising, and their sweat rate is lower. (Balbus & Malina, 2009; Cheng & Brown, 2020).

### 3.6.2 BioMet

As part of ENVI-met, PET is calculated using Bio-Met, a tool that calculates various human thermal comfort indexes from ENVI-met model files. This task obviously requires a number of ENVI-met atmospheric output files such air temperature, MRT, relative humidity, and wind speed in order to achieve it.

In the following chapter, the results of outdoor thermal comfort simulations for 12 months will be discussed after ENVI-met simulations of the baseline and mitigation scenarios are completed.

# CHAPTER 4

# RESULTS

The previous chapter described a methodology for developing new weather files based on various scenarios, as well as parameters of energy simulations. As part of the goal of improving the energy and comfort conditions of the existing school, this chapter examines the impact of scenarios as UHI mitigation. The results of potential intervention scenarios, as well as a performance assessment, will be discussed.

## 4.1 Comparison of UHI Modified Weather File and the Weather Station File for the Baseline

As discussed in the literature review, the weather files that are used for energy and thermal comfort calculations do not consider urban parameters. The weather data, therefore, are collected from rural areas or airport stations where the effect of UHI is absent. It is necessary to calculate the UHI effect in this study by using statistical weather data files in .epw format. The weather file has 8760 hourly data, and modifying all year is expensive in a time manner. Therefore, 12 representative days are selected for each month and the air temperature values are changed with ENVI-Met simulation outputs. The hourly air temperature data from 16 receptors is extracted and compared with the weather station data for each representative day to analyze UHI effect. Only first level receptors are selected to compare with the baseline because the air temperature difference between levels is negligible.

Moreover, ENVI-Met is not very sensitive to minus degrees based on previous studies in the literature, which means that the results for winter and fall are a bit overrated due to the limitations of ENVI-Met.

*Winter*

The measurements shown in Table 4.1 indicate a 4–5 °C difference between the site area (BL), and the rural areas (EPW) in Ankara during winter as a result of UHI. Even though the air temperature drops after sunset, the stored heat cannot be released to the atmosphere because of the urban canopy. Therefore, the air temperature during the night is higher than in rural areas. Appendix C shows more in detail.

Table 4.1. *UHI effect in winter*

| | **31st December** | **5th January** | **23rd February** |
|---|---|---|---|
| **a1** | 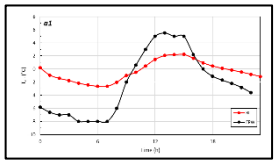 | 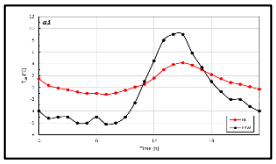 | 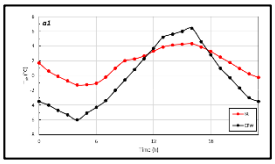 |
| **b1** | 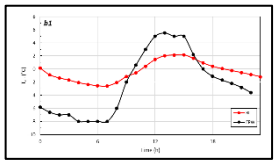 | 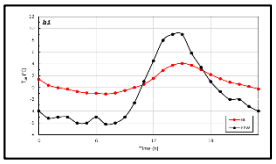 | 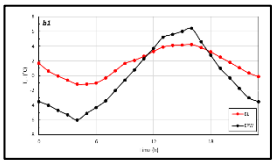 |
| **c1** | 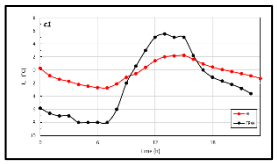 | 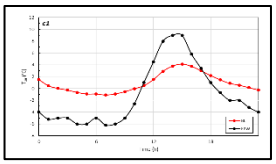 | 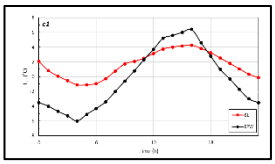 |
| **d1** | 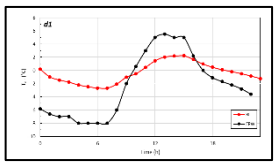 | 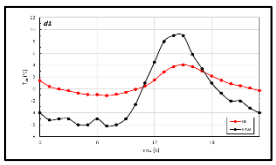 | 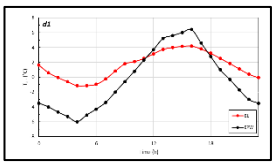 |
| **e1** | 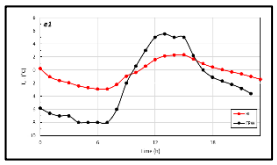 | 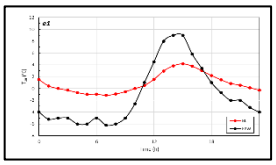 | 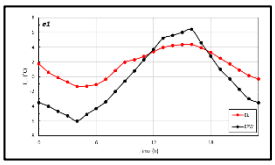 |
| **f1** | 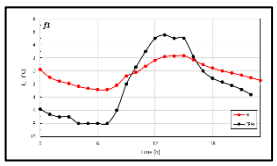 | 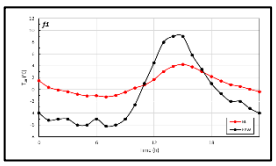 | 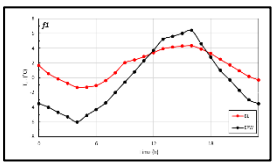 |

*Spring*

In the spring, the difference in air temperature between Baseline and EPW decreases when compared with winter. According to Table 4.2, this difference in air temperature decreases from 3-4 °C in March to 1-2 °C in May. Appendix C shows more in detail.

Table 4.2. *UHI effect in spring*

| | **22nd March** | **5th April** | **23rd May** |
|---|---|---|---|
| **a1** | 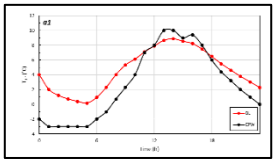 | 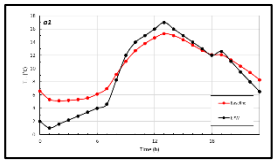 | 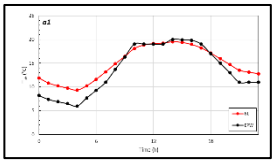 |
| **b1** | 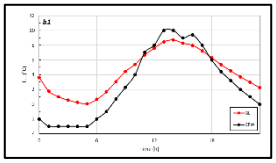 | 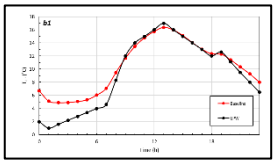 | 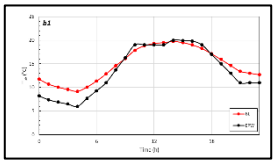 |
| **c1** | 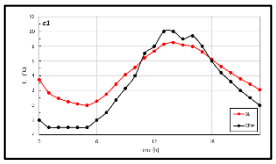 | 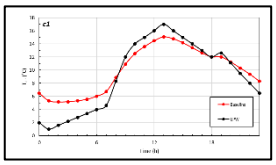 | 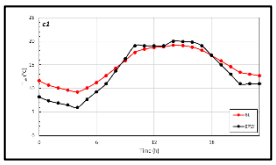 |
| **d1** | 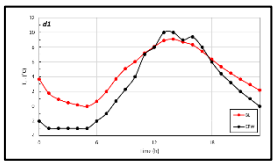 | 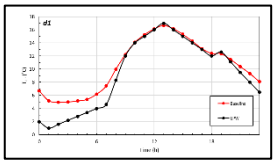 | 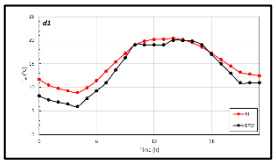 |
| **e1** | 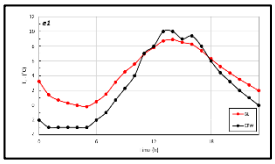 | 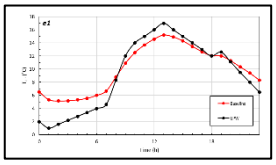 | 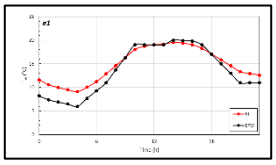 |
| **f1** | 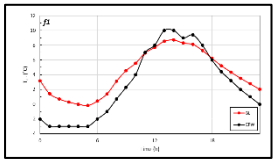 | 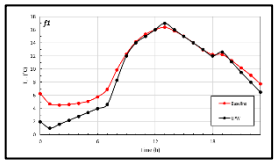 | 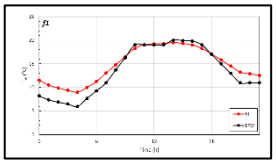 |

*Summer*

In summer, the air temperature difference during the night is approximately 3-4°C as shown in Table 4.3. In the evenings, the Baseline air temperature drops below EPW, but increases during the night. In consequence, city centers are unable to cool down themselves before the sun rises up again as a result of this situation. Appendix C shows more in detail.

Table 4.3. *UHI effect in summer*

| | **21st June** | **31st July** | **17th August** |
|---|---|---|---|
| **a1** | 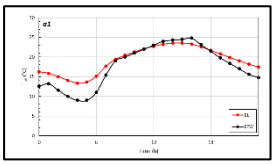 | 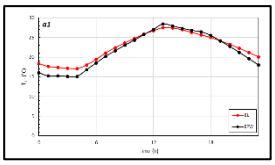 | 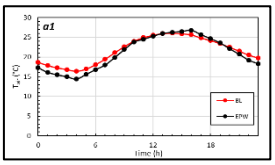 |
| **b1** | 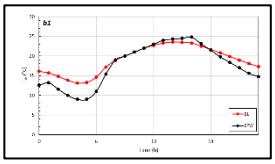 | 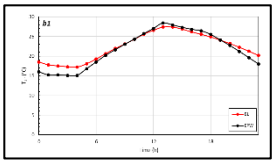 | 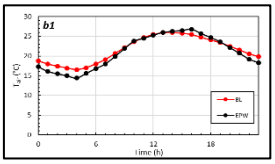 |
| **c1** | 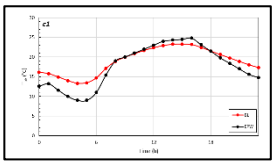 | 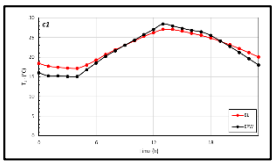 | 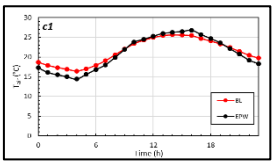 |
| **d1** | 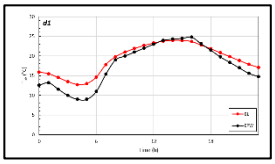 | 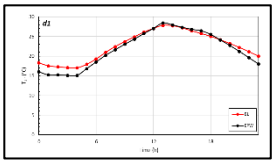 | 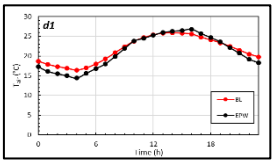 |
| **e1** | 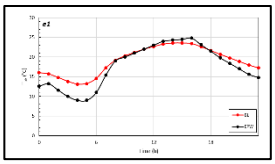 | 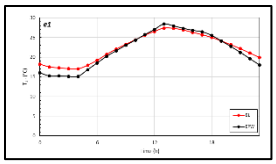 | 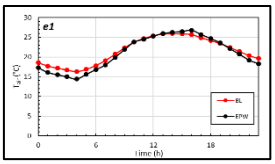 |
| **f1** | 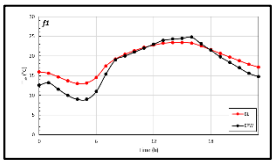 | 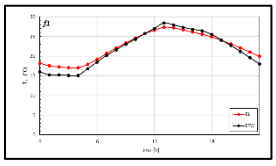 | 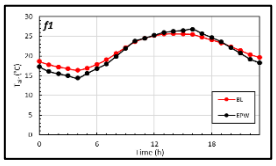 |

*Fall*

There is a temperature difference of 2-3°C during the night in fall. However, there may be a difference of up to 5°C between Baseline and the rural area. Appendix C shows more in detail.

Table 4.4. *UHI effect in fall*

| | **21st September** | **9th October** | **16th November** |
|---|---|---|---|
| **a1** | 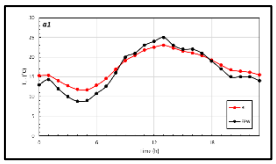 | 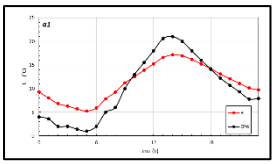 | 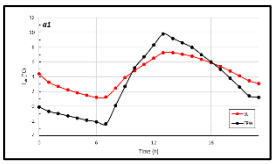 |
| **b1** | 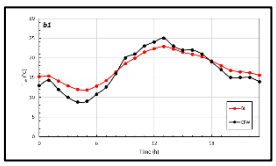 | 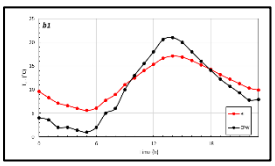 | 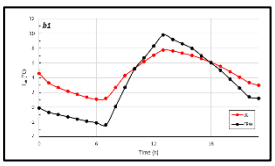 |
| **c1** | 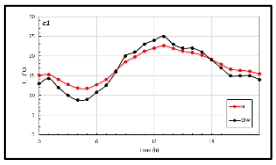 | 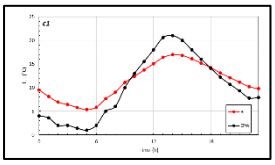 | 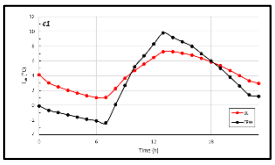 |
| **d1** | 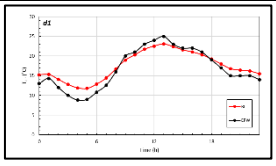 | 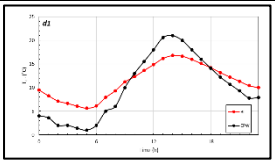 | 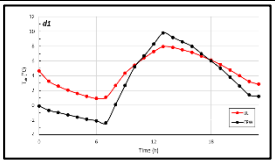 |
| **e1** | 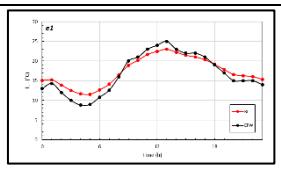 | 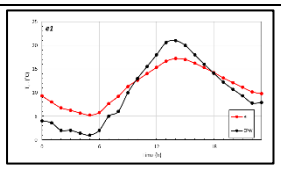 | 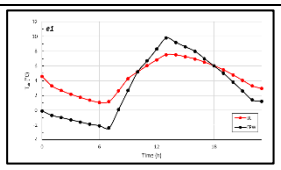 |
| **f1** | 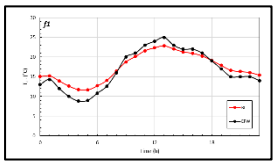 | 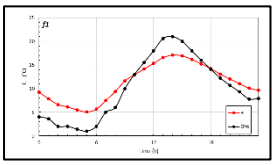 | 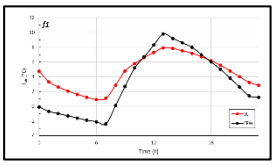 |

## 4.2 Impact of Scenarios on Air Temperature

Six different UHI mitigation scenarios are evaluated using the classroom's receptor hourly air temperature data over 12 representative days.

*Cool Pavement Scenario (CP)*

The parameters of the Cool Pavement scenario are the same as those of the baseline scenario, but the pavement material differs. As previously explained, the ground floor material of the schoolyard will be replaced with a material with a high albedo (0.8), known as light concrete pavement.

Considering the air temperature data of each receptor for all scenarios, the cool pavement scenario represents the best scenario for reducing air temperature among other possible scenarios. Table 4.5 indicates that the impact of the cool pavement is greatest on the first floor and gradually diminishes for the upper floors. The highest levels are found in classroom A receptors as a result of exposure to a large area of cool pavement. Furthermore, it decreases the air temperature between 12pm and 14pm by 0.6-0.8°C.

Table 4.5. *Cool Pavement receptors' air temperature data*

| **a1** | **a2** | **a3** |
|---|---|---|
| 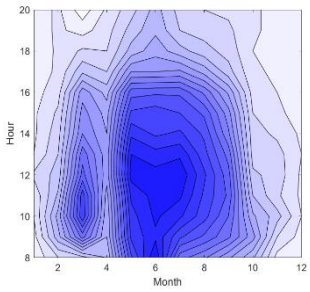 | 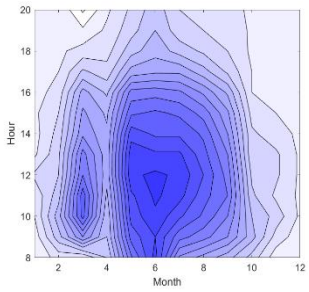 | 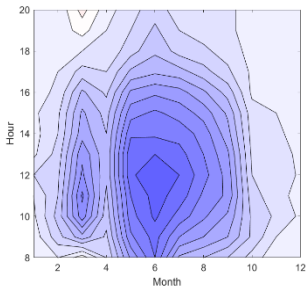 |
| **b1** | **b2** | **b3** |
| 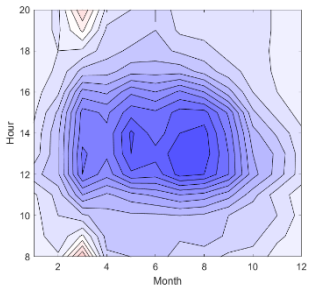 | 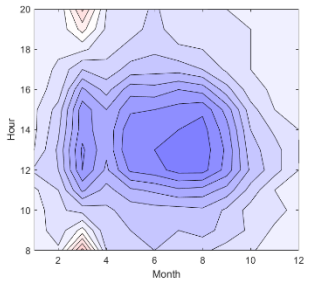 | 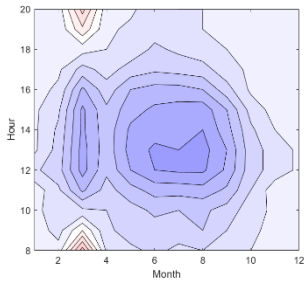 |
| **c1** | **c2** | **c3** |
| 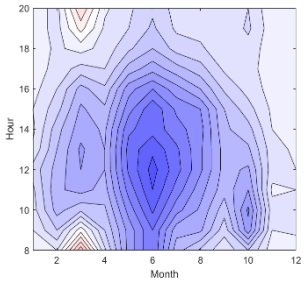 | 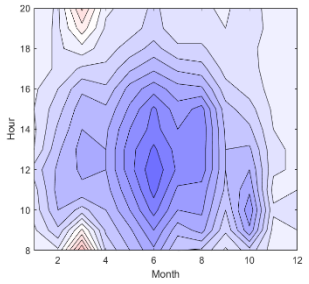 | 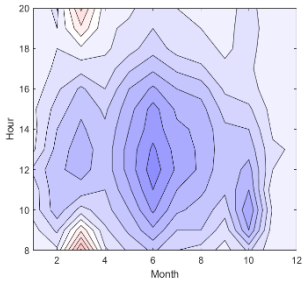 |

Table 4.5 (continued)

| d1 | d2 | d3 |
|---|---|---|
| 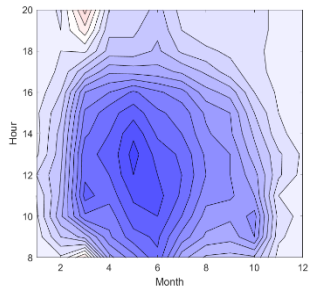 | 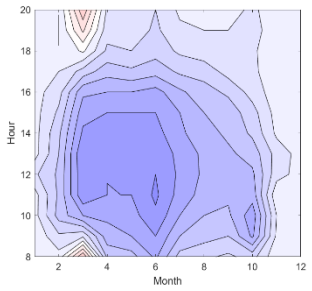 | 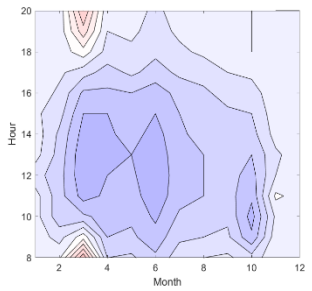 |
| **e1** | **e2** | |
| 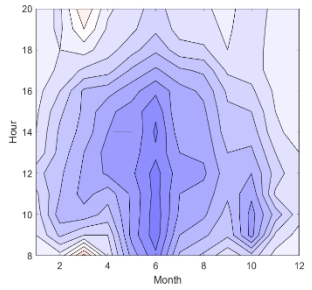 | 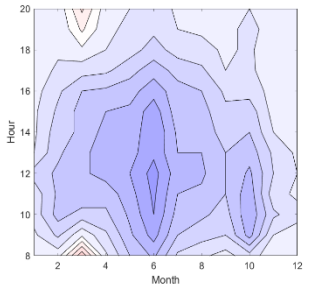 | 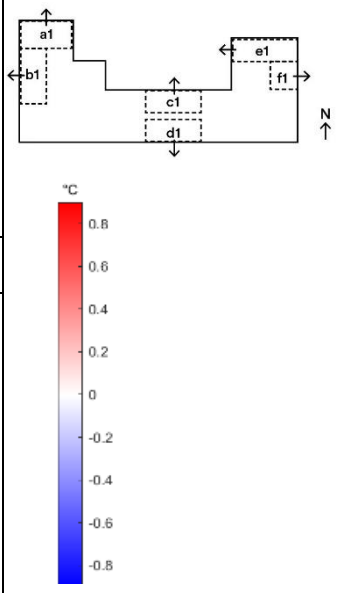 |
| **f1** | **f2** | |
| 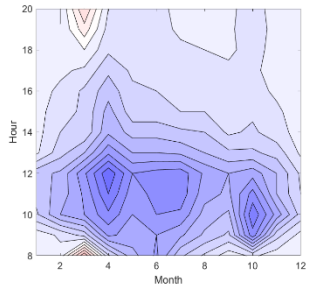 | 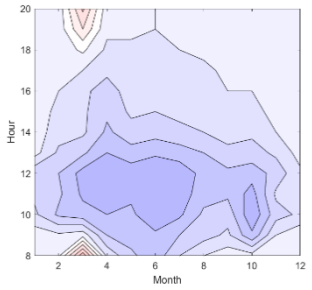 | |

*Green Scenario (GR)*

The Green scenario has more trees around the schoolyard. The other parameters were not changed and kept as same in the Baseline. The number of trees is multiplied 4 times by the current amount that there are 16 trees in four different directions in the schoolyard in this scenario.

Classroom A, C and E in three floors are the less affected rooms due to their locations. The addition trees are not right in front of these classrooms therefore, the impact of green scenario is not as significant as in other classrooms such as classroom D, B and F in three floors. The dense trees cast shadow over these classrooms' windows. Thus, trees can decrease the air temperature more than 0.8°C between 14 pm and 16pm during spring and summer. However, the cooling effect decreases for upper levels due to the less shadow.

Moreover, trees help to increase air temperature during fall and winter. A study in the literature shows that cooling air temperature by trees in cool seasons is considerably smaller than hot seasons, and trees can even warming the air up during day time (Meili et al., 2021).

Table 4.6. *Green receptors' air temperature data*

| **a1** | **a2** | **a3** |
|---|---|---|
| 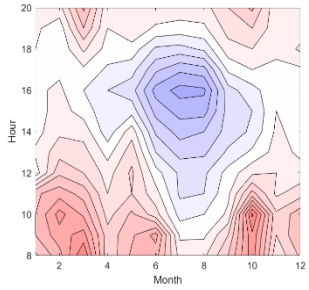 | 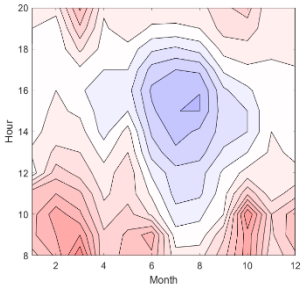 | 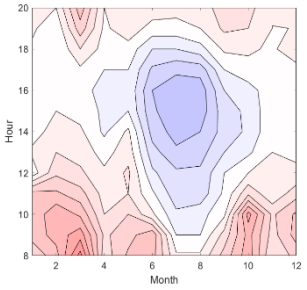 |
| **b1** | **b2** | **b3** |
| 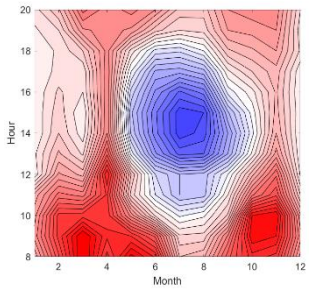 | 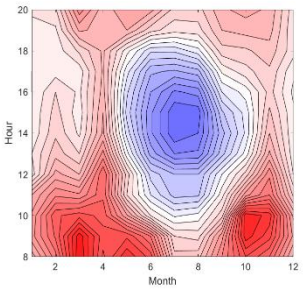 | 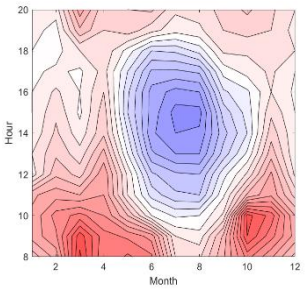 |
| **c1** | **c2** | **c3** |
| 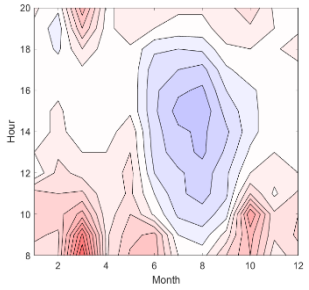 | 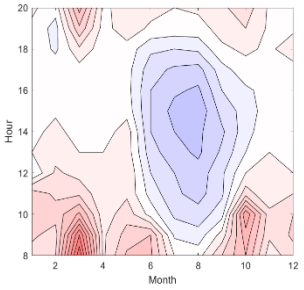 | 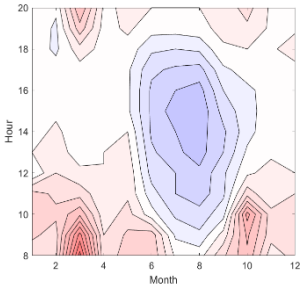 |

Table 4.6 (continued)

| d1 | d2 | d3 |
|---|---|---|
| 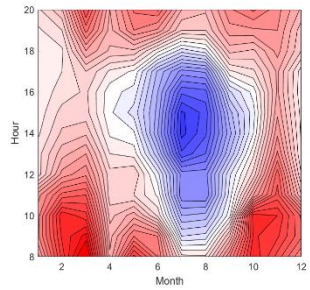 | 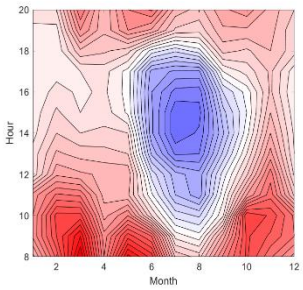 | 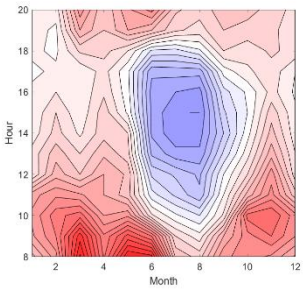 |
| **e1** | **e2** | |
| 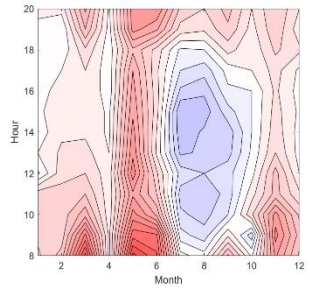 | 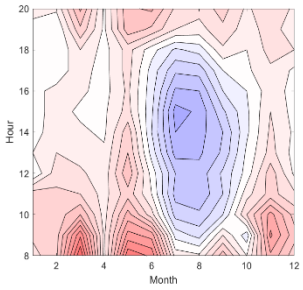 | 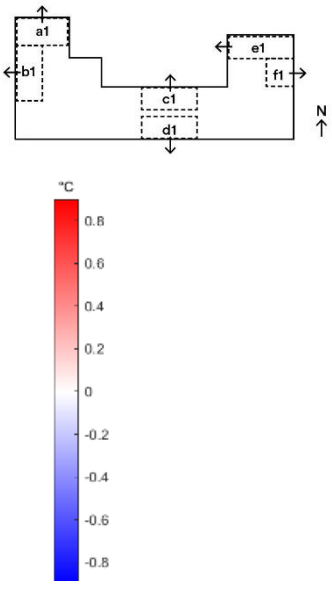 |
| **f1** | **f2** | |
| 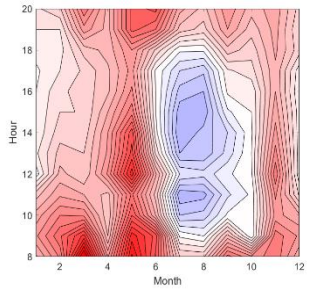 | 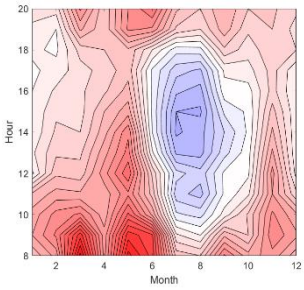 | |

*Cool Facade (CF)*

The Cool Facade scenario has the same schoolyard floor material and the amount of vegetation as the Baseline; however, it differs in the facade material in the light color plaster with 0.6 albedo is replaced with the 0.3 albedo plaster.

It is the least effective intervention to decrease the air temperature among other scenarios. However, Cool Façade scenario can reduce 0.1-0.2°C.

Classroom B and D in three levels that are facing to west and south respectively. They get benefit cool façade from February to April; November to December between 12pm and 16pm.

Table 4.7. *Cool Facade receptors' air temperature data*

| **a1** | **a2** | **a3** |
|---|---|---|
| 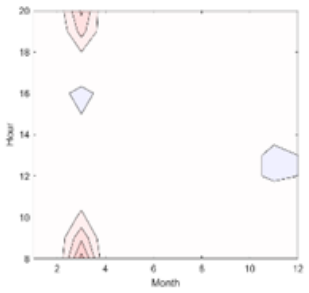 | 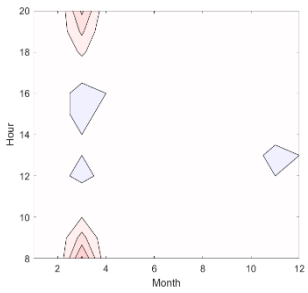 | 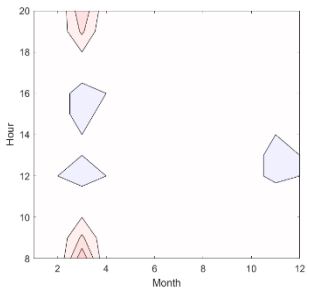 |
| **b1** | **b2** | **b3** |
| 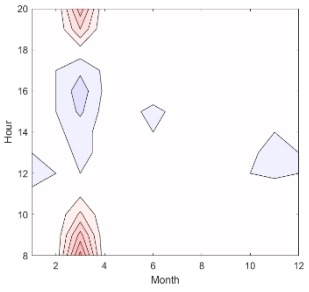 | 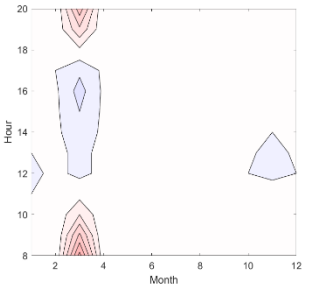 | 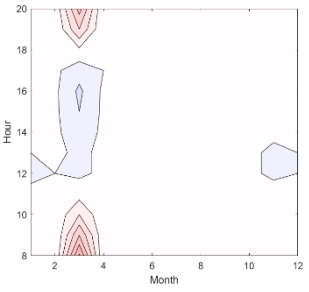 |

Table 4.7 (continued)

| c1 | c2 | c3 |
|---|---|---|
| 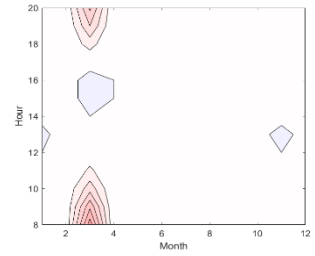 | 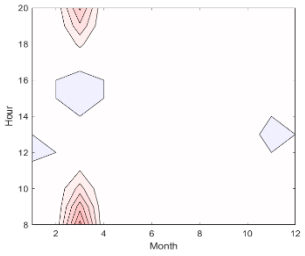 | 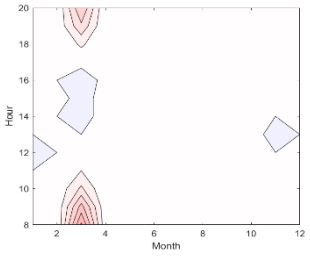 |
| **d1** | **d2** | **d3** |
| 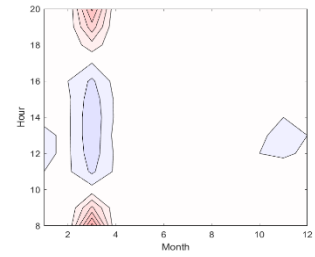 | 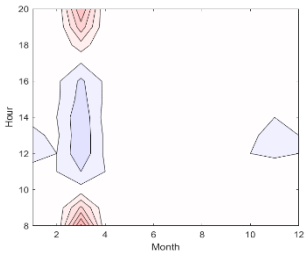 | 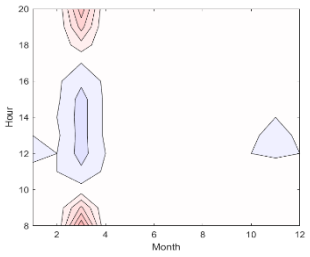 |
| **e1** | **e2** | 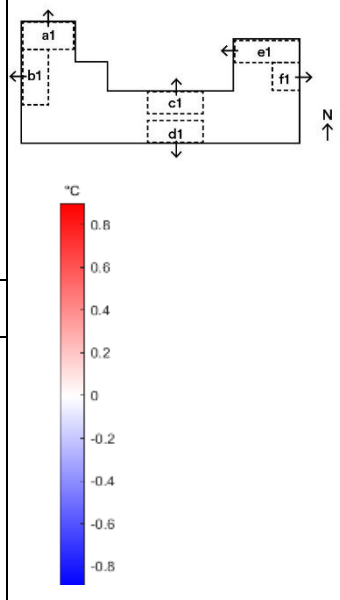 |
| 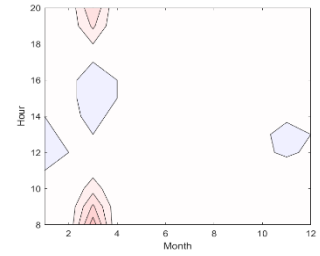 | 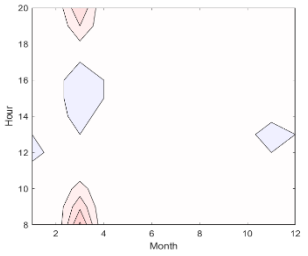 | |
| **f1** | **f2** | |
| 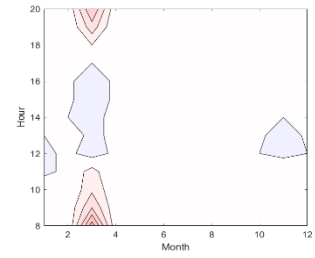 | 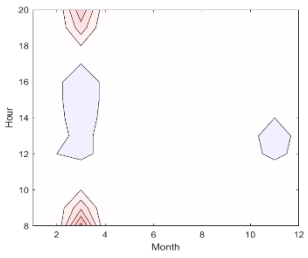 | |

*Cool Façade + Green (CFGR)*

The Cool Facade + Green intervention has the same schoolyard floor material with 0.3 albedo. The building facade material is replaced with the 0.6 albedo material and has 4 times more trees in the schoolyard.

CFGR results are similar to Green scenario because the impact of Cool Façade on air temperature is negligible.

Table 4.8. *Cool Façade + Green receptors' air temperature data*

| **a1** | **a2** | **a3** |
|---|---|---|
| 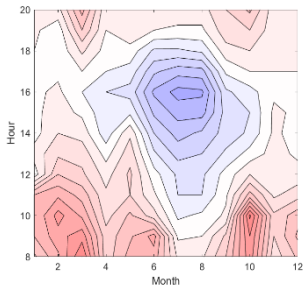 | 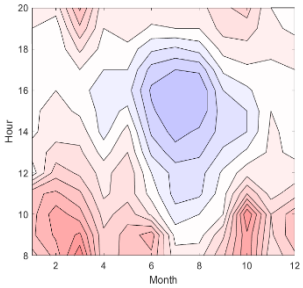 | 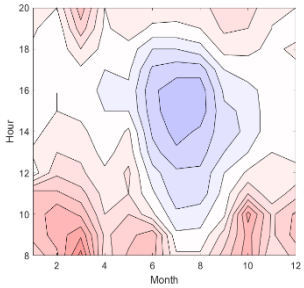 |
| **b1** | **b2** | **b3** |
| 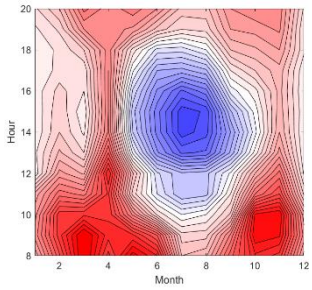 | 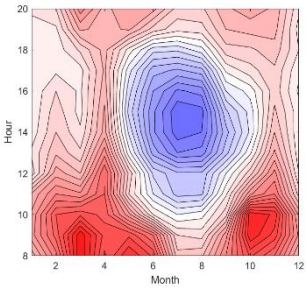 | 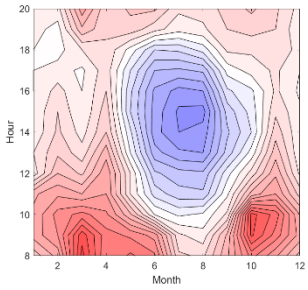 |

Table 4.8 (continued)

| c1 | c2 | c3 |
|---|---|---|
| 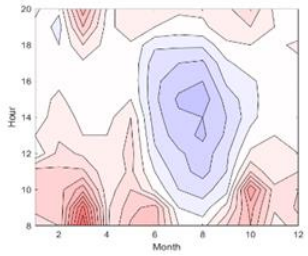 | 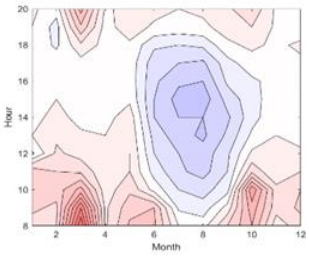 | 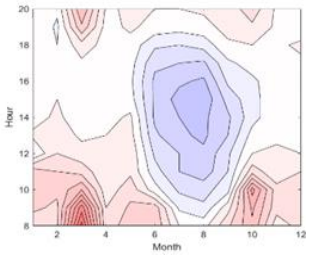 |
| **d1** | **d2** | **d3** |
| 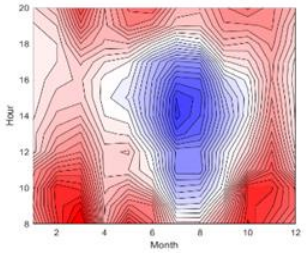 | 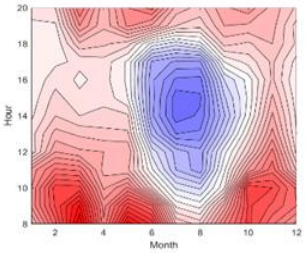 | 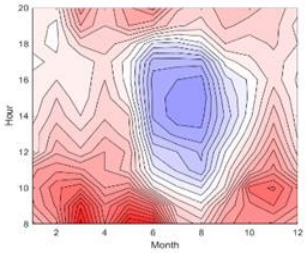 |
| **e1** | **e2** | |
| 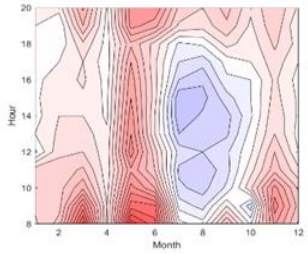 | 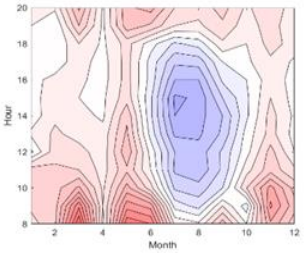 | 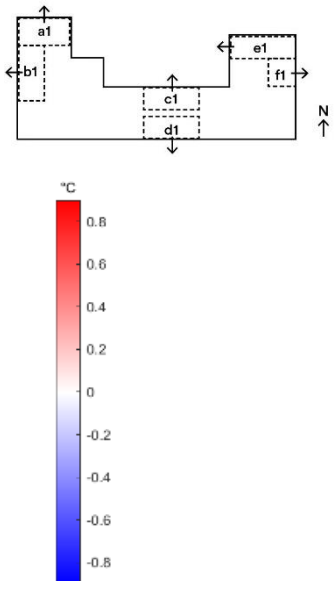 |
| **f1** | **f2** | |
| 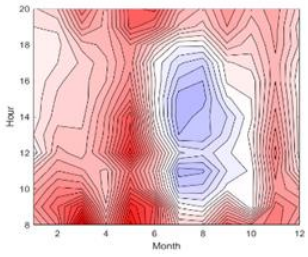 | 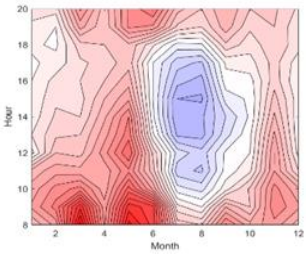 | |

*Cool Pavement + Green (CPGR)*

The Cool Pavement + Green intervention has light material with 0.8 albedo on the schoolyard floor rather than high albedo facade plaster. The building's facade plaster albedo, 0.3, is the same as in the Baseline. In addition, it has 16 trees in the schoolyard.

CPGR scenario results are similar to those of the Green scenario; however, its impact is more extensive throughout the year. Green scenario can reduce air temperature up to 0.8°C between May and August during daytime; however, CPGR scenario can decrease air temperature throughout the year, not just in the spring and summer. The impact of this phenomenon can also be observed between February and April, and in early autumn.

There is a significant temperature drop in classrooms C and A in three levels due to the large amount of cool pavement exposed to them, as well as the fact that they are not very close to trees that create heat traps at night.

Table 4.9. *Cool Pavement + Green receptors' air temperature data*

| **a1** | **a2** | **a3** |
|---|---|---|
| 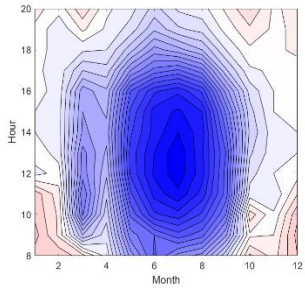 | 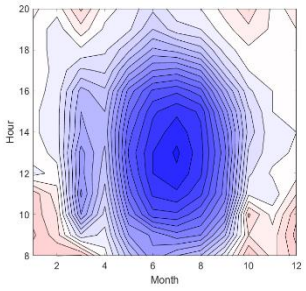 | 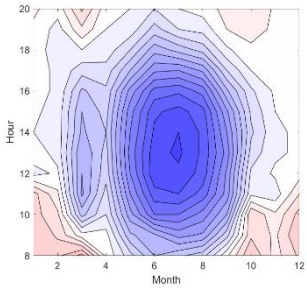 |
| **b1** | **b2** | **b3** |
| 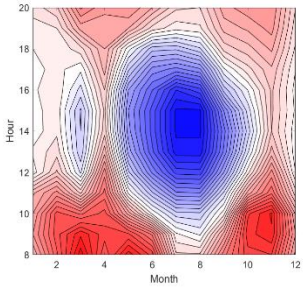 | 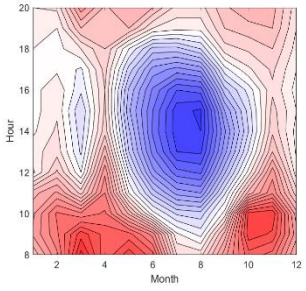 | 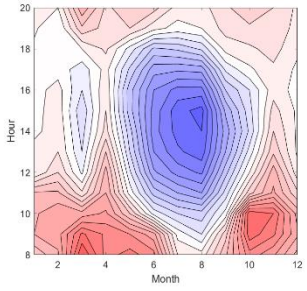 |
| **c1** | **c2** | **c3** |
| 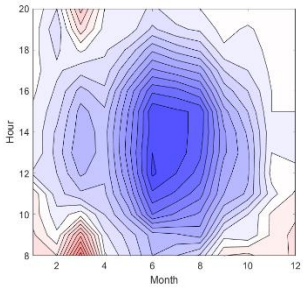 | 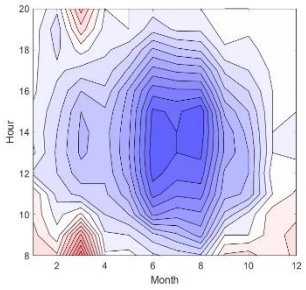 | 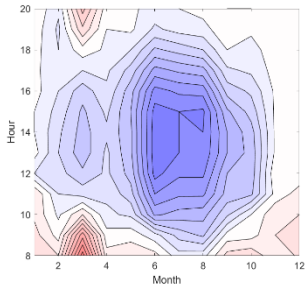 |

Table 4.9 (continued)

| d1 | d2 | d3 |
|---|---|---|
| 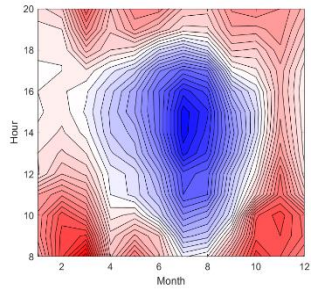 | 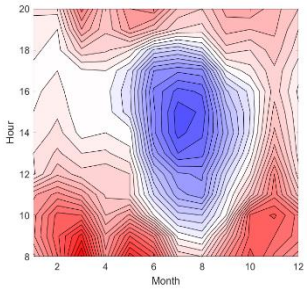 | 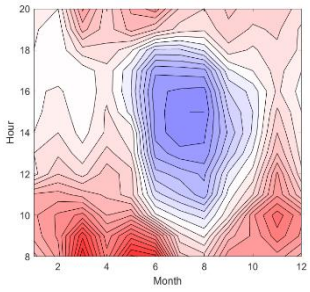 |
| **e1** | **e2** | |
| 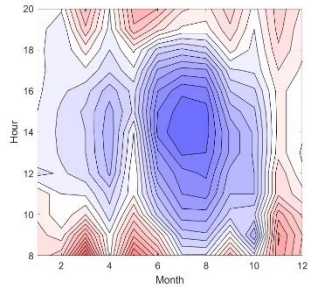 | 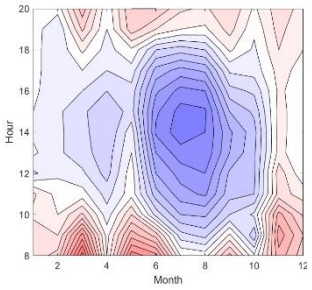 | 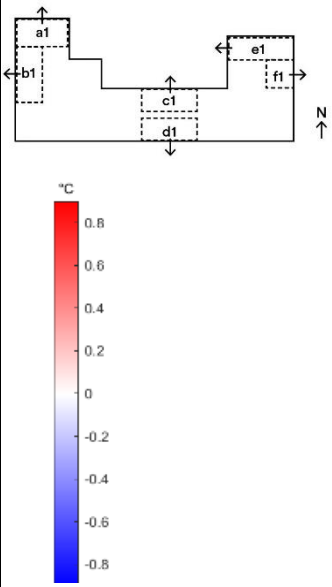 |
| **f1** | **f2** | |
| 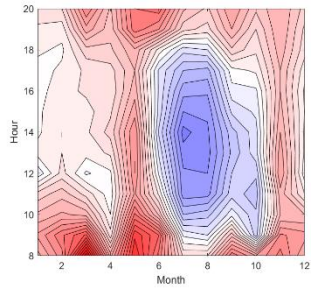 | 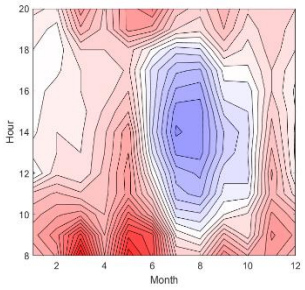 | |

*Cool Façade + Cool Pavement + Green (CFCPGR)*

This last scenario contains three different scenarios, with high albedo materials overlaying both the facade (0.6) and the schoolyard floor (0.8), and more greenery at the same time. According to Table 4.10, the results are similar to Cool Pavement + Green scenario due to the insignificant impact of the cool façade.

Table 4.10. *Cool Façade +Cool Pavement+ Green receptors' air temperature data*

| **a1** | **a2** | **a3** |
|---|---|---|
| 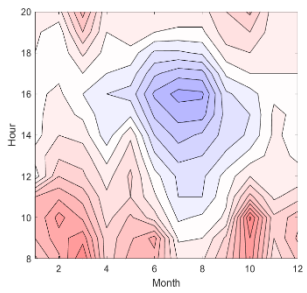 | 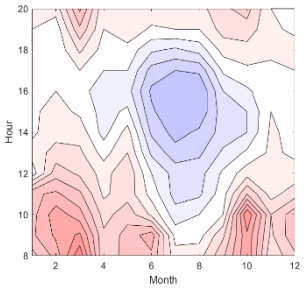 | 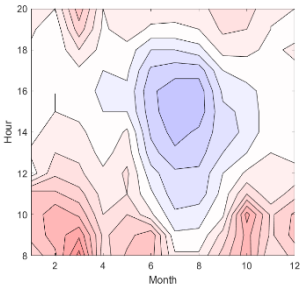 |
| **b1** | **b2** | **b3** |
| 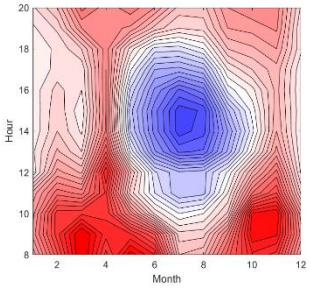 | 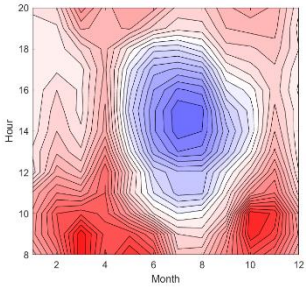 | 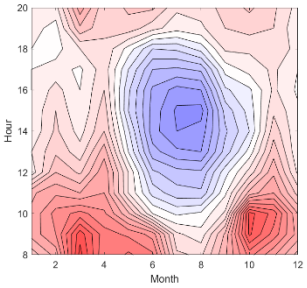 |

Table 4.10 (continued)

| c1 | c2 | c3 |
|---|---|---|
| 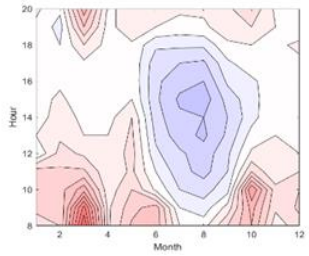 | 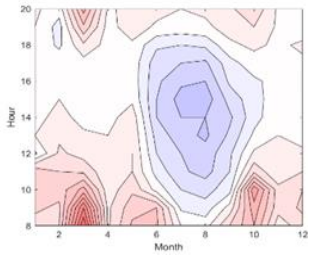 | 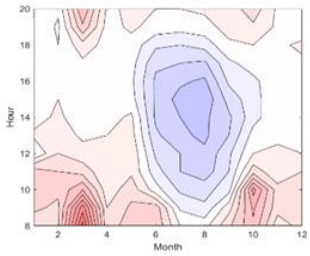 |
| **d1** | **d2** | **d3** |
| 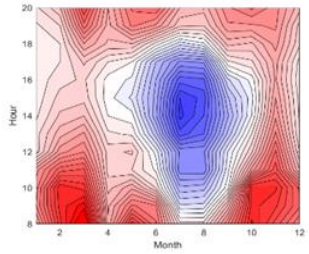 | 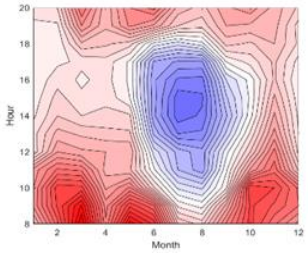 | 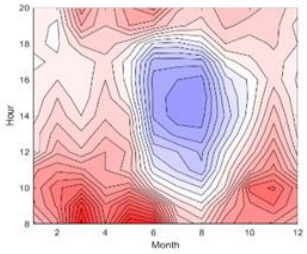 |
| **e1** | **e2** | 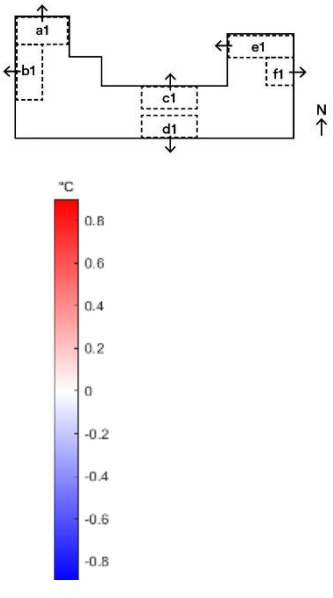 |
| 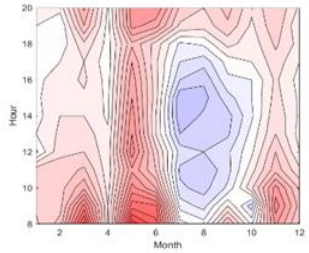 | 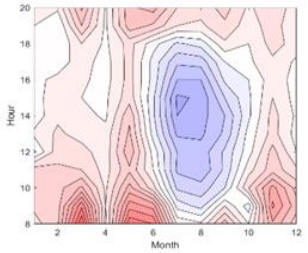 | |
| **f1** | **f2** | |
| 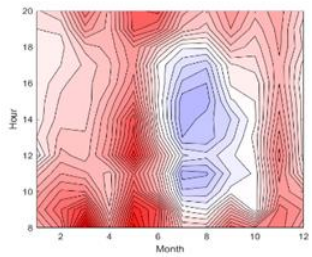 | 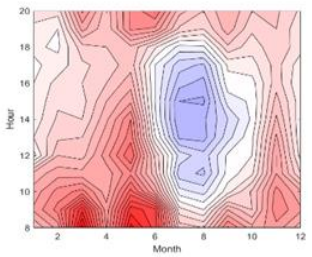 | |

## 4.3 Impact of Scenarios on Indoor Overheating Degrees (IODs)

Six different UHI mitigation scenarios are evaluated using each classroom's IODs over 12 representative days.

*Cool Pavement Scenario (CP)*

Using a cool pavement, it is evident that indoor overheating degrees have increased due to solar reflection toward the facade from the ground. Its effect diminishes when solar reflection reaches the upper floors less.

Between 12 p.m. and 13 p.m. during the summer, it is particularly useful for classrooms A and B on the first floor, while classrooms D and F are adversely affected by the cool pavement. A and B have a 0.2°C decrease in IOD as compared to the baseline. However, D and F have a 0.2-0.4°C increase. The reason is that A and B have under the shadow between 12 p.m. and 13 p.m.

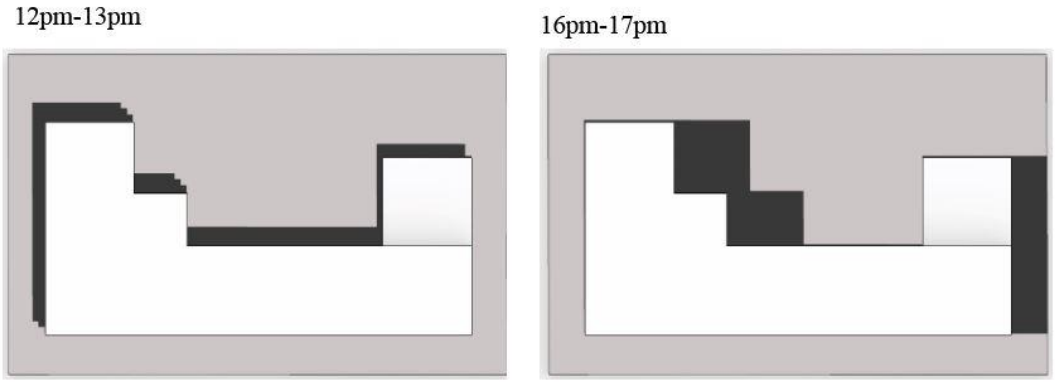


*Figure 4.1.* Shadow studies in different times during summer

In this regard, classrooms C and E are also under the shadow at the time as A and B. However, they are exposed by the more reflective hard surface causing overheating.

Table 4.11. *Cool Pavement IODs*

| **a1** | **a2** | **a3** |
|---|---|---|
| 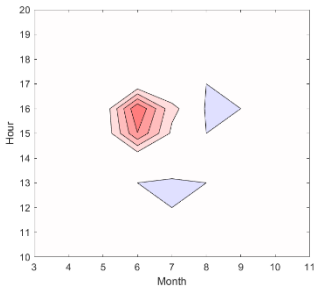 | 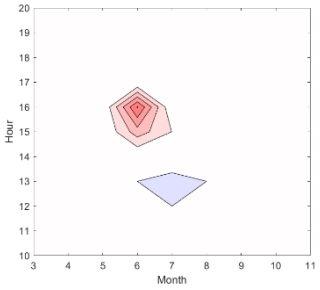 | 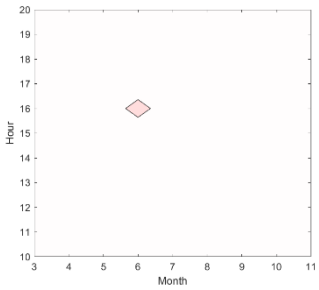 |
| **b1** | **b2** | **b3** |
| 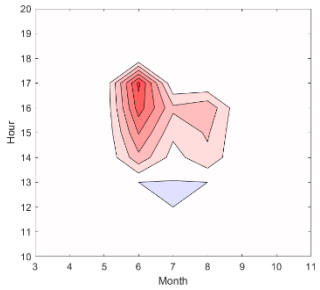 | 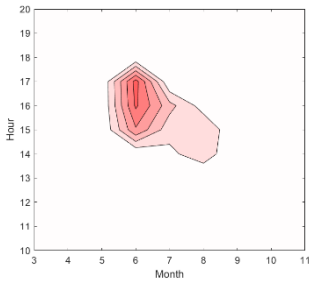 | 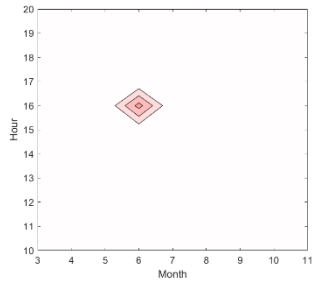 |
| **c1** | **c2** | **c3** |
| 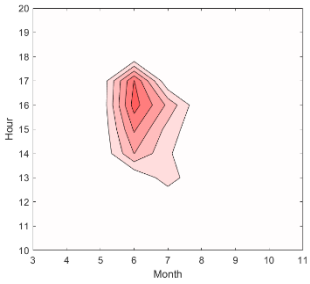 | 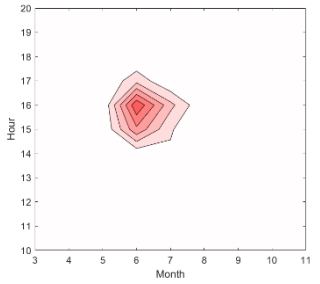 | 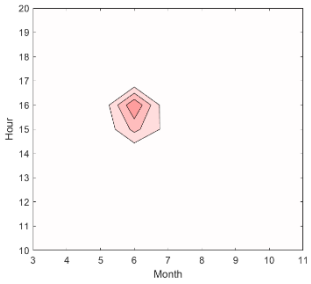 |

Table 4.11 (continued)

| d1 | d2 | d3 |
|---|---|---|
| 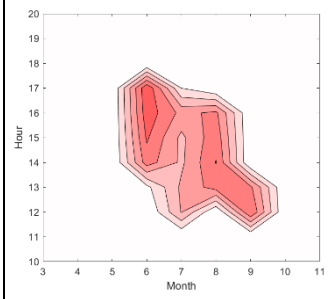 | 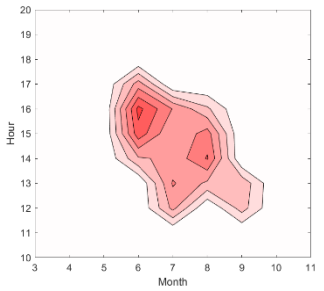 | 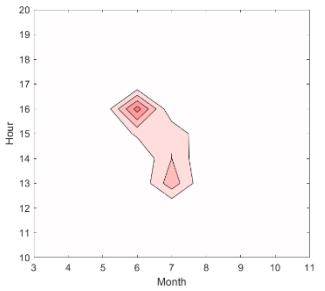 |
| **e1** | **e2** | |
| 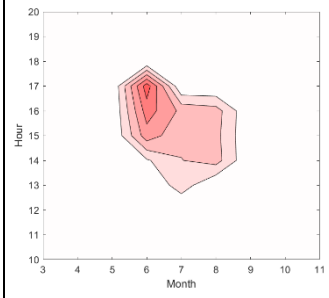 | 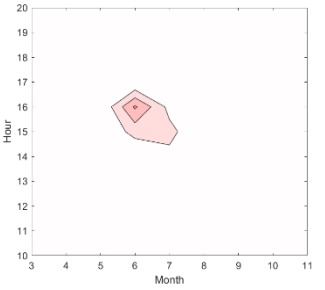 | 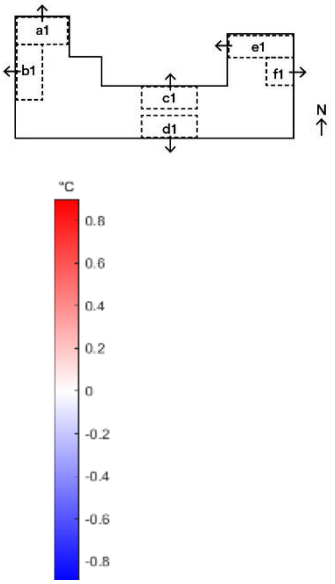 |
| **f1** | **f2** | |
| 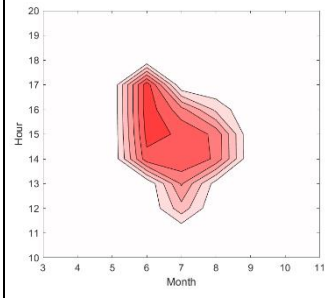 | 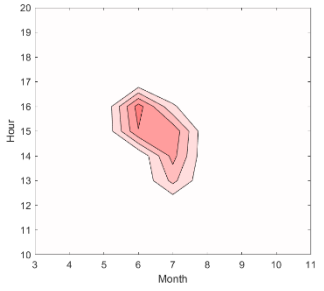 | |

*Cool Façade Scenario (CF)*

In comparison to a Cool Pavement scenario, a Cool Facade is an effective method of decreasing indoor overheating. According to the literature, high reflective materials reflect solar radiation and keep the surface cool. As a result of the cool facade scenario, in this thesis, the indoor temperature can be reduced by up to 0.8C.

On the south facade of Classroom D, the impact of the cool facade can be more clearly observed due to the greater reflection of radiation.

Table 4.12. *Cool Façade IODs*

| **a1** | **a2** | **a3** |
|---|---|---|
| 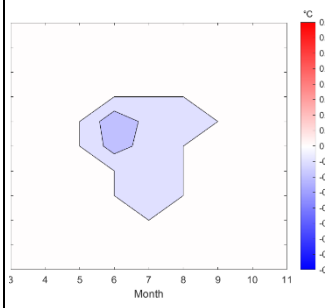 | 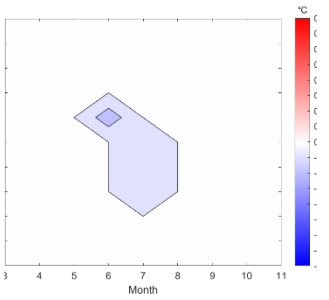 | 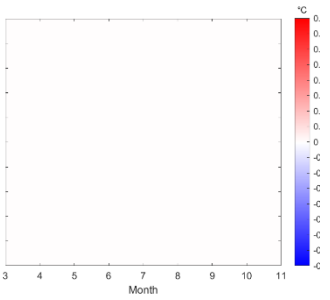 |
| **b1** | **b2** | **b3** |
| 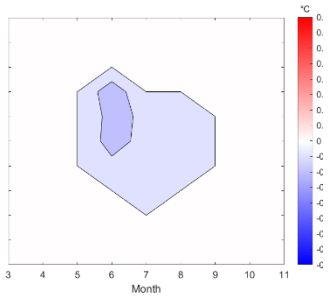 | 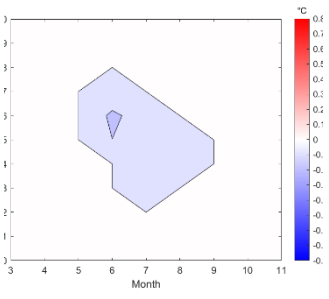 | 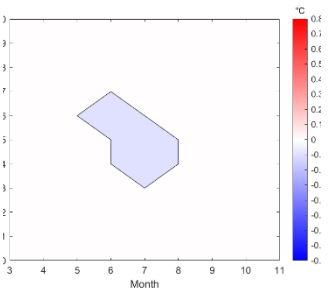 |

Table 4.12 (continued)

| c1 | c2 | c3 |
|---|---|---|
| 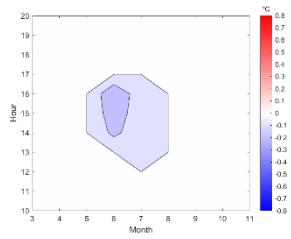 | 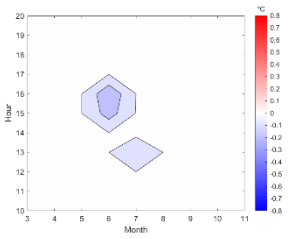 | 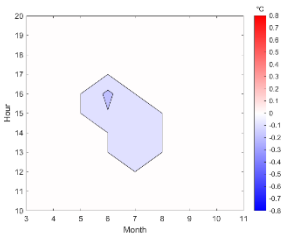 |
| **d1** | **d2** | **d3** |
| 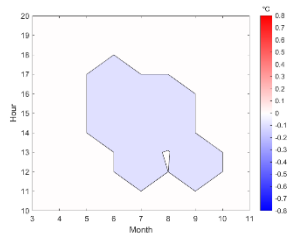 | 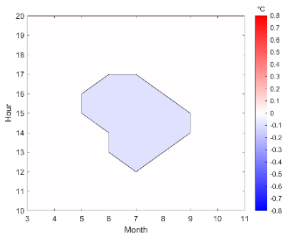 | 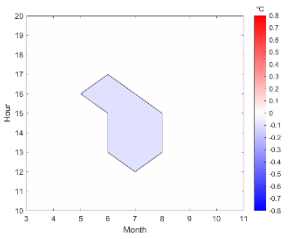 |
| **e1** | **e2** | |
| 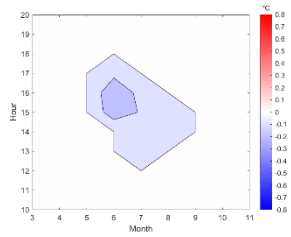 | 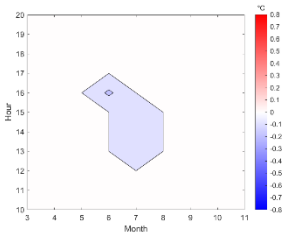 | 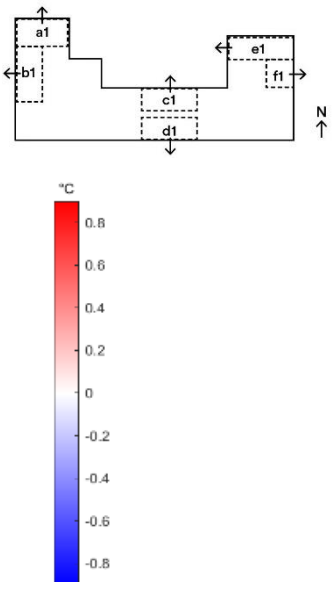  |
| **f1** | **f2** | |
| 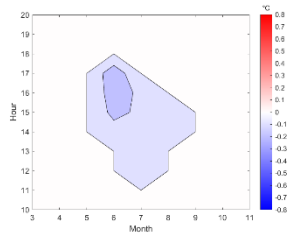 | 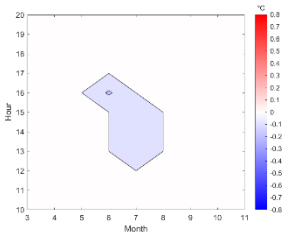 | |

*Green Scenario (GR)*

It has been demonstrated that greenery casts shadows on windows and decreases overheating. As a result, classrooms D and B experienced a greater drop in temperature between the hours of 13 p.m. and 15 p.m. during the summer compared to other classrooms. Due to the short distance of trees to these two rooms and the lack of shadow cast by the building, the impact is more apparent.

Table 4.13. *Green IODs*

| **a1** | **a2** | **a3** |
|---|---|---|
| 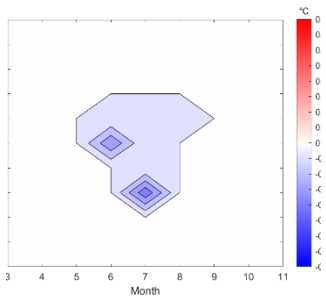 | 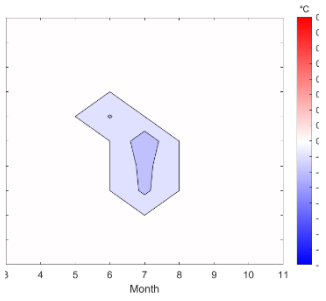 | 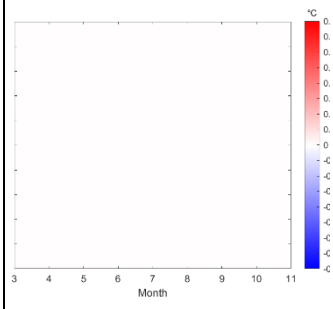 |
| **b1** | **b2** | **b3** |
| 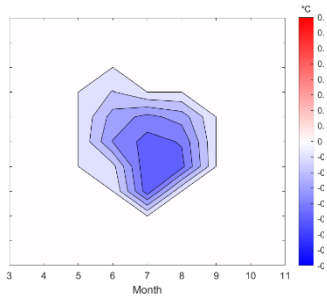 | 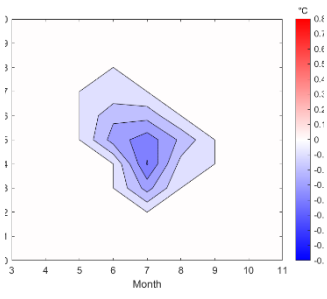 | 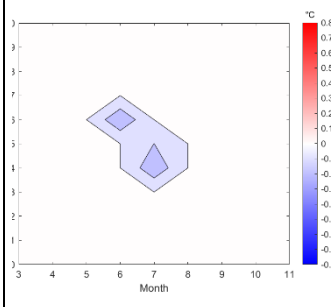 |

Table 4.13 (continued)

| d1 | d2 | d3 |
|---|---|---|
| 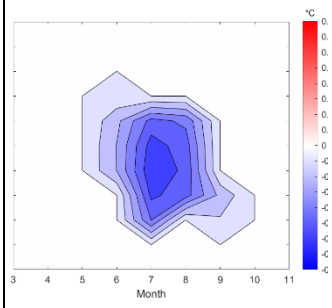 | 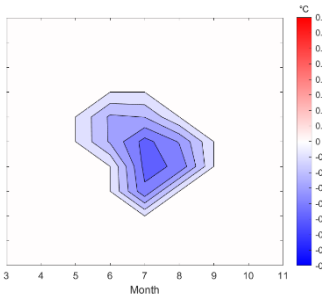 | 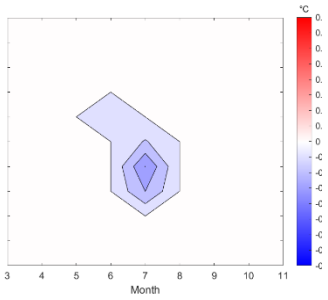 |
| **e1** | **e2** | |
| 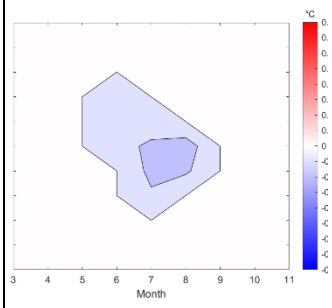 | 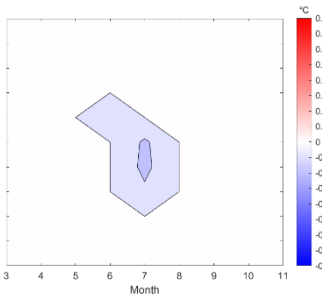 | 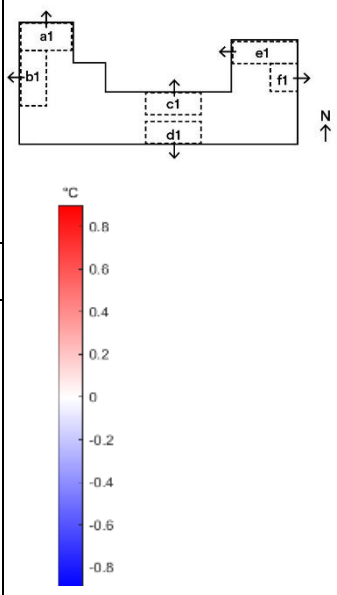 |
| **f1** | **f2** | |
| 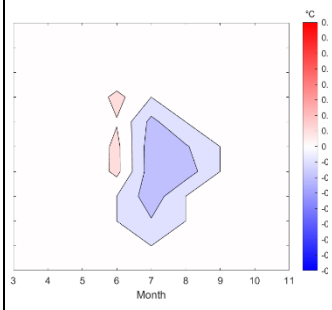 | 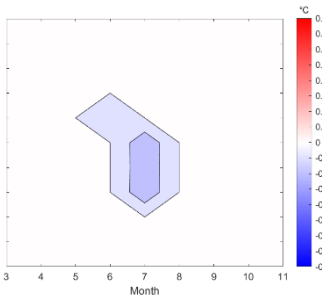 | |

*Cool Pavement + Green (CPGR)*

Considering this scenario, it can be argued that when vegetation is combined with a cool pavement, the greenery reduces overheating. For Classrooms A and B, CPGR could extend the air temperature drop until 17pm instead of 13pm. The D and F rooms were the worst in the CP scenario, however adding vegetation had a positive impact. There is no significant impact of greenery on classrooms C and E because there are no trees close to the windows in these classrooms.

Table 4.14. *Cool Pavement + Green IODs*

| **a1** | **a2** | **a3** |
|---|---|---|
| 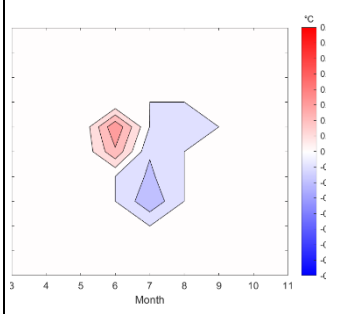 | 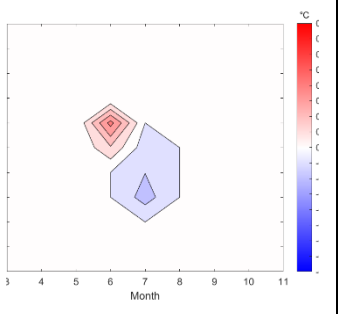 | 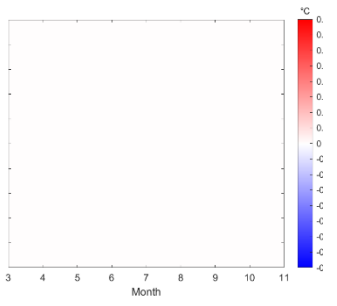 |
| **b1** | **b2** | **b3** |
| 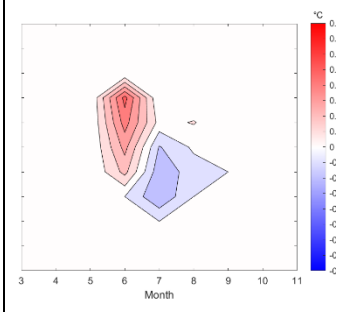 | 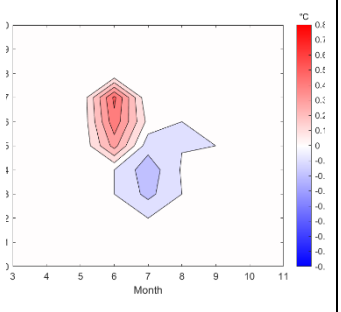 | 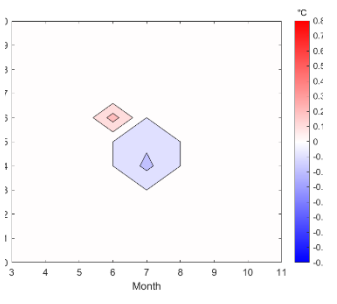 |

Table 4.14 (continued)

| d1 | d2 | d3 |
|---|---|---|
| 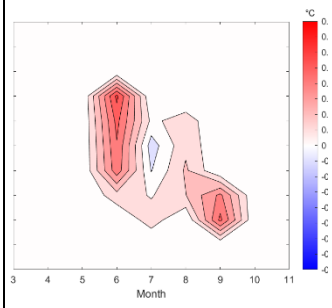 | 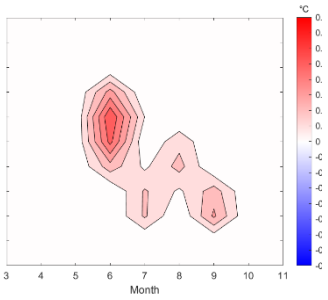 | 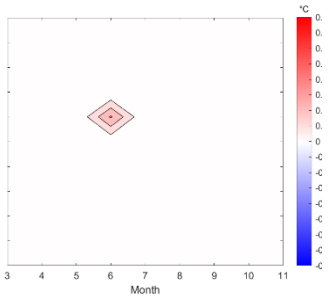 |
| **e1** | **e2** | |
| 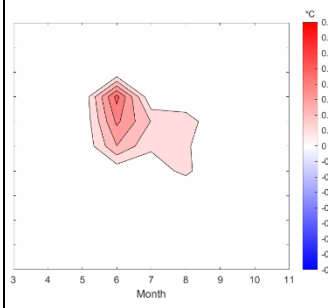 | 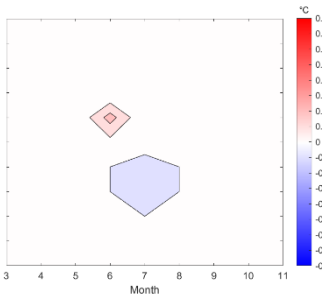 | 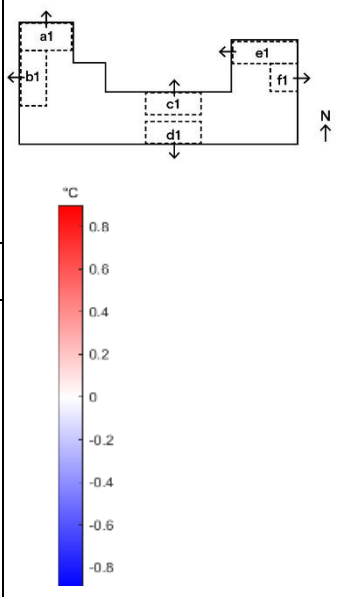 |
| **f1** | **f2** | |
| 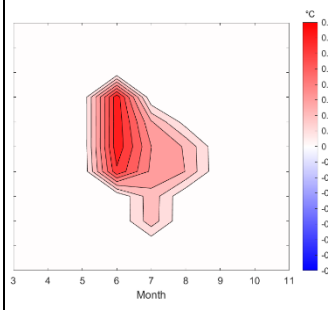 | 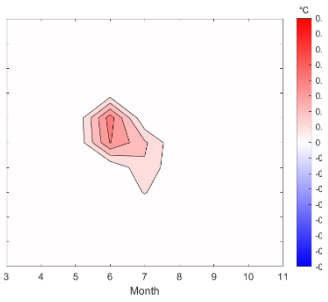 | |

*Cool Façade+ Green (CFGR)*

It is shown that the combination of two effective scenarios has the greatest impact on decreasing overheating degrees during summer. The temperature drops by 0.6 C in all classrooms between 14 p.m. and 16 p.m. The most significant difference is found in Classrooms B and D, since they are located near greenery in front of their windows and reflect radiation due to their orientation.

Table 4.15. *Cool Façade + Green IODs*

| **a1** | **a2** | **a3** |
|---|---|---|
| 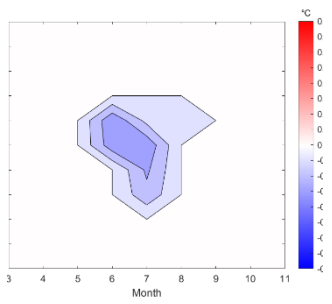 | 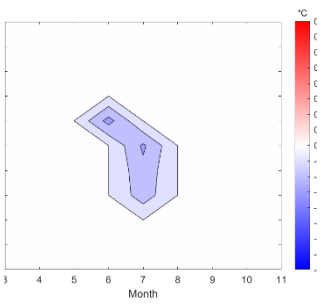 | 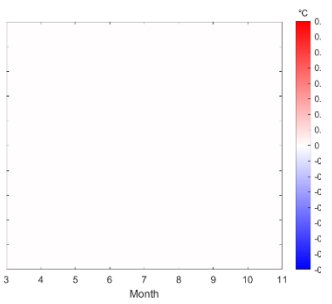 |
| **b1** | **b2** | **b3** |
| 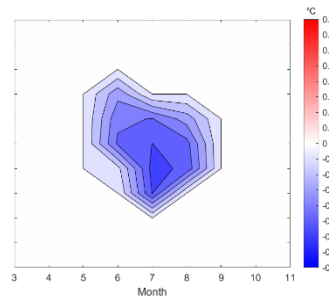 | 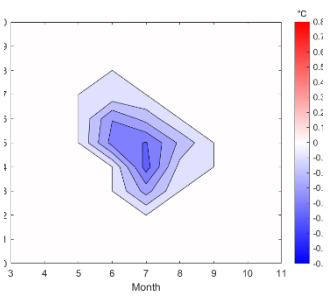 | 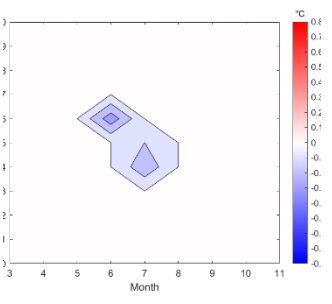 |

Table 4.15 (continued)

| d1 | d2 | d3 |
|---|---|---|
| 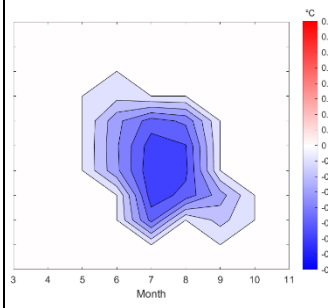 | 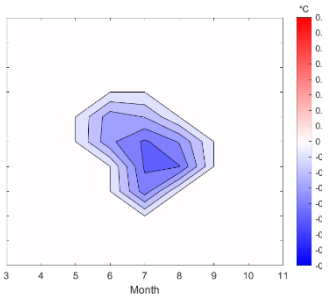 | 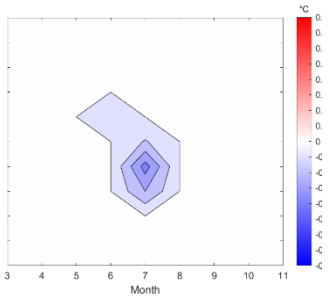 |
| **e1** | **e2** | |
| 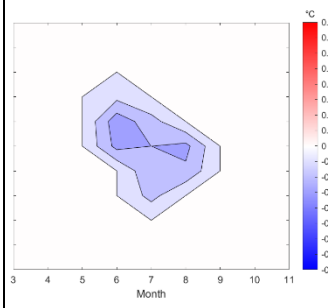 | 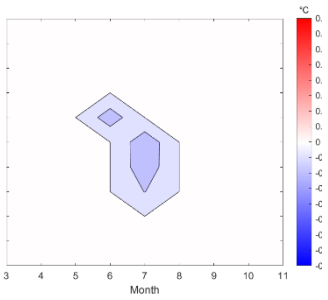 | 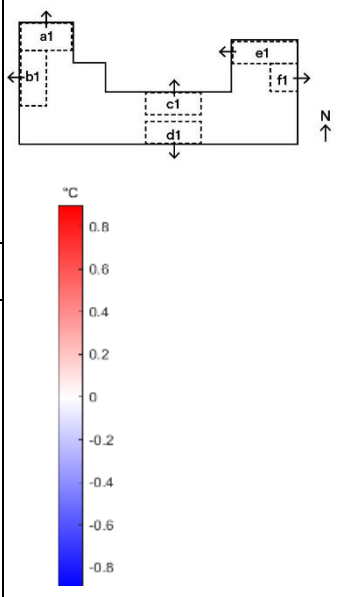 |
| **f1** | **f2** | |
| 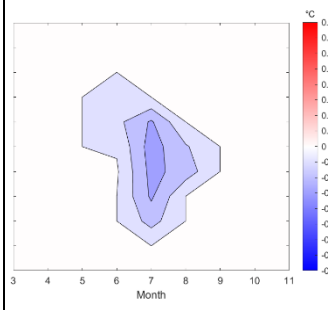 | 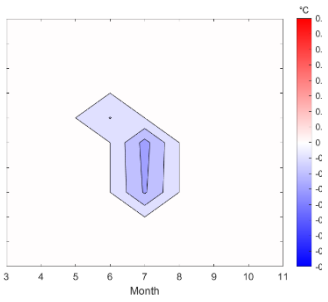 | |

*Cool Façade + Cool Pavement + Green (CFCPGR)*

Using both cool facade and trees to mitigate the negative effects of cool pavement, the combined scenario performs better than the CPGR scenario. There was a drop of 0.2 degrees between 13 p.m. and 16 p.m. in Classroom D on the first floor in July, which was not the case in CPGR scenarios. Between May and June, classrooms A, B, C, and E experienced an increase of 0.2-0.4C in the afternoon, but a decrease of up to 0.8C during the summer months.

Table 4.16. *Cool Façade + Cool Pavement + Green IODs*

| **a1** | **a2** | **a3** |
|---|---|---|
| 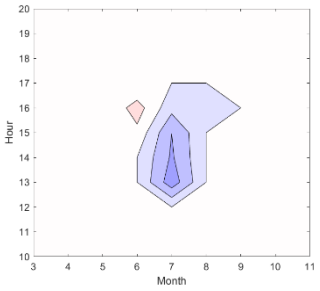 | 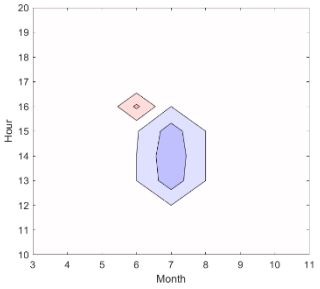 | 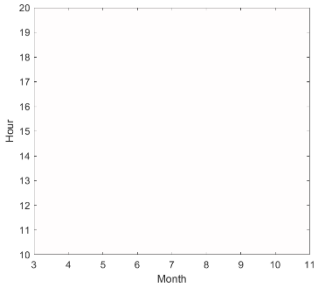 |
| **b1** | **b2** | **b3** |
| 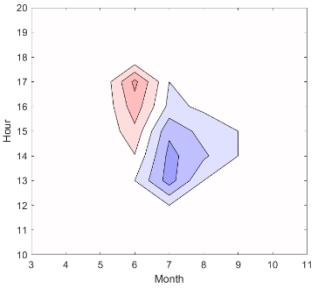 | 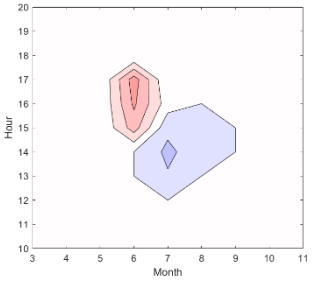 | 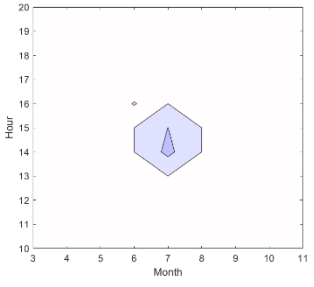 |

Table 4.16 (continued)

| d1 | d2 | d3 |
|---|---|---|
| 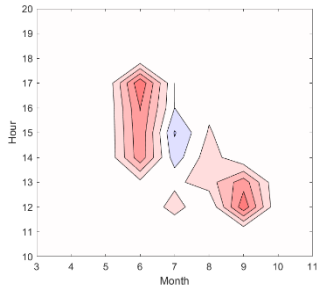 | 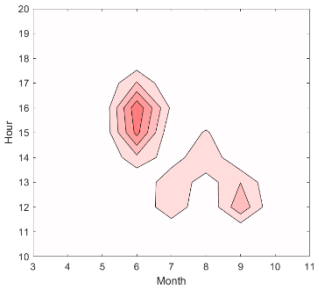 | 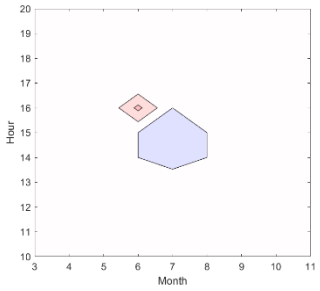 |
| **e1** | **e2** | |
| 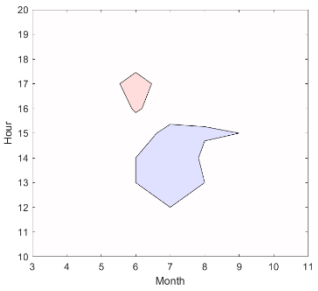 | 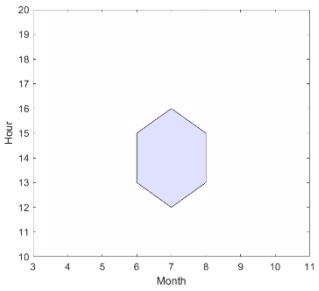 | 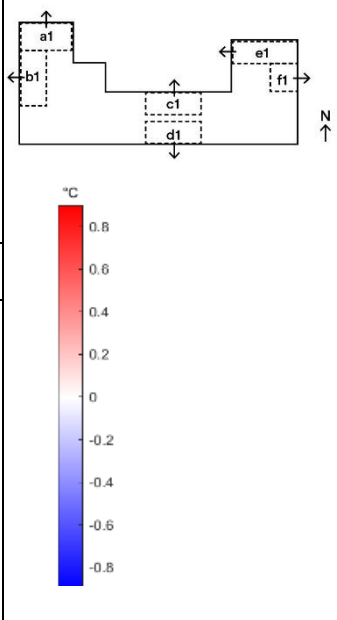 |
| **f1** | **f2** | |
| 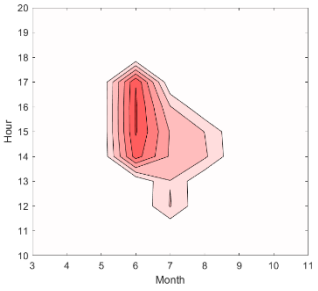 | 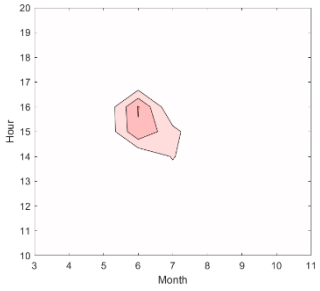 | |

## 4.4 Impact of Scenarios on Heating Load

The methodology discusses the difficulty of investigating microclimate impact on energy consumption studies that require the input of annual weather data. Therefore, 12 representative days are selected, and new annual weather files are created. Following the energy simulations, the heating loads are examined. The impact of six different UHI mitigation scenarios on heating loads has been calculated over 12 representative days. To note that heating is not working during warm months. After this process, the hourly loads for each day have been multiplied by 30 to calculate the monthly heating loads. Finally, the yearly heating loads for each classroom have been determined by summing up the monthly results. The impact of scenarios on annual heating load results can be seen on Table 4.17 for each classroom. The numbers represent the difference between each scenario and the baseline.

Table 4.17. *Annual heating loads (kwh/m$^2$)*

| | cp | cf | gr | cfgr | cpgr | cfcpgr |
|---|---|---|---|---|---|---|
| **a1** | -15.0 | 4.2 | 0.7 | 4.7 | -13.9 | -6.1 |
| **a2** | -11.6 | 5.3 | 1.5 | 6.5 | -10.7 | -3.3 |
| **a3** | -13.6 | 4.3 | 0.3 | 5.2 | -14.7 | -7.8 |
| **b1** | -8.6 | 3.5 | 3.8 | 6.9 | -5.3 | 0.3 |
| **b2** | -8.7 | 3.2 | 4.3 | 7.1 | -4.5 | -0.3 |
| **b3** | -9.2 | 3.1 | 4.1 | 6.9 | -4.9 | 0.7 |
| **c1** | -9.5 | 2.3 | -1.3 | 1.6 | -10.5 | -4.9 |
| **c2** | -8.9 | 2.1 | -1.1 | 1.3 | -9.9 | -4.9 |
| **c3** | -10.5 | 2.2 | -1.1 | 1.4 | -11.3 | -5.5 |
| **d1** | -3.7 | 0.8 | 1.9 | 5.5 | -5.9 | 0.0 |
| **d2** | -1.5 | 0.7 | 1.0 | 3.2 | -5.0 | -1.8 |
| **d3** | -11.2 | 3.7 | 15.5 | 16.0 | 2.8 | 9.2 |
| **e1** | -12.2 | 3.3 | 1.5 | 5.2 | -10.0 | -4.3 |
| **e2** | -10.9 | 3.6 | 3.4 | 7.2 | -8.2 | -2.8 |
| **f1** | -9.3 | 2.1 | 3.7 | 6.0 | -6.6 | -2.6 |
| **f2** | -10.7 | 2.5 | 10.1 | 12.7 | -1.9 | 4.0 |

In cool pavement scenario, a result, the indoor temperature is increased by the reflection of radiation from cool pavement through the windows. Thus, the energy consumption for heating decreases compared to baseline heating loads. The more significant difference can be seen in rooms such as A, C and E due to being more exposed to high reflective pavement rather than other rooms.

In a scenario where there is a cool façade, all the rooms will have increased heating loads, as the cool façade reflects solar radiation and keeps the surface temperature of the walls low. Thus, interiors will need a higher heating load during the cold months to maintain a comfortable temperature.

During a green scenario, all rooms' heating loads increase except classroom C, which is the least affected by the trees. In a green scenario, indoor temperatures are lowered.

Combining a cool façade with green (CFGR), heating loads increase as a result of the cool façade, but its results are not superior to the cool façade due to the green scenario.

Cool pavement and green (CPGR) scenarios result in decreased heating loads, with the exception of room D on the third floor, which loses heat from the roof while being cooled by many trees in front of the window.

Since cool façades are also involved, the last scenario results in a somewhat lower reduction of heating load than CP and CPGR.

In conclusion, UHI mitigation scenarios do not work well for third floor classrooms since they lose heat from the roof as other rooms are defined as adiabatic rooms. The combination of cool façade, green, and the combination of two is not appropriate for the strategy of decreasing heating load, as both cause a cooling effect on interiors. The best scenario for less heating load is Cool Pavement and its combinations.

## 4.5 Impact of Scenarios on Outdoor Thermal Comfort

When compared to other months, August has the highest air temperature at 14:00, and PET simulations are conducted at that time by using Bio-Met in ENVI-Met. Results are normally read at 1.5m, but because of the children's height, they are read at 1.00m.

A boxplot illustrates the comparison between scenarios compared with the baseline. Cool pavements are more effective at maintaining thermal comfort when they are shaded. In all scenarios, including the green scenario, the perceived temperature significantly decreases. Cool façades also increase MRT in their surroundings, which can be seen as an increase in perceived temperatures.

A green scenario and its variations can reduce perceived temperature by an average of four degrees. By using reflective materials for the facade and the pavement, the perception of temperature is increased by two degrees on average.

Therefore, while the air temperature is high in the summer months, planting more trees is the most reasonable strategy. Additionally, using cool pavement under the shadow of trees can also contribute to a decrease in perceived temperature during the summer months.

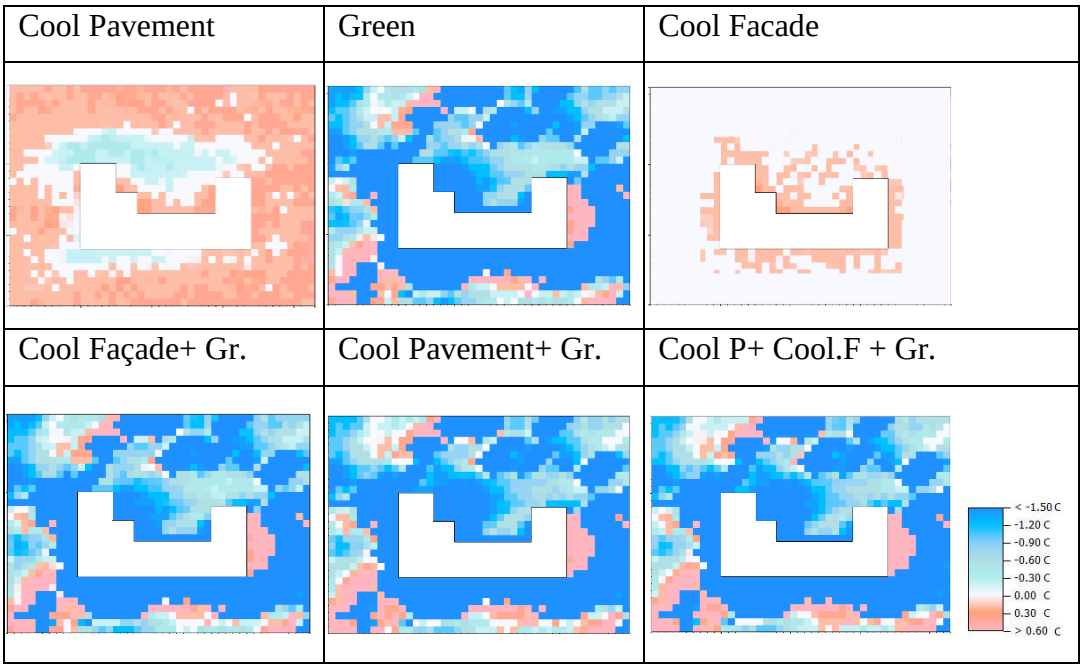


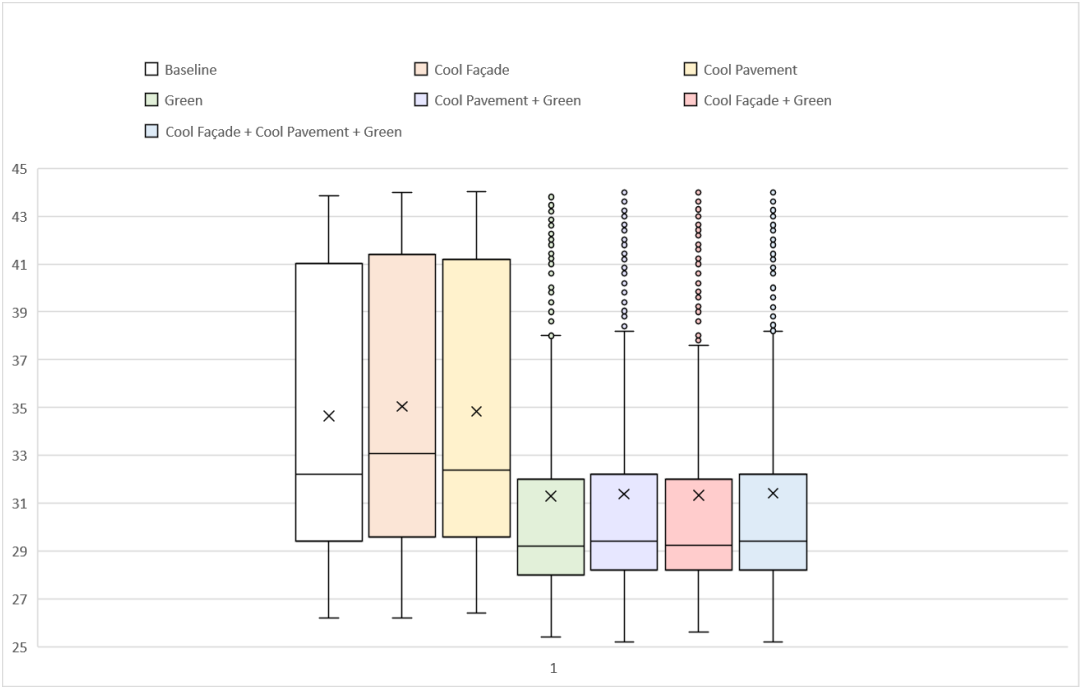


*Figure 4.2.* Comparison of PET result

# CHAPTER 5

# CONCLUSION

This study aimed to develop a computational method to assess the impact of UHI mitigation scenarios by coupling urban microclimate with energy and indoor overheating calculations, as well as outdoor thermal comfort. The study was conducted in the neighborhood of Bahçelievler, Ankara, and the results were presented in five stages. By analyzing the methodology and general framework of the research, this chapter will discuss the findings of the thesis. As such, the results of the proposed methodology will be discussed through the research questions, the promising contributions of the study to the field of research will be described, and the limitations of the present study will be acknowledged. At the end of this chapter, suggestions for further research will be presented.

## 5.1 The Outcomes of the Proposed Methodology

Through the research questions, the outcomes of the proposed methodology will be summarized. The main research question was what the most relevant mitigation scenarios are for tackling UHI effect, energy efficiency, low overheating degrees and better outdoor thermal comfort. This question can be answered by explaining each scenario's impact separately. To begin, Figure 5.1 shows suitable UHI mitigation scenarios for discussed aspects. In the following section, some suggestions are provided.

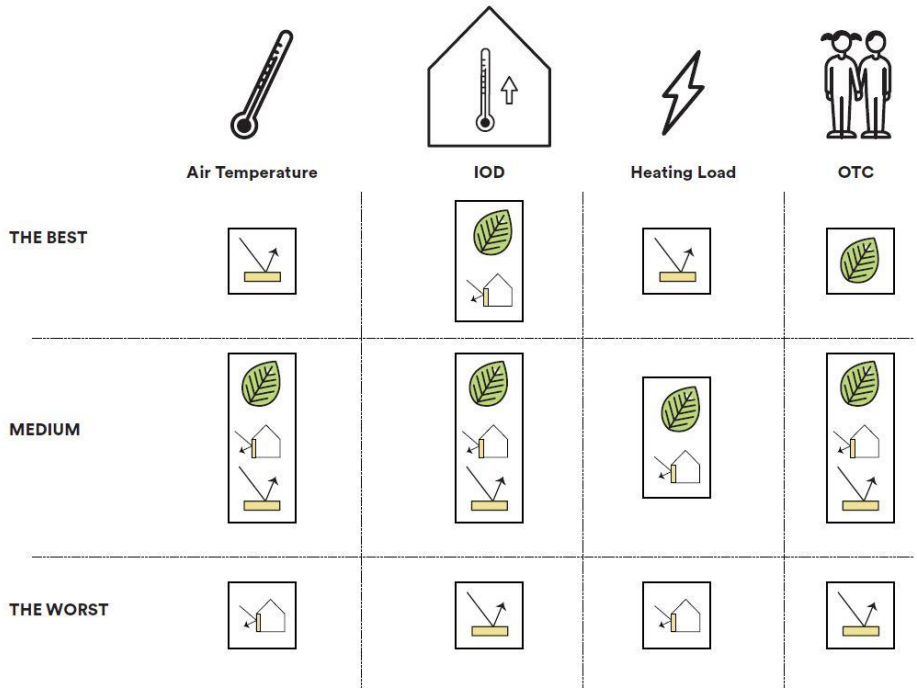


*Figure 5.1.* Comparison of UHI mitigation scenarios

For mitigating UHI effects, Cool Pavement (CP) is the most reasonable alternative. The medium option is to combine Cool Pavement with vegetation and Cool Facade. Cool Pavement will help to decrease the temperature by up to 0.8°C-1°C. However, the impact of Cool Facade scenario on reducing air temperature is negligible. Classrooms A, C, E facing toward North get benefit Cool Pavement scenario more than other rooms in order to be exposed to large amount of high reflective ground material.

In terms of reducing indoor overheating degrees, Cool Façade + Green (CFGR) scenario is more effective than simply applying high reflective materials to the façade. The most significant difference is found in Classrooms B and D, which are facing to West and East, respectively, since they are located near greenery in front of their windows and reflect radiation due to their orientation. The worst scenario is Cool Pavement that reflects the radiation from ground to inside of the rooms. Therefore, it causes overheating during the warm months.

During the cold months, Cool Pavement (CP) or Cool Façade + Green (CFGR) are more effective in reducing the amount of heating energy required per square meter whereas Cool Façade causes to increase heating loads due to cooling indoors.

The Green scenario (GR) achieves a higher reduction in perceived temperatures during the summer months. However, Cool Façade + Green (CFGR) is another option for thermal comfort. However, areas close to the building may be uncomfortable. Cool Pavement scenario is the worst option among the other scenarios due to high reflection of radiation. As a consequence, it is recommended that high reflective materials be employed in well shaded areas.

The second question was what the impact of UHI on microclimate is. It has been found that a difference of 3-4 degrees was seen at night due to the urban heat island, while there is a difference of 2-3 degrees during the day.

The third question was related to in how the impact of UHI can be measured, which computational tool should be used for the UHI modeling. There are many tools to allow investigating UHI impact such as Urban Weather Generator (UWG), Rayman Model, Urban Multi-scale Environmental Predictor (UMEP). However, ENVI-Met has been decided after the literature review to conduct the study due to its ability of high-resolution simulations. It allows to calculate the atmosphere's state based on the interaction between buildings, vegetation, hard ground properties, soil, and climatic conditions. Based on the laws of fluid dynamics and thermodynamics, the model simulates the evolution of climate variables throughout the day.

The fourth question was about demonstrating the reason of choosing the educational building typology rather than selecting other types of buildings, such as residential, commercial, or industrial. Aside from their large size, high occupant density, and schedule for energy savings throughout the year, educational buildings present a number of unique challenges among other building typologies (Palme et al., 2020). Moreover, children and adults react to heat stress differently due to UHI effect.

Children's physical conditions affect their perceived temperature and make them more vulnerable on warm days (Balbus & Malina, 2009; Cheng & Brown, 2020). Due to the fact that there is a gap in the literature regarding institutional facilities, an educational building was selected for the purpose of this study.

The fifth question was addressing to which UHI mitigation strategies are applicable for an existing educational facility. There are many different mitigation strategies such as changing façade, ground, and roof reflectiveness, using greenery, adding water elements or the combination of each individual strategy. However, six scenarios are investigated that they are Cool Pavement (CP), Cool Façade (CF), Green (GR), Cool Pavement+Green (CPGR), Cool Façade+Green(CFGR) and combination of three of them, which is Cool Facade+Cool Pavement+Green (CFCPGR) based on the research in the literature. Only façade and schoolyard's hard surface albedo changes and new trees are added due to capability of ENVI-Met.

The last research question was to what extent can a method be developed to investigate UHI mitigation scenarios to evaluate the energy performance of educational buildings, pupil perception of outdoor temperatures, and degree of indoor overheating. According to previous studies in the literature, there is a lack of investigation of the impact of UHI mitigations on different aspects and understanding the relationship between them due to computational cost in the context of educational building. This study has found that the developed methodology can couple urban microclimate with building energy and indoor comfort as well as outdoor perceived temperature simulations.

## 5.2 The Limitations and Future Studies

It is the objective of the thesis to develop a methodology to investigate how UHI mitigation strategies impact building energy consumption, indoor comfort, and children's perceived outdoor temperature. Based on previous studies in the literature, an accurate 3D urban microclimate modeling tool was selected as a method for investigating the UHI effect. However, the limitations of this thesis are primarily due to the computational costs associated with it. The first limitation involves the length of simulations. Although the selected tool has been validated for the investigation of UHI effects, it requires considerable simulation time, particularly when the analysis grid resolution is set to coarse. However, this might lead to a loss of information. To optimize result accuracy and simulation duration, several grid resolutions were tested in this thesis. The grid size for the XY analysis area is defined as 3mx3m in order to optimize result accuracy. In future studies, simulations can be performed at a finer grid resolution to improve the accuracy of the results.

A second limitation is the lack of design options. In addition to simulations of urban microclimates, the research intends to couple simulations of energy consumption with simulations of urban microclimate, which requires matching two models. During the energy calculation part of the research, the Rhino model and EnergyPlus were utilized, both of which provide flexible design environments for users. ENVI-Met, however, provides grid-based simulations of urban microclimates with pixelated design alternatives. Therefore, UHI mitigation scenarios were limited. However, it is possible to study the impact of different types of material on interior overheating degrees and heating loads through the use of different types of materials for walls and roofs for the future studies.

## REFERENCES


Ash, C., B. Jasny, L. Robert, R. Stone and A.Sugden (2008) Reimagining cities.Science319.5864, 739.

Wang, K., Wang, J., Wang, P., Sparrow, M., Yang, J., & Chen, H. (2007). Influences of urbanization on surface characteristics as derived from the Moderate-Resolution Imaging Spectroradiometer: A case study for the Beijing metropolitan area. Journal of Geophysical Research: Atmospheres, 112(D22).

Kong, F., Yan, W., Zheng, G., Yin, H., Cavan, G., Zhan, W., Cheng, L., 2016. Retrieval of three-dimensional tree canopy and shade using terrestrial laser scanning (TLS) data to analyze the cooling effect of vegetation. Agric. For. Meteorol. 217, 22–34.

Yang, W., Wong, N. H., & Li, C. Q. (2016). Effect of street design on outdoor thermal comfort in an urban street in Singapore. *Journal of Urban Planning and Development*, *142*(1), 05015003.

Huang, K.T., Lin, T.P., Lien, H.C., 2015., N. (2013). Street design and urban microclimate: analyzing the effects of street geometry and orientation on airflow and solar access in urban canyons. *Journal of clean energy technologies*, *1*(1).

Kovats, R. S., & Hajat, S. (2008). Heat stress and public health: a critical review. *Annu. Rev. Public Health*, *29*, 41-55.

Luber, G., & McGeehin, M. (2008). Climate change and extreme heat events. *American journal of preventive medicine*, *35*(5), 429-435.

Sanusi, R., Johnstone, D., May, P., & Livesley, S. J. (2016). Street orientation and side of the street greatly influence the microclimatic benefits street trees can provide in summer. *Journal of environmental quality*, *45*(1), 167-174.

Climate Change. (2022, August 19). US EPA. Retrieved September 11, 2022, from https://www.epa.gov/climate-change

Shaftel, H. (n.d.). Overview: Weather, Global Warming and Climate Change. Climate Change: Vital Signs of the Planet. Retrieved September 11, 2022, from https://climate.nasa.gov/global-warming-vs-climate-change/

Causes and Effects of Climate Change. (n.d.). Thailand. Retrieved September 11, 2022, from https://thailand.un.org/en/174652-causes-and-effects-climate-change

Rohde, R. (2022, February 14). Global Temperature Report for 2021. Berkeley Earth. Retrieved September 11, 2022, from http://berkeleyearth.org/global-temperature-report-for-2021/

Abreu-Harbich, L. V., Labaki, L. C., & Matzarakis, A. (2015). Effect of tree planting design and tree species on human thermal comfort in the tropics. *Landscape and Urban Planning*, *138*, 99–109. https://doi.org/10.1016/j.landurbplan.2015.02.008

Akköse, G. (2019). *Architectural Design For Climate Change Mitigation And Adaptation Strategies In Existing Buildings* (Vol. 126, Issue 1). Middle East Technical University.

AlFaris, F., Juaidi, A., & Manzano-Agugliaro, F. (2016). Improvement of efficiency through an energy management program as a sustainable practice in schools. *Journal of Cleaner Production*, *135*, 794–805. https://doi.org/10.1016/J.JCLEPRO.2016.06.172

Antoniadis, D., Katsoulas, N., Papanastasiou, D., Christidou, V., & Kittas, C. (2016). Evaluation of thermal perception in schoolyards under Mediterranean climate conditions. *International Journal of Biometeorology*, *60*(3), 319–334. https://doi.org/10.1007/s00484-015-1027-5

Antoniadis, Dimitrios, Katsoulas, N., & Papanastasiou, D. (2020). Thermal environment of urban schoolyards: Current and future design with respect to children's thermal comfort. *Atmosphere*, *11*(11). https://doi.org/10.3390/atmos11111144

ASHRAE Standard. (2004). Thermal Environmental Conditions for Human Occupancy 55-2004. *American Society of Heating, Refrigerating and Air-Conditioning Engineers, Inc.*, *2004*(ANSI/ASHRAE Standard 55-2004), 1–34.

Balbus, J. M., & Malina, C. (2009). Identifying vulnerable subpopulations for climate change health effects in the United States. *Journal of Occupational and Environmental Medicine*, *51*(1), 33–37. https://doi.org/10.1097/JOM.0b013e318193e12e

Beck, H. E., Zimmermann, N. E., Mcvicar, T. R., Vergopolan, N., Berg, A., & Wood, E. F. (2018). *Data Descriptor: Present and future Köppen-Geiger climate classification maps at 1-km resolution*. https://doi.org/10.1038/sdata.2018.214

Berghauser Pont, M., Salvalai, G., Mosteiro-Romero, M., Maiullari, D., Esch, P. M., Pijpers-van Esch, M., & Schlueter, A. (2020). *An Integrated Microclimate-Energy Demand Simulation Method for the Assessment of Urban Districts*. https://doi.org/10.3389/fbuil.2020.553946

Billmore, B., Brooke, J., Booth, R., Funnell, K., & Bubb, M. (1999). *The Outdoor Classroom: Educational Use, Landscape Design, & Management of School Grounds*.

Błazejczyk, K., Jendritzky, G., Bröde, P., Fiala, D., Havenith, G., Epstein, Y., Psikuta, A., & Kampmann, B. (2013). An introduction to the Universal thermal climate index (UTCI). *Geographia Polonica*, *86*(1), 5–10. https://doi.org/10.7163/GPol.2013.1

Bueno, B., Norford, L., Hidalgo, J., & Pigeon, G. (2013). The urban weather generator. *Journal of Building Performance Simulation*, *6*(4), 269–281. https://doi.org/10.1080/19401493.2012.718797

Chan, A. L. S. (2011). Developing a modified typical meteorological year weather file for Hong Kong taking into account the urban heat island effect. *Building and Environment*, *46*(12), 2434–2441. https://doi.org/10.1016/J.BUILDENV.2011.04.038

Chatzipoulka, C., Nikolopoulou, M., Watkins, R., & Building, M. (2015). The impact of urban geometry on the radiant environment in outdoor spaces. *ICUC9 - 9th International Conference on Urban Climate Jointly with 12th Symposium on the Urban Environment*, 1–6.

Cheng, W., & Brown, R. D. (2020). An energy budget model for estimating the thermal comfort of children. *International Journal of Biometeorology*, *64*(8), 1355–1366. https://doi.org/10.1007/s00484-020-01916-x

Chung, W., & Yeung, I. M. H. (2020). A study of energy consumption of secondary school buildings in Hong Kong. *Energy and Buildings*, *226*, 110388. https://doi.org/10.1016/j.enbuild.2020.110388

Çiçek, İ., & Yılmaz, E. (2013). *Ankara Şehrinde Isı adası Oluşumu*.

Corgnati, S. P., Ansaldi, R., & Filippi, M. (2009). Thermal comfort in Italian classrooms under free running conditions during mid seasons: Assessment through objective and subjective approaches. *Building and Environment*, *44*(4), 785–792. https://doi.org/10.1016/j.buildenv.2008.05.023

Costanzo, V., Evola, G., & Marletta, L. (2021). Urban Heat Stress and Mitigation Solutions. In *Urban Heat Stress and Mitigation Solutions*. https://doi.org/10.1201/9781003045922

Dall'O, G., & Sarto, L. (2013). Potential and limits to improve energy efficiency in space heating in existing school buildings in northern Italy. *Energy and Buildings*, *67*, 298–308. https://doi.org/10.1016/J.ENBUILD.2013.08.001

Duman Yüksel, Ü., & Yilmaz, O. (2008). Ankara kentinde kentsel isi adasi etkisinin yaz aylarinda uzaktan algilama ve meteorolojik gözlemlere dayali olarak saptanmasi ve değerlendirilmesi. *Journal of the Faculty of Engineering and Architecture of Gazi University*, *23*(4), 937–952.

Flax, L., Korthals Altes, R., Kupers, R., & Mons, B. (2020). Greening schoolyards - An urban resilience perspective. *Cities*, *106*(August), 102890. https://doi.org/10.1016/j.cities.2020.102890

Gál, C. V., & Kántor, N. (2020). Modeling mean radiant temperature in outdoor spaces, A comparative numerical simulation and validation study. *Urban Climate*, *32*, 100571. https://doi.org/10.1016/J.UCLIM.2019.100571

Hamdy, M., Carlucci, S., Hoes, P. J., & Hensen, J. L. M. (2017). The impact of climate change on the overheating risk in dwellings—A Dutch case study. *Building and Environment*, *122*(August 2003), 307–323. https://doi.org/10.1016/j.buildenv.2017.06.031

Höppe, P. (1999). The physiological equivalent temperature - a universal index for the biometeorological assessment of the thermal environment. *International Journal of Biometeorology*, *43*(2), 71–75. http://www.embase.com/search/results?subaction=viewrecord&from=export&id=L129347950

Höppe, P. (2002). Different aspects of assessing indoor and outdoor thermal comfort. *Energy and Buildings*, *34*(6), 661–665. https://doi.org/10.1016/S0378-7788(02)00017-8

Hove, L. W. a Van, Steeneveld, G. J., Jacobs, C. M. J., Heusinkveld, B. G., Elbers, J. a, Moors, E. J., & Holtslag, a a M. (2011). Exploring the Urban Heat Island Intensity of Dutch cities. *Climate Science and Urban Design*, *June*, 1–60. http://edepot.wur.nl/171621

Huttner, S. (2012). Further development and application of the 3D microclimate simulation ENVI-met. *Mainz: Johannes Gutenberg-Universitat in Mainz*, 147. http://ubm.opus.hbz-nrw.de/volltexte/2012/3112/

IPCC. (2022). *Climate Change 2022 Impacts, Adaptation and Vulnerability*.

Janssen, W. D., Blocken, B., & van Hooff, T. (2013). Pedestrian wind comfort around buildings: Comparison of wind comfort criteria based on whole-flow field data for a complex case study. *Building and Environment*, *59*, 547–562. https://doi.org/10.1016/J.BUILDENV.2012.10.012

Jeong, D., Park, K., Song, B., & Kim, G. (2015). Validation of ENVI-met PMV values by in-situ measurements. *ICUC9 - 9th International Conference on Urban Climate Jointly with 12th Symposium on the Urban Environment*.

Joong-Bin LIM; Jinhang YU; Ju-Yeol LEE; Kyoo-Seock LEE. (2015). Comparison of Thermal Effects of Different School Ground Surface Materials. *Journal of the Korean Association of Geographic Information Studies*, *18*(2), 28–44. http://www.riss.kr/link?id=A100543263

Karachaliou, P., Santamouris, M., & Pangalou, H. (2016). Experimental and numerical analysis of the energy performance of a large scale intensive green roof system installed on an office building in Athens. *Energy and Buildings*, *114*, 256–264. https://doi.org/10.1016/j.enbuild.2015.04.055

Katafygiotou, M. C., & Serghides, D. K. (2014). Thermal comfort of a typical secondary school building in Cyprus. *Sustainable Cities and Society*, *13*, 303–312. https://doi.org/10.1016/j.scs.2014.03.004

Khatoon, S., & Kim, M.-H. (2020). *Thermal Comfort in the Passenger Compartment Using a 3-D Numerical Analysis and Comparison with Fanger's Comfort Models*. https://doi.org/10.3390/en13030690

Kim, T. W., Lee, K. G., & Hong, W. H. (2012). Energy consumption characteristics of the elementary schools in South Korea. *Energy and Buildings*, *54*, 480–489. https://doi.org/10.1016/J.ENBUILD.2012.07.015

Kleerekoper, L., Van Esch, M., & Salcedo, T. B. (2012). How to make a city climate-proof, addressing the urban heat island effect. *Resources, Conservation and Recycling*, *64*, 30–38. https://doi.org/10.1016/j.resconrec.2011.06.004

La Roche, P. M. (2016). Carbon-neutral architectural design. In *Carbon-Neutral Architectural Design*. https://doi.org/10.1201/9781315119649-2

Lalošević, M. D., Komatina, M. S., Miloš, M. V, & Rudonja, N. R. (2018). *Green Roofs and Cool Materials As Retrofitting Strategies for*. *22*(6), 2309–2324.

Li, X., Zhou, Y., Yu, S., Jia, G., Li, H., & Li, W. (2019). Urban heat island impacts on building energy consumption: A review of approaches and findings. *Energy*, *174*, 407–419. https://doi.org/10.1016/J.ENERGY.2019.02.183

Lin, T. P., Ho, Y. F., & Huang, Y. S. (2007). Seasonal effect of pavement on outdoor thermal environments in subtropical Taiwan. *Building and Environment*, *42*(12), 4124–4131. https://doi.org/10.1016/j.buildenv.2006.11.031

Lindberg, F., Grimmond, C. S. B., Gabey, A., Huang, B., Kent, C. W., Sun, T., Theeuwes, N. E., Järvi, L., Ward, H. C., Capel-Timms, I., Chang, Y., Jonsson, P., Krave, N., Liu, D., Meyer, D., Olofson, K. F. G., Tan, J., Wästberg, D., Xue, L., & Zhang, Z. (2018). Urban Multi-scale Environmental Predictor (UMEP): An integrated tool for city-based climate services. *Environmental Modelling & Software*, *99*, 70–87. https://doi.org/10.1016/J.ENVSOFT.2017.09.020

Lourenço, P., Pinheiro, M. D., & Heitor, T. (2014). From indicators to strategies: Key Performance Strategies for sustainable energy use in Portuguese school buildings. *Energy and Buildings*, *85*, 212–224.

Manteghi, G., Bin Limit, H., & Remaz, D. (2015). Water bodies an urban microclimate: A review. *Modern Applied Science*, *9*(6), 1–12. https://doi.org/10.5539/mas.v9n6p1

Matzarakis, A., Mayer, H., & Iziomon, M. G. (1999). Applications of a universal thermal index: Physiological equivalent temperature. *International Journal of Biometeorology*, *43*(2), 76–84. https://doi.org/10.1007/s004840050119

Meili, N., Manoli, G., Burlando, P., Carmeliet, J., Chow, W. T. L., Coutts, A. M., Roth, M., Velasco, E., Vivoni, E. R., & Fatichi, S. (2021). Tree effects on urban microclimate : Diurnal , seasonal , and climatic temperature differences explained by separating radiation , evapotranspiration , and roughness effects. *Urban Forestry & Urban Greening*, *58*, 126970. https://doi.org/10.1016/j.ufug.2020.126970

Meng, F., Guo, J., Ren, G., Zhang, L., & Zhang, R. (2020). Impact of urban heat island on the variation of heating loads in residential and office buildings in Tianjin. *Energy and Buildings*, *226*, 110357. https://doi.org/10.1016/J.ENBUILD.2020.110357

Moogk-Soulis, C. (2002). *Schoolyard Heat Islands: A Case Study in Waterloo, Ontario*. 1–7.

Naboni, E., Meloni, M., Coccolo, S., Kaempf, J., & Scartezzini, J. L. (2017). An overview of simulation tools for predicting the mean radiant temperature in an outdoor space. *Energy Procedia*, *122*, 1111–1116. https://doi.org/10.1016/J.EGYPRO.2017.07.471

Oke, T. . (1988). *Boundary Layer Climates* (second). Routledge.

Palme, M., Clemente, C., Baiani, S., Calice, C., & Salvati, A. (2020). Energy Consumption of Institutional Buildings Considering the Urban Climate in Rome. *Proceedings of Building Simulation 2019: 16th Conference of IBPSA*, *16*(September), 3765–3770. https://doi.org/10.26868/25222708.2019.211271

Pérez-Lombard, L., Ortiz, J., & Pout, C. (2008). A review on buildings energy consumption information. *Energy and Buildings*, *40*(3), 394–398. https://doi.org/10.1016/J.ENBUILD.2007.03.007

Perez, Y. V., & Capeluto, I. G. (2009). Climatic considerations in school building design in the hot–humid climate for reducing energy consumption. *Applied Energy*, *86*(3), 340–348. https://doi.org/10.1016/J.APENERGY.2008.05.007

Radhi, H., & Sharples, S. (2013). Quantifying the domestic electricity consumption for air-conditioning due to urban heat islands in hot arid regions. *Applied Energy*, *112*, 371–380. https://doi.org/10.1016/J.APENERGY.2013.06.013

Salcedo-Rahola, Baldiri, Van Oppen, Peter, Mulder, K. (2009). *Heat in the city An inventory of knowledge and knowledge* (Issue April 2014).

Salvati, A., Kolokotroni, M., Kotopouleas, A., Watkins, R., Giridharan, R., & Nikolopoulou, M. (2022). Impact of reflective materials on urban canyon albedo, outdoor and indoor microclimates. *Building and Environment*, *207*, 108459.

Santamouris, M. (2014). Cooling the cities - A review of reflective and green roof mitigation technologies to fight heat island and improve comfort in urban environments. *Solar Energy*, *103*, 682–703. https://doi.org/10.1016/j.solener.2012.07.003

Santamouris, M., Ding, L., Fiorito, F., Oldfield, P., Osmond, P., Paolini, R., Prasad, D., & Synnefa, A. (2017). Passive and active cooling for the outdoor built environment – Analysis and assessment of the cooling potential of mitigation technologies using performance data from 220 large scale projects. *Solar Energy*, *154*, 14–33. https://doi.org/10.1016/j.solener.2016.12.006

Santamouris, M., Papanikolaou, N., Livada, I., Koronakis, I., Georgakis, C., Argiriou, A., & Assimakopoulos, D. N. (2001). On the impact of urban climate on the energy consumption of buildings. *Solar Energy*, *70*(3), 201–216. https://doi.org/10.1016/S0038-092X(00)00095-5

Santamouris, M., & Vasilakopoulou, K. (2021). Present and future energy consumption of buildings: Challenges and opportunities towards decarbonisation. *E-Prime - Advances in Electrical Engineering, Electronics and Energy*, *1*, 100002. https://doi.org/10.1016/J.PRIME.2021.100002

Santamouris, Mat. (2016). Cooling the buildings – past, present and future. *Energy and Buildings*, *128*,617–638. https://doi.org/10.1016/J.ENBUILD.2016.07.034

Skoulika, Fotini; Santamouris, Mattheos; Kolokotsa, D. (n.d.). *The Thermal Characteristics And The Mitigation Potential Of A Medium Size*.

Stewart, I. D. ;Mill. G. (2018). The Urban Heat Island A Guidebook. In *Angewandte Chemie International Edition, 6(11), 951–952.*

Street, M., Reinhart, C., Norford, L., & Ochsendorf, J. (2013). Urban heat island in boston - An evaluation of urban airtemperature models for predicting building energy use. *Proceedings of BS 2013: 13th Conference of the International Building Performance Simulation Association*, 1022–1029.

Taleghani, M., Sailor, D., & Ban-Weiss, G. A. (2016). Micrometeorological simulations to predict the impacts of heat mitigation strategies on pedestrian thermal comfort in a Los Angeles neighborhood. *Environmental Research Letters*, *11*(2). https://doi.org/10.1088/1748-9326/11/2/024003

Teli, D., Jentsch, M. F., & James, P. A. B. (2012). Naturally ventilated classrooms: An assessment of existing comfort models for predicting the thermal sensation and preference of primary school children. *Energy and Buildings*, *53*, 166–182. https://doi.org/10.1016/j.enbuild.2012.06.022

Thewes, A., Maas, S., Scholzen, F., Waldmann, D., & Zürbes, A. (2014). Field study on the energy consumption of school buildings in Luxembourg. *Energy and Buildings*, *68*(PARTA), 460–470. https://doi.org/10.1016/J.ENBUILD.2013.10.002

Tsoka, S., Theodosiou, T., Tsikaloudaki, K., & Flourentzou, F. (2018). Modeling the performance of cool pavements and the effect of their aging on outdoor surface and air temperatures. *Sustainable Cities and Society*, *42*(July), 276–288. https://doi.org/10.1016/j.scs.2018.07.016

Tsoka, S., Tolika, K., Theodosiou, T., Tsikaloudaki, K., & Bikas, D. (2018). A method to account for the urban microclimate on the creation of 'typical weather year' datasets for building energy simulation, using stochastically generated data. *Energy and Buildings*, *165*, 270–283. https://doi.org/10.1016/J.ENBUILD.2018.01.016

U.S. Department of Energy. (2015). Chapter 5: Increasing Efficiency of Building Systems and Technologies. *Quadrennial Technology Review, An Assessment of Energy Technologies and Research Opportunities*, *September*, 143–181. https://www.energy.gov/sites/prod/files/2017/03/f34/qtr-2015-chapter5.pdf

Ürge-Vorsatz D, et al. (2012). *Energy End-Use: Buildings*.

Van Hoof, J. (2008). Forty years of Fanger's model of thermal comfort: Comfort for all? *Indoor Air*, *18*(3), 182–201. https://doi.org/10.1111/J.1600-0668.2007.00516.X

Vanos, J. K., Herdt, A. J., & Lochbaum, M. R. (2017). Effects of physical activity and shade on the heat balance and thermal perceptions of children in a playground microclimate. *Building and Environment*, *126*, 119–131. https://doi.org/10.1016/j.buildenv.2017.09.026

Wang, Y., Berardi, U., & Akbari, H. (2016). Comparing the effects of urban heat island mitigation strategies for Toronto, Canada. *Energy and Buildings*, *114*, 2–19. https://doi.org/10.1016/j.enbuild.2015.06.046

Yamamoto, Y. (2005). Measures to Mitigate Urban Heat Islands. *Environmental and Energy Research Unit. Quaterly Review*, *18*, 65–83.

Yavaş, M., & Yılmaz, S. (2019). *Soğuk İklim Bölgesinde Kentsel Mikro İklimin Değerlendirilmesi : Erzurum Kentsel Dönüşüm Alanı Örneği Evaluation of Urban Micro-Climate in Cold Climate Cities : The Case of Urban Transformation Area in Erzurum*. *7*(2), 103–114.

Younger, M., Morrow-Almeida, H. R., Vindigni, S. M., & Dannenberg, A. L. (2008). The Built Environment, Climate Change, and Health: Opportunities for Co-Benefits. *American Journal of Preventive Medicine*, *35*(5), 517–526. https://doi.org/10.1016/J.AMEPRE.2008.08.017

Zhang, A., Bokel, R., van den Dobbelsteen, A., Sun, Y., Huang, Q., & Zhang, Q. (2017). An integrated school and schoolyard design method for summer thermal comfort and energy efficiency in Northern China. *Building and Environment*, *124*, 369–387. https://doi.org/10.1016/j.buildenv.2017.08.024

Zinzi, M., & Carnielo, E. (2017). Impact of urban temperatures on energy performance and thermal comfort in residential buildings. The case of Rome, Italy. *Energy and Buildings*, *157*, 20–29. https://doi.org/10.1016/J.ENBUILD.2017.05.021

Zomorodian, Z. S., Tahsildoost, M., & Hafezi, M. (2016). Thermal comfort in educational buildings: A review article. *Renewable and Sustainable Energy Reviews*, *59*, 895–906. https://doi.org/10.1016/j.rser.2016.01.033

# APPENDICES

## A. ENVI-Met Baseline Model INX File Inputs

| **Building Material Inputs based on a typical school building in Turkey** | | | | | | | |
|---|---|---|---|---|---|---|---|
| Material | Absorp. | Transmission | Albedo | Emissivity | Specific Heat | Thermal Conductivity | Density |
| Concrete | 0,7 | 0 | 0,3 | 0,9 | 840 | 1,3 | 2000 |
| Brick | 0,6 | 0 | 0,4 | 0,9 | 650 | 0,44 | 1500 |
| Tile | 0,5 | 0 | 0,5 | 0,9 | 800 | 0,84 | 1900 |

| **Hardsurface and Natural Surface Input** | | |
|---|---|---|
| | Albedo | Emissivity |
| Aged Concrete | 0,3 | 0,9 |
| Asphalt | 0,2 | 0,9 |
| Sandy Soil | 0 | 0,9 |

| Greenery | Albedo | Transmittance | Height(m) | Root area depth(m) | Leaf Area Density |
|---|---|---|---|---|---|
| Grass | 0,2 | 0,3 | 0,25 | 0,20 | high |
| Deciduous | 0,18 | 0,3 | 15 | 12 | high |

## B. Details of Zones

| Levels | Zone Names | Zone Program | Zone Floor Area (m2) | Zone Window-Wall Ratio (%) | Orientation |
|---|---|---|---|---|---|
| First Floor | A1 | Classroom | 90 | 0,3 | North |
| | B1 | Classroom | 60 | 0,23 | West |
| | C1 | Classroom | 49,5 | 0,18 | North |
| | D1 | Classroom | 50,4 | 0,36 | South |
| | E1 | Classroom | 112,5 | 0,3 | West |
| | F1 | Classroom | 45 | 0,3 | East |
| Second Floor | A2 | Classroom | 90 | 0,3 | North |
| | B2 | Classroom | 60 | 0,23 | West |
| | C2 | Classroom | 49,5 | 0,18 | North |
| | D2 | Classroom | 50,4 | 0,36 | South |
| | E2 | Classroom | 112,5 | 0,3 | West |
| | F2 | Classroom | 45 | 0,3 | East |
| Third Floor | A3 | Classroom | 90 | 0,3 | North |
| | B3 | Classroom | 60 | 0,23 | West |
| | C3 | Classroom | 49,5 | 0,18 | North |
| | D3 | Classroom | 50,4 | 0,36 | South |
| Summary | 16 Zones | Classroom | 66,54 | 0,27 | |

## C. Comparison of UHI Modified Weather File and the Weather Station File for the Baseline

| | a1 |
|---|---|
| 31st December | 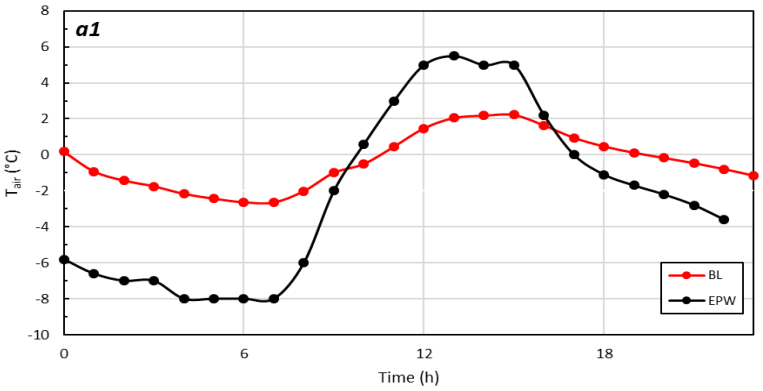 |
| 5th January | 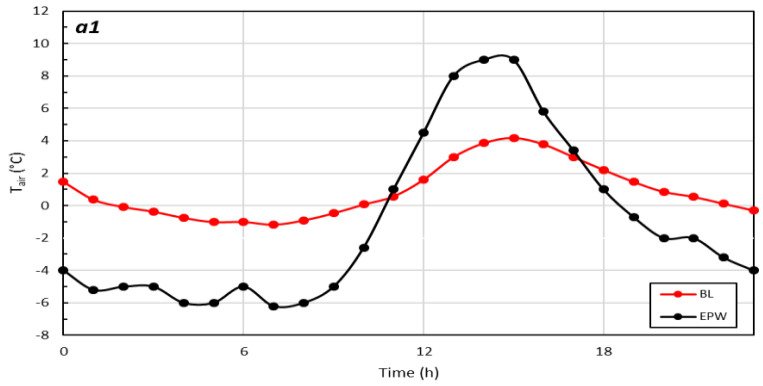 |
| 23rd February | 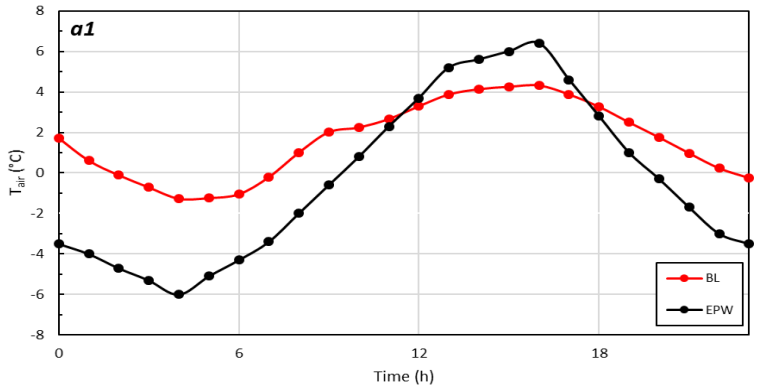 |

| | b1 |
|---|---|
| 31st December | 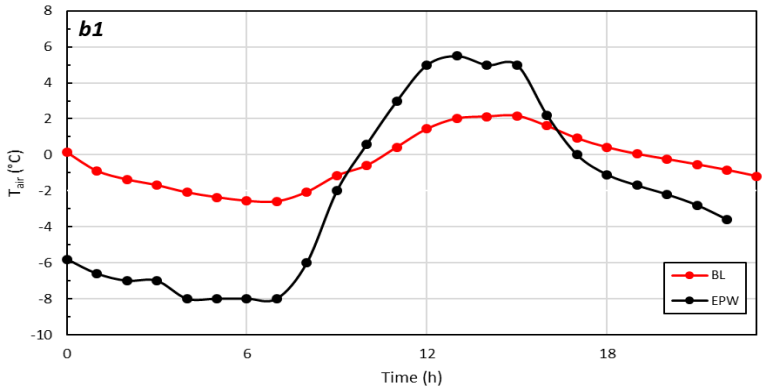 |
| 5th January | 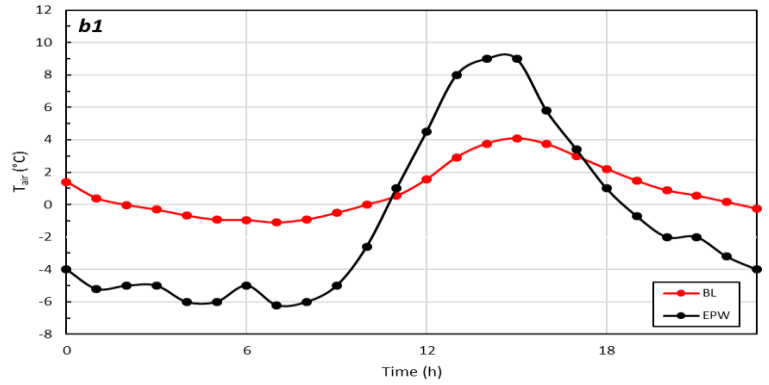 |
| 23rd February | 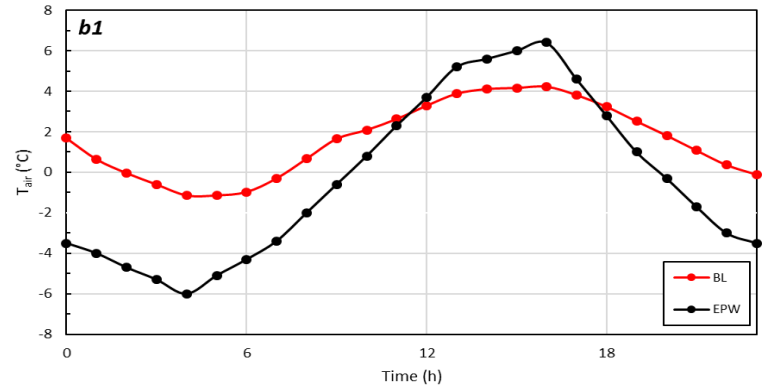 |

| | c1 |
|---|---|
| 31st December | 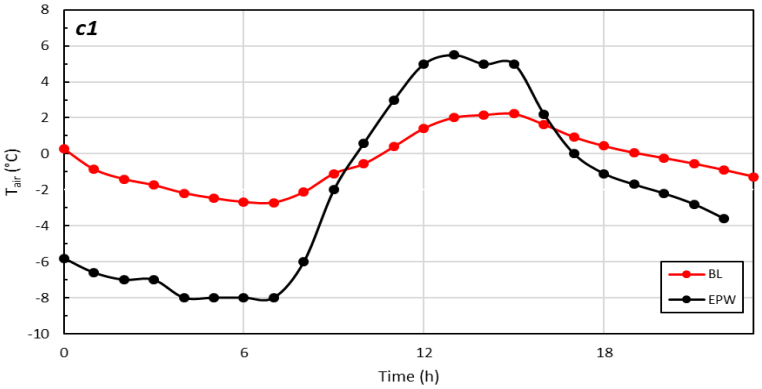 |
| 5th January | 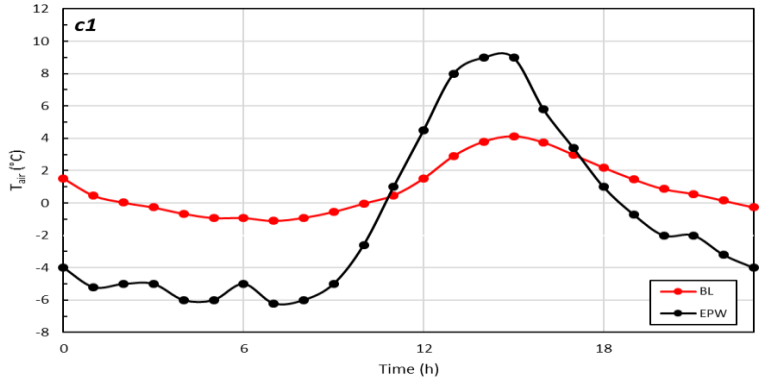 |
| 23rd February | 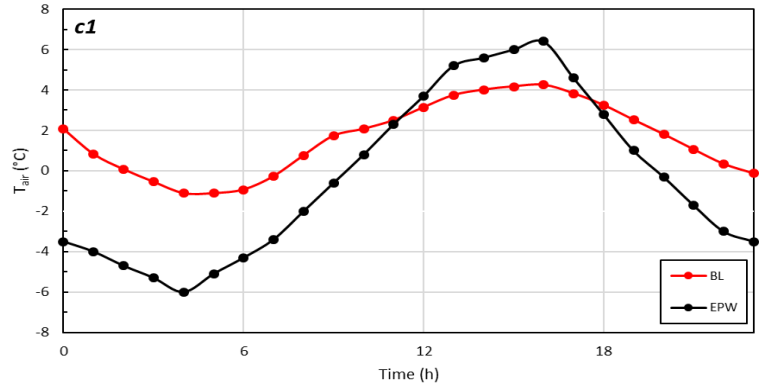 |

| | d1 |
|---|---|
| 31st December | 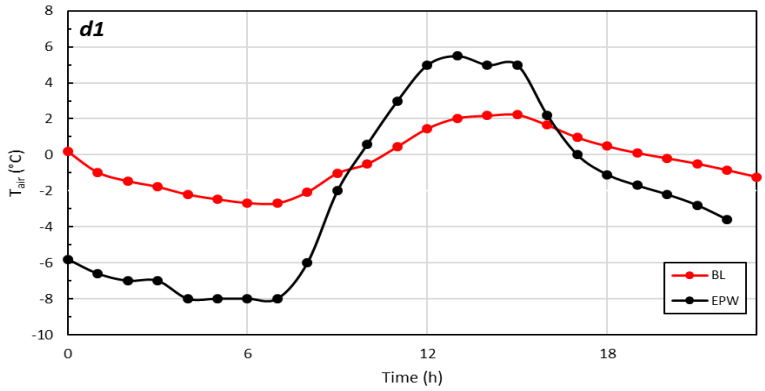 |
| 5th January | 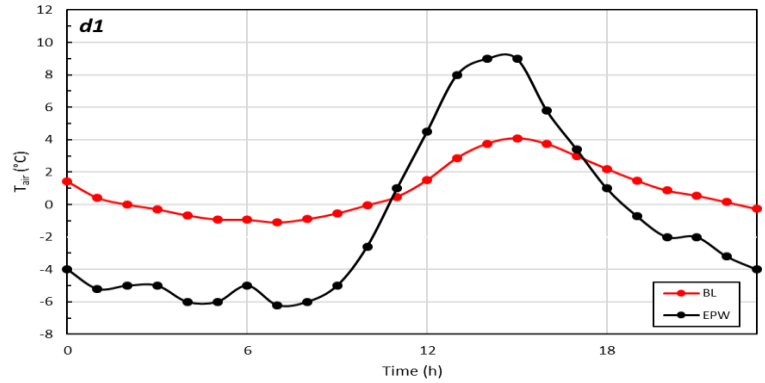 |
| 23rd February | 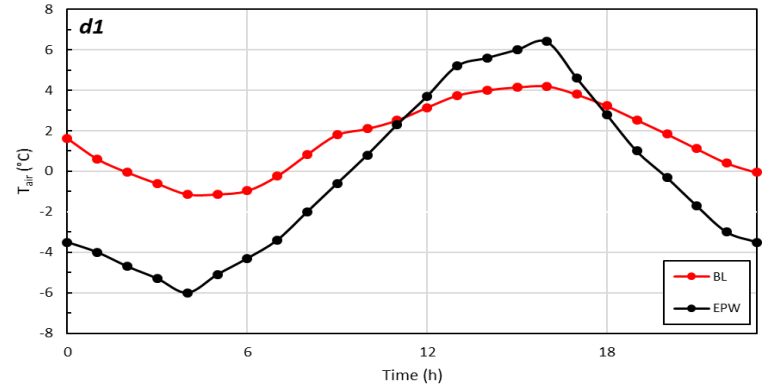 |

| | e1 |
|---|---|
| 31st December | 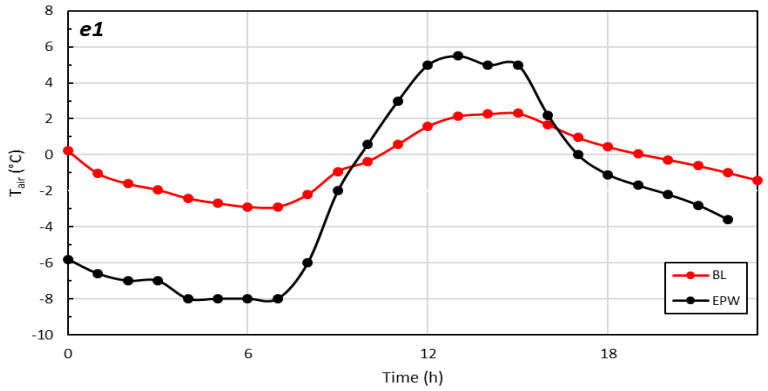 |
| 5th January | 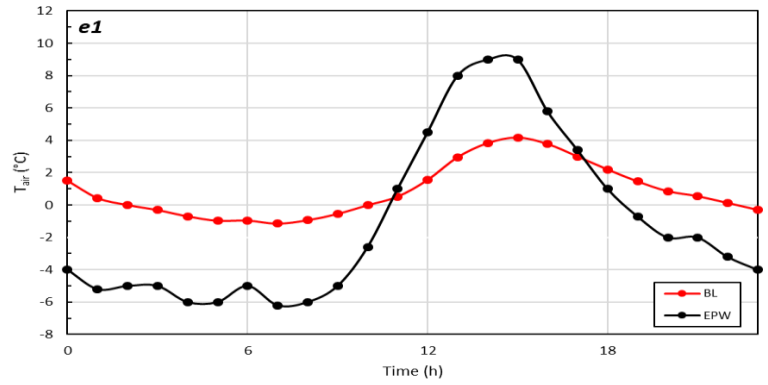 |
| 23rd February | 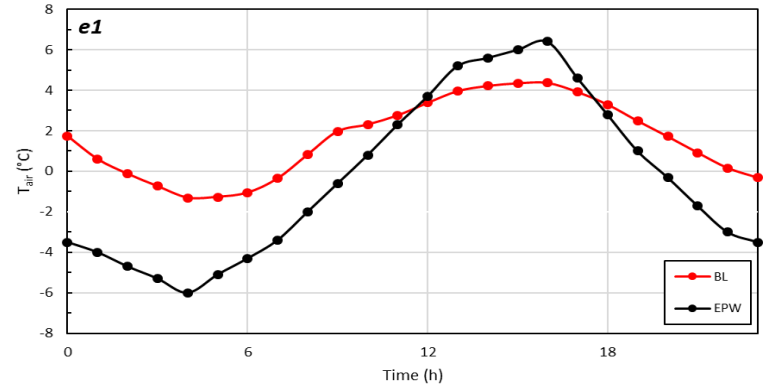 |

| | f1 |
|---|---|
| 31st December | 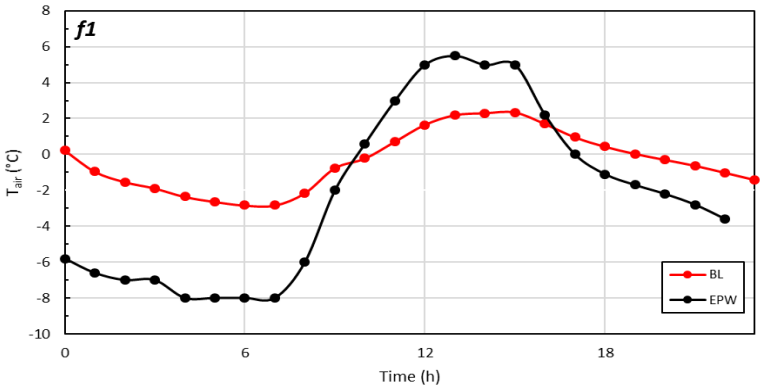 |
| 5th January | 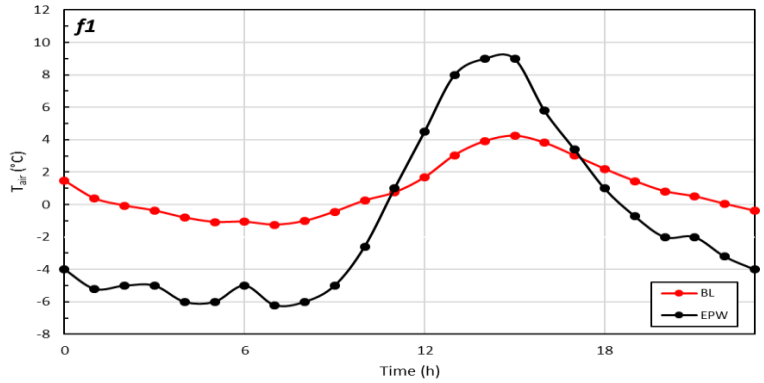 |
| 23rd February | 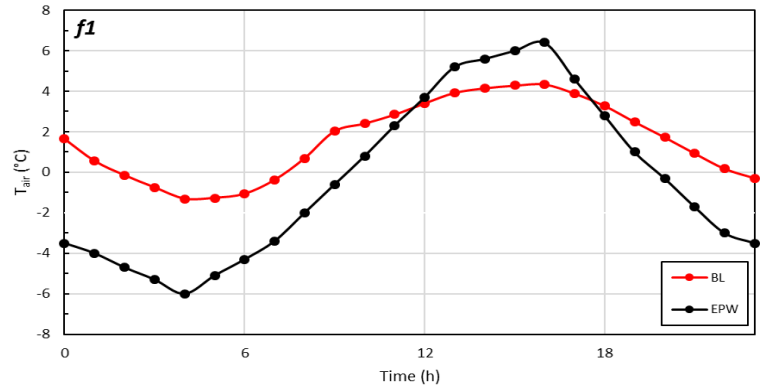 |

| | a1 |
|---|---|
| 22nd March | 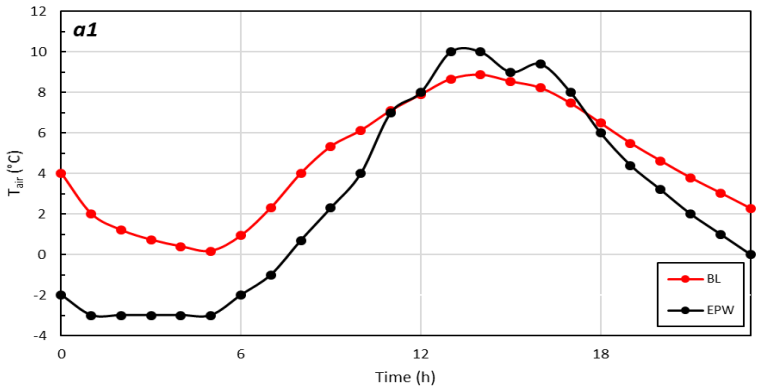 |
| 5th April | 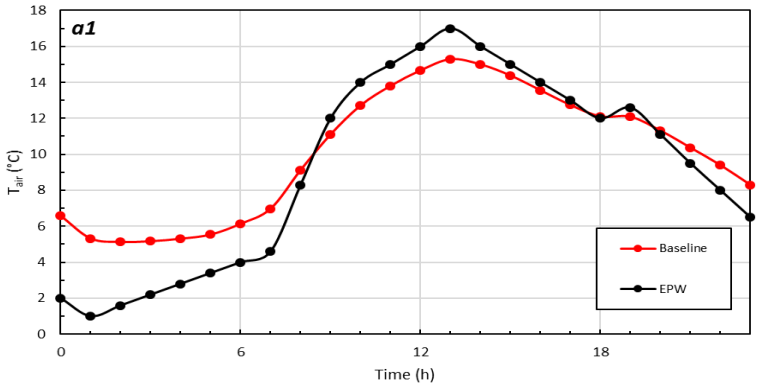 |
| 23rd May | 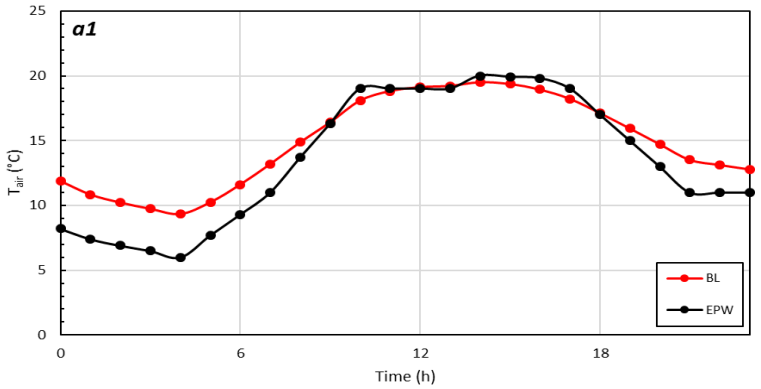 |

| | b1 |
|---|---|
| 22nd March | 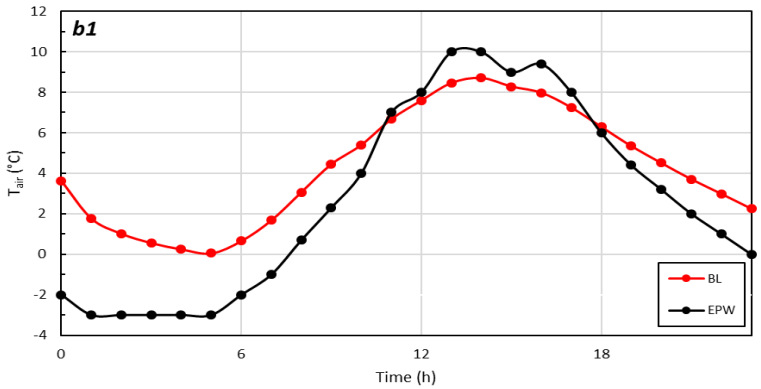 |
| 5th April | 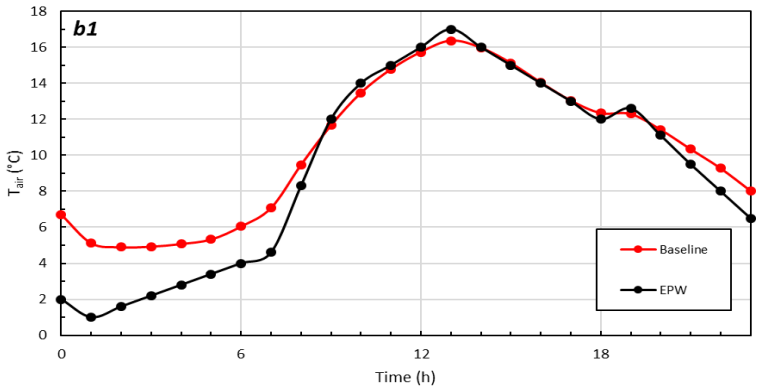 |
| 23rd May | 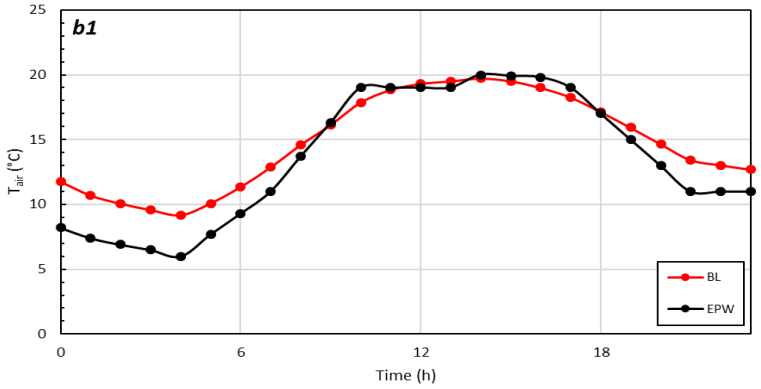 |

| | c1 |
|---|---|
| 22nd March | 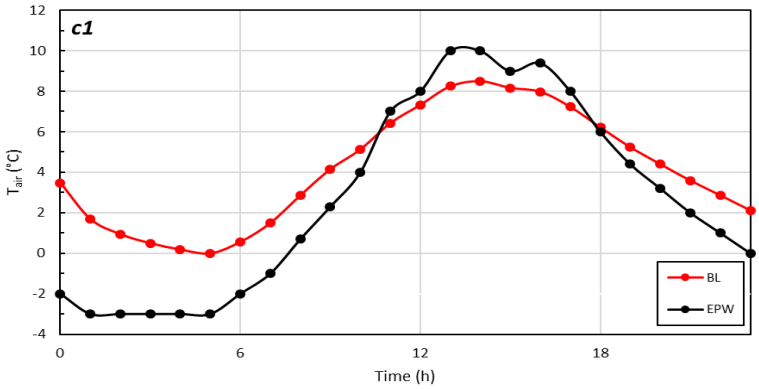 |
| 5th April | 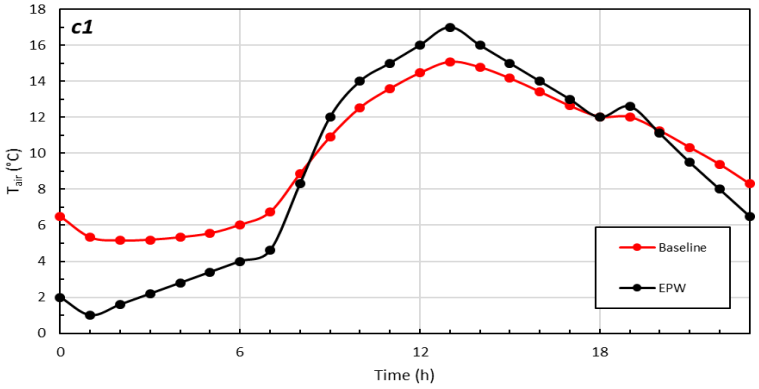 |
| 23rd May | 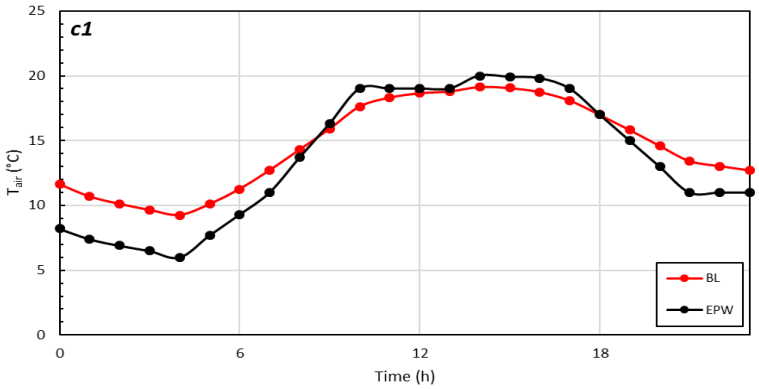 |

| | d1 |
|---|---|
| 22nd March | 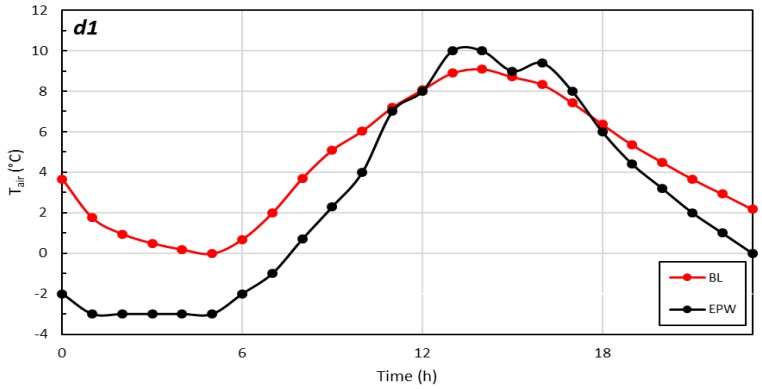 |
| 5th April | 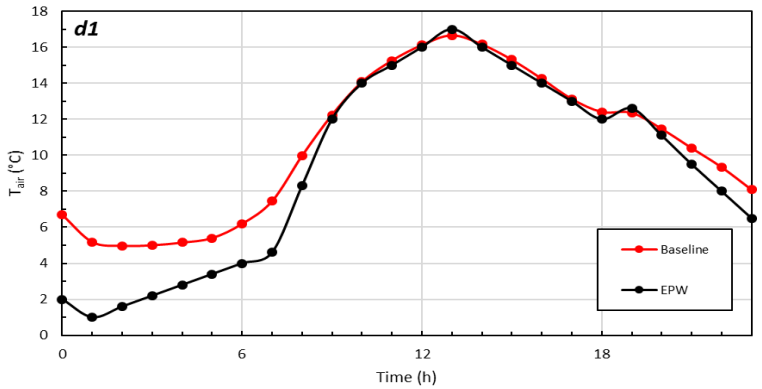 |
| 23rd May | 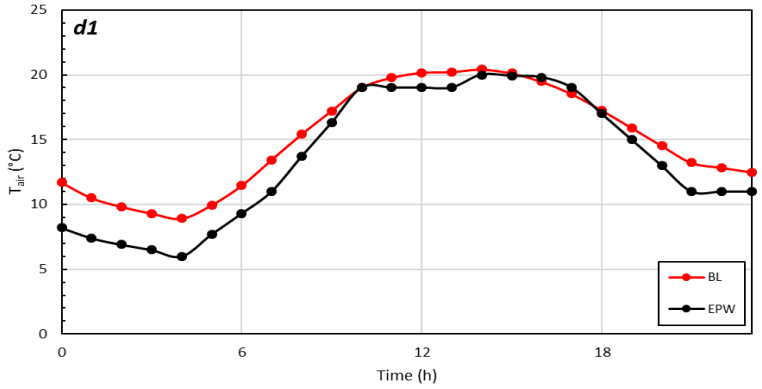 |

| | e1 |
|---|---|
| 22nd March | 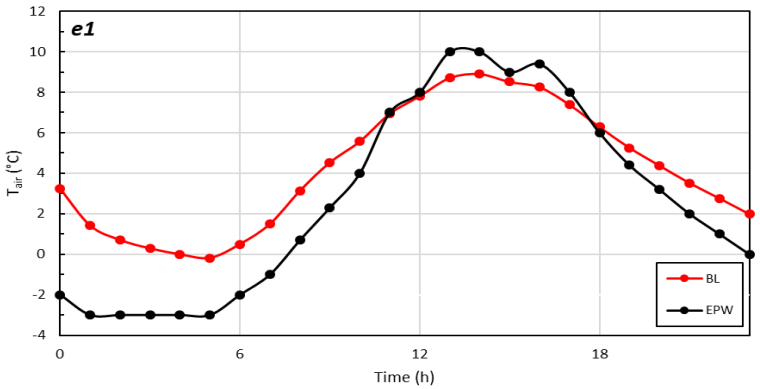 |
| 5th April | 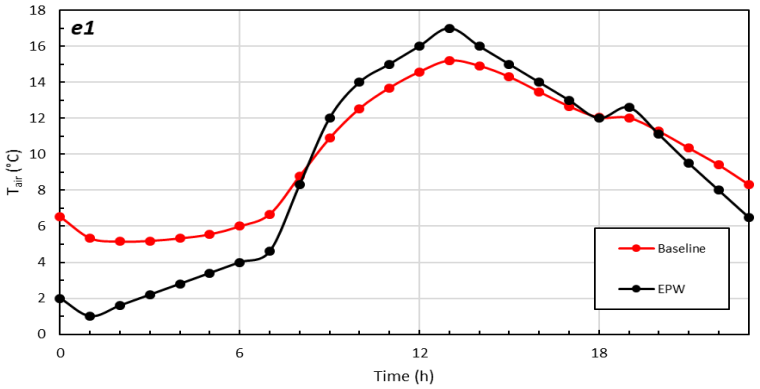 |
| 23rd May | 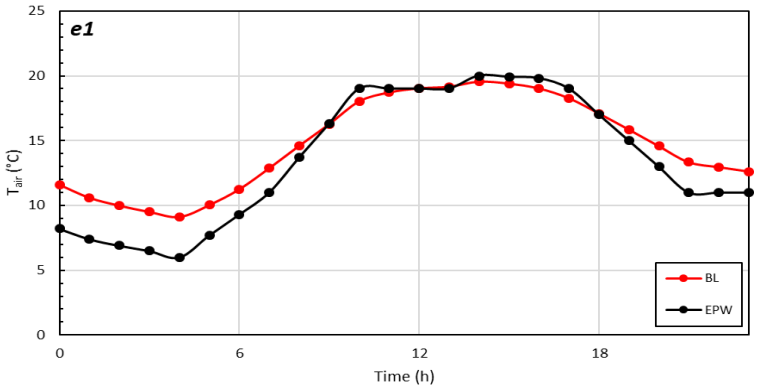 |

| | f1 |
|---|---|
| 22nd March | 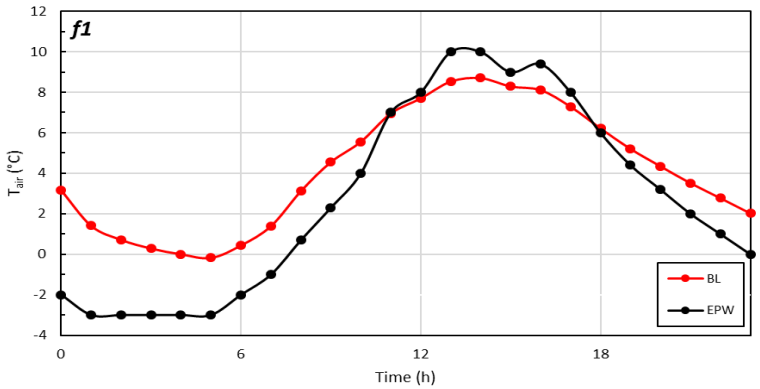 |
| 5th April | 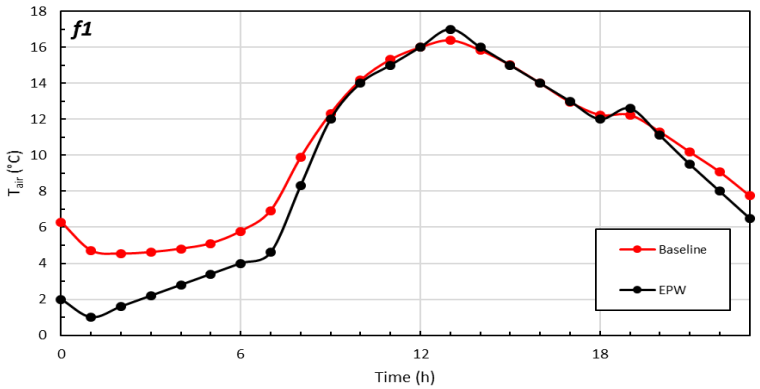 |
| 23rd May | 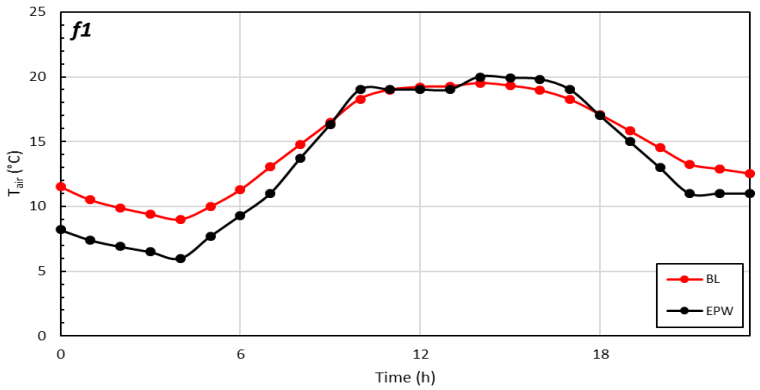 |

| | a1 |
|---|---|
| 21st June | 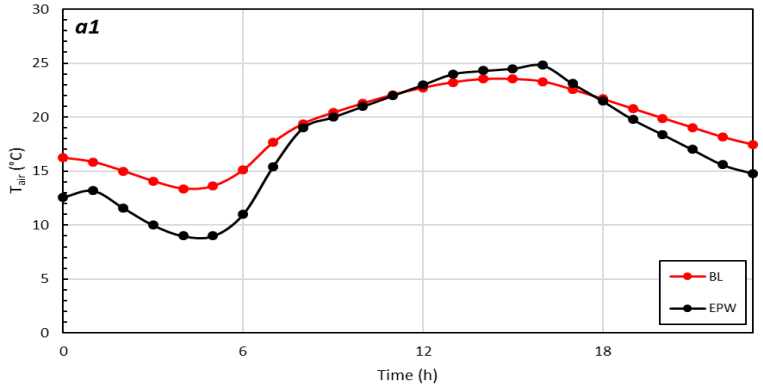 |
| 31st July | 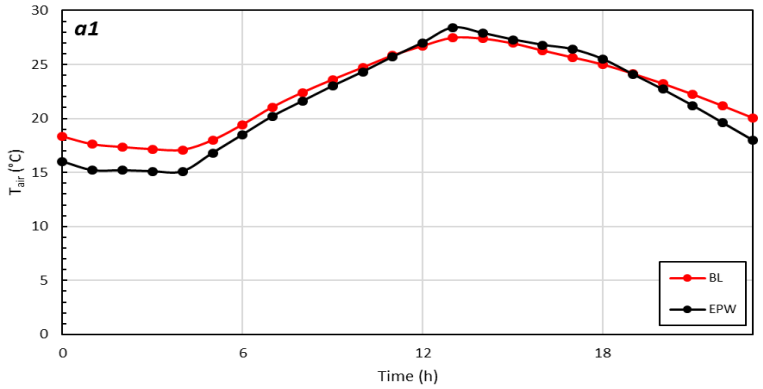 |
| 17th August | 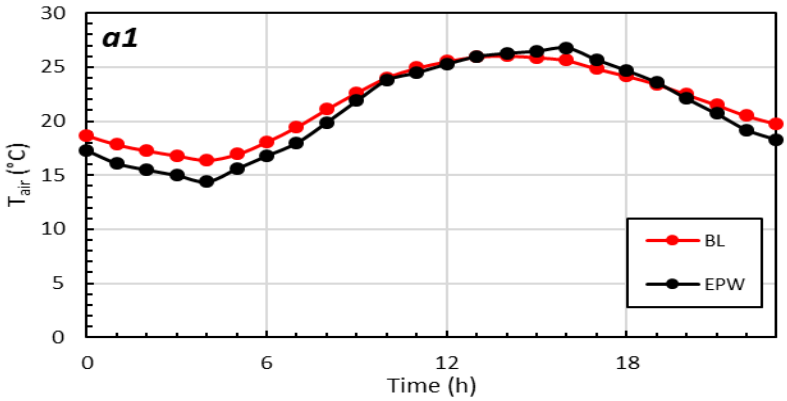 |

| | b1 |
|---|---|
| 21st June | 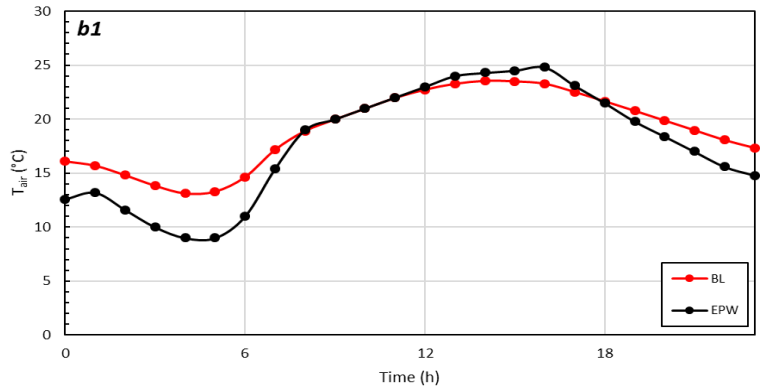 |
| 31st July | 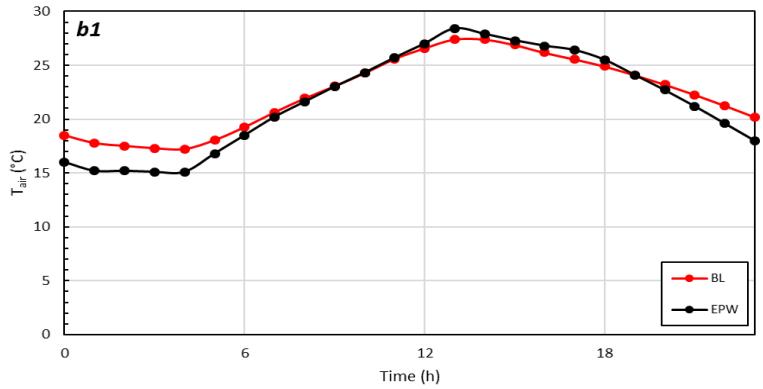 |
| 17th August | 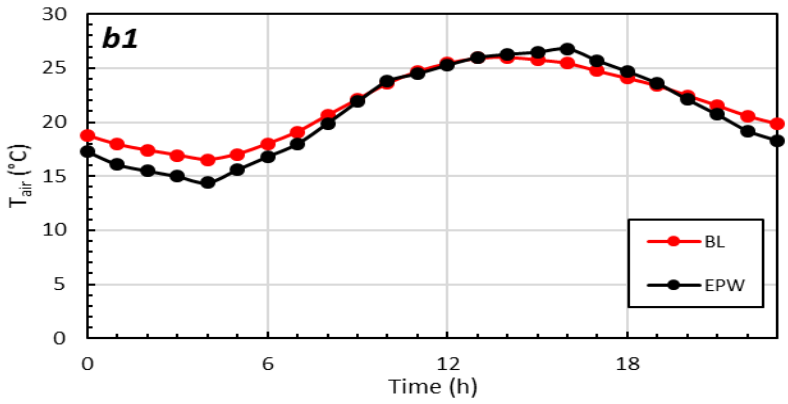 |

| | c1 |
|---|---|
| 21st June | 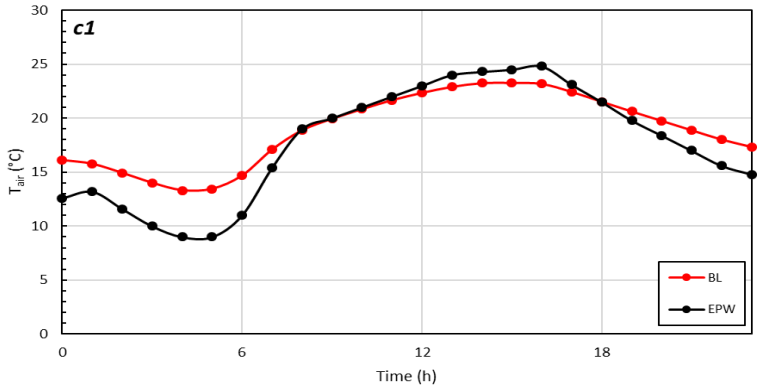 |
| 31st July | 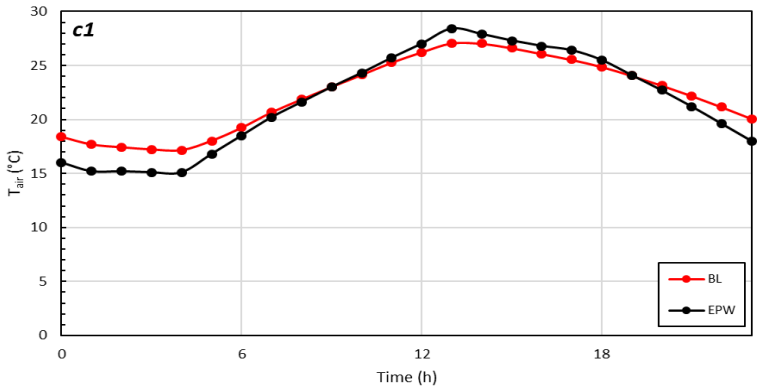 |
| 17th August | 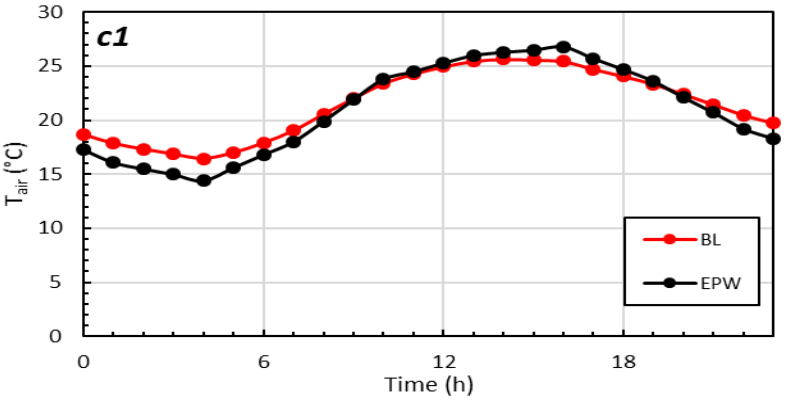 |

| | d1 |
|---|---|
| 21st June | 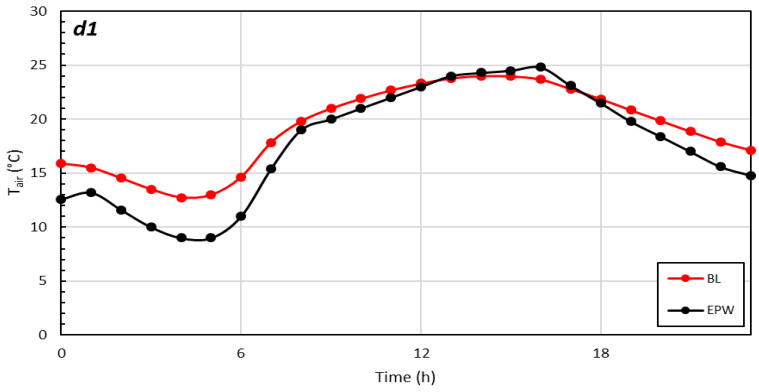 |
| 31st July | 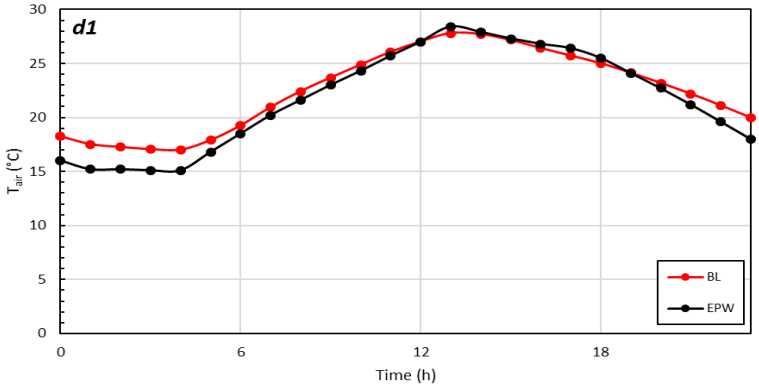 |
| 17th August | 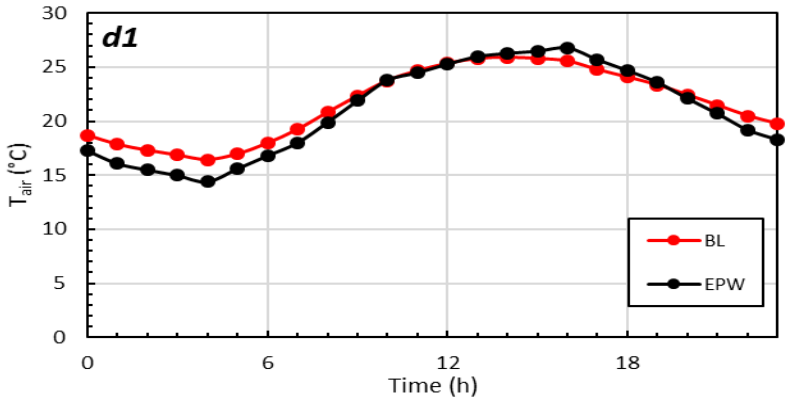 |

| | e1 |
|---|---|
| 21st June | 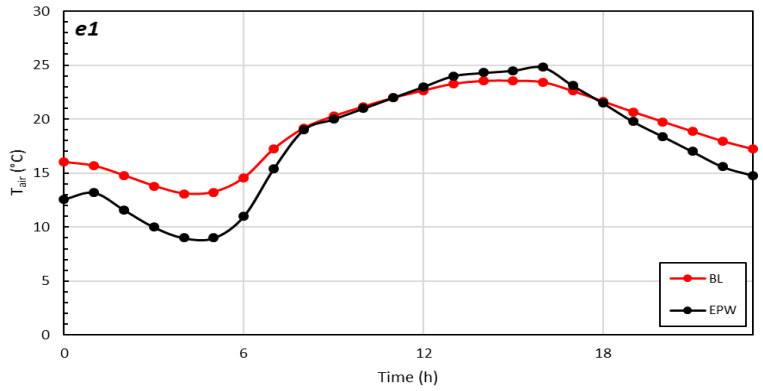 |
| 31st July | 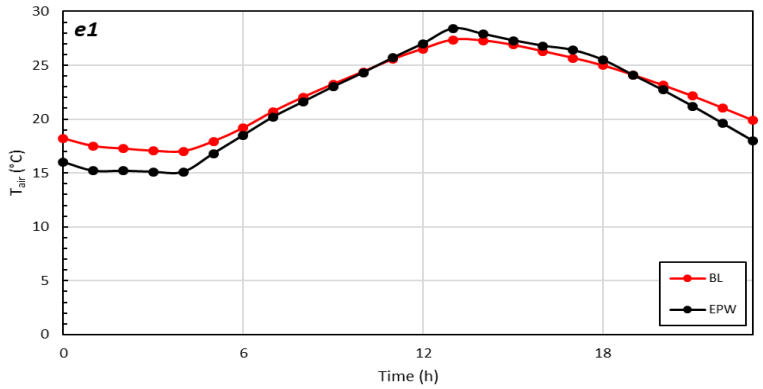 |
| 17th August | 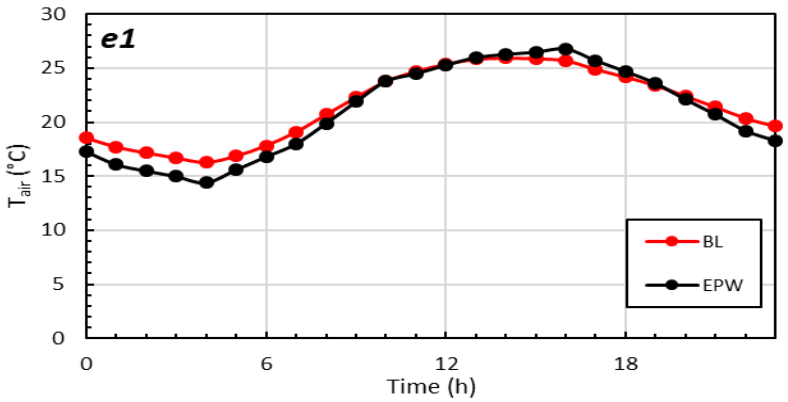 |

| | f1 |
|---|---|
| 21st June | 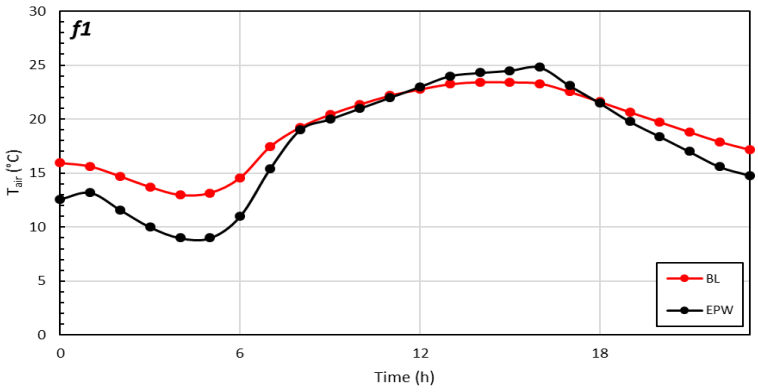 |
| 31st July | 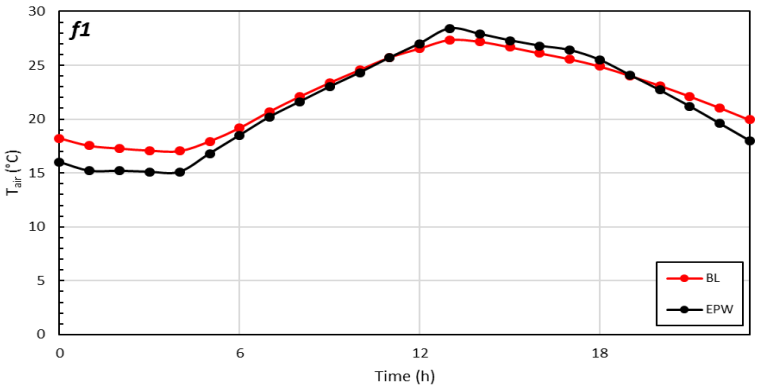 |
| 17th August | 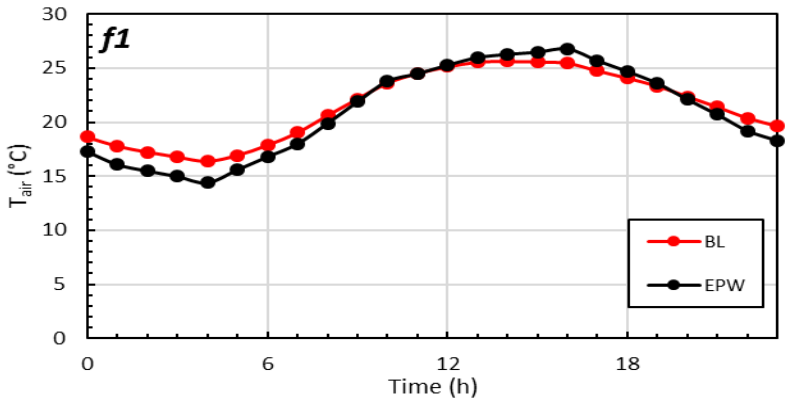 |

| | a1 |
|---|---|
| 21st September | 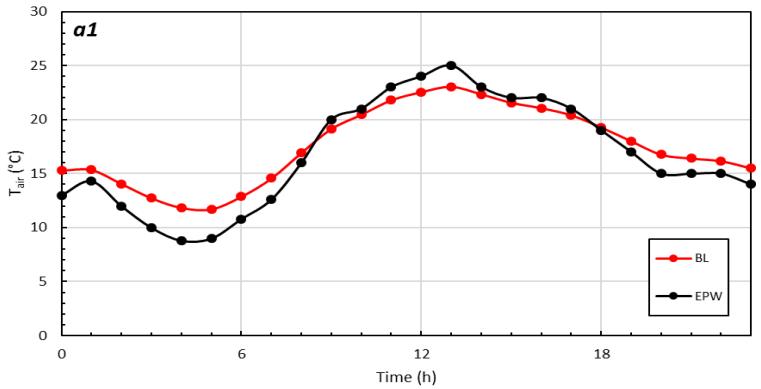 |
| 9th October | 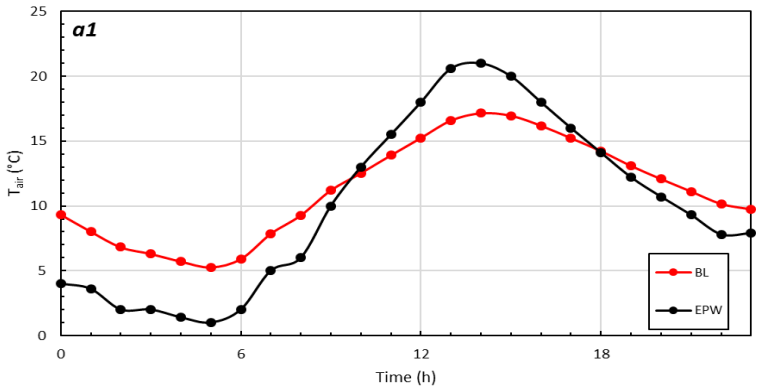 |
| 16th November | 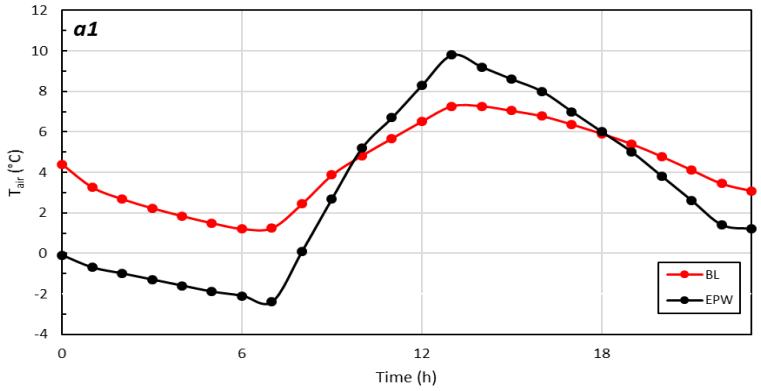 |

| | b1 |
|---|---|
| 21st September | 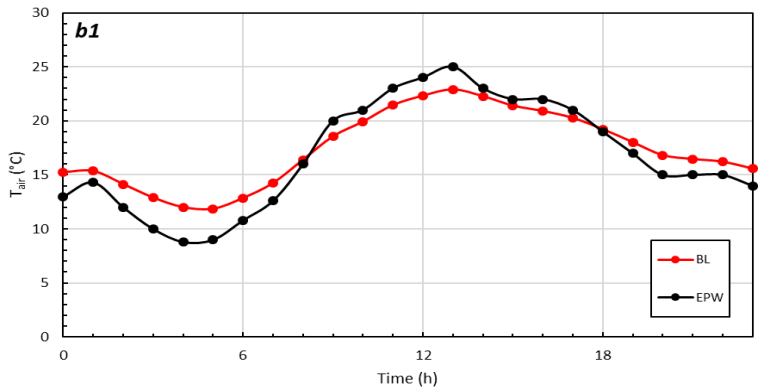 |
| 9th October | 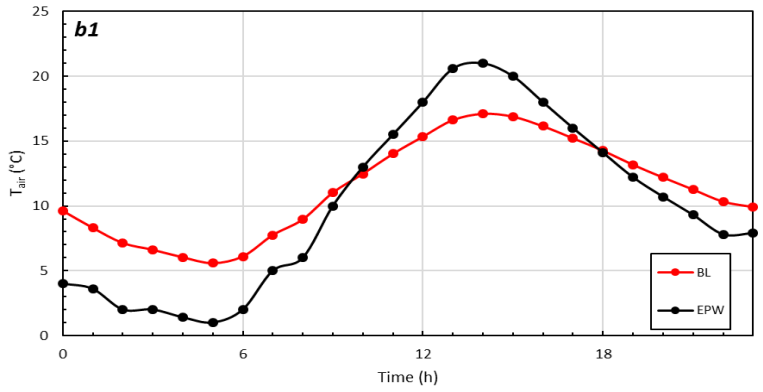 |
| 16th November | 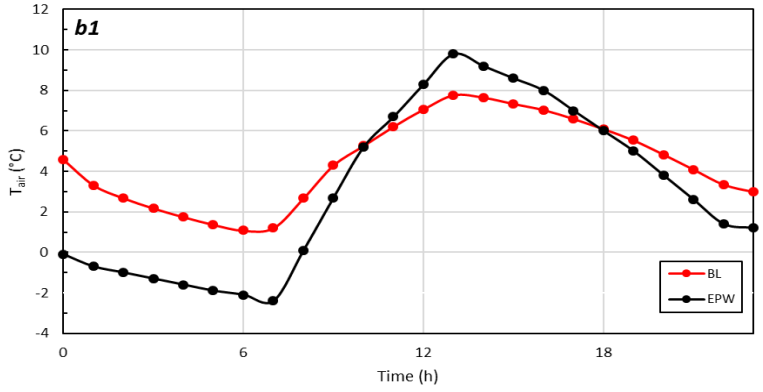 |

| | c1 |
|---|---|
| 21st September | 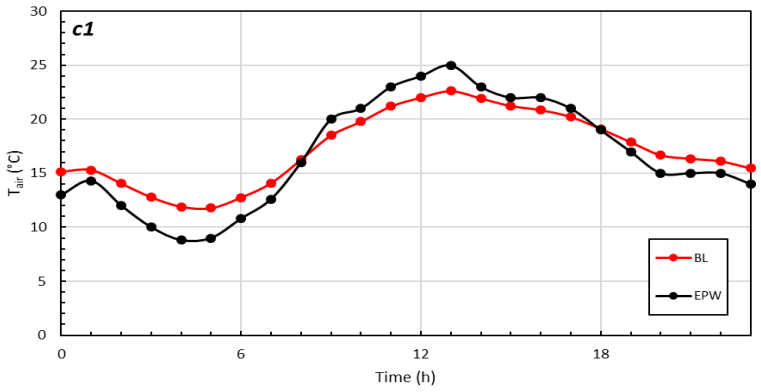 |
| 9th October | 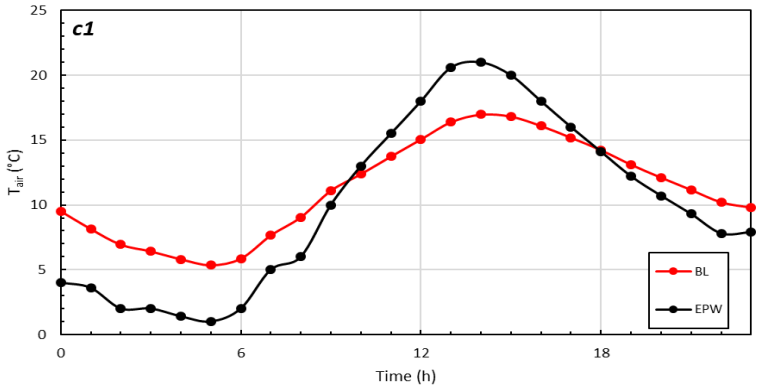 |
| 16th November | 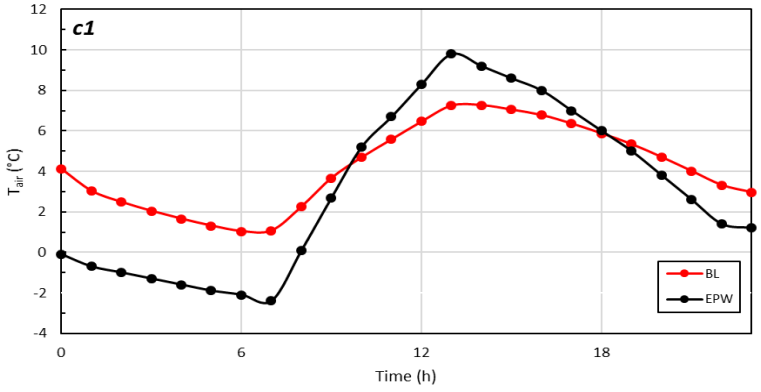 |

| | d1 |
|---|---|
| 21st September | 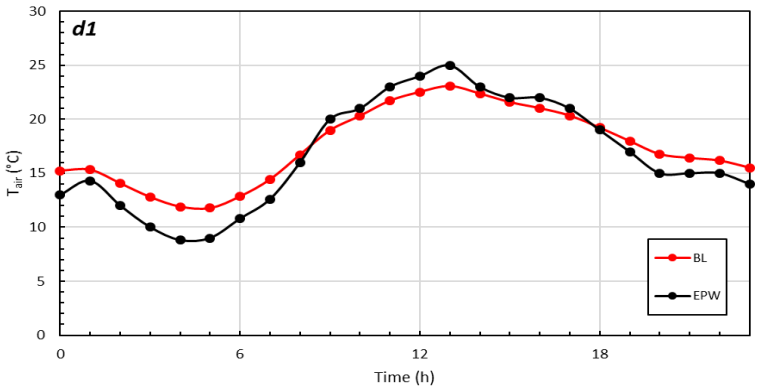 |
| 9th October | 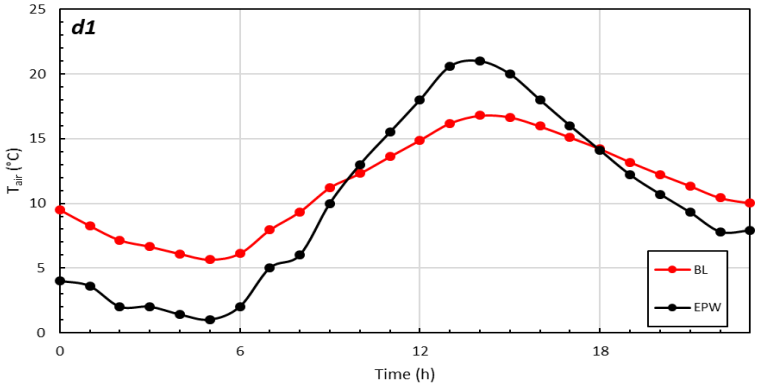 |
| 16th November | 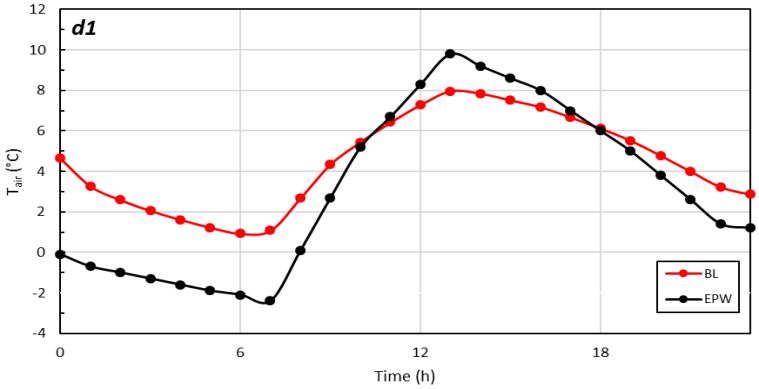 |

| | e1 |
|---|---|
| 21st September | 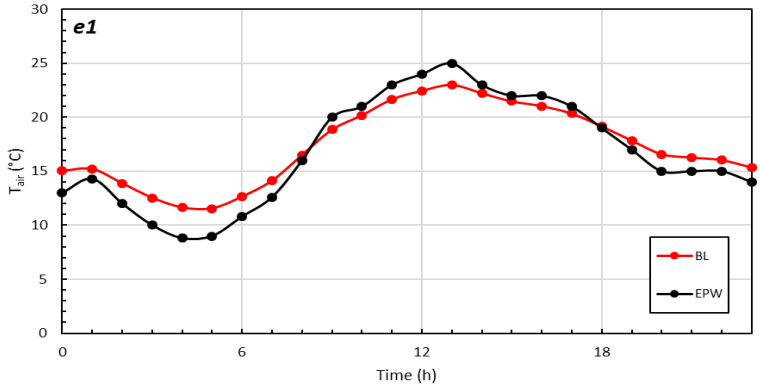 |
| 9th October | 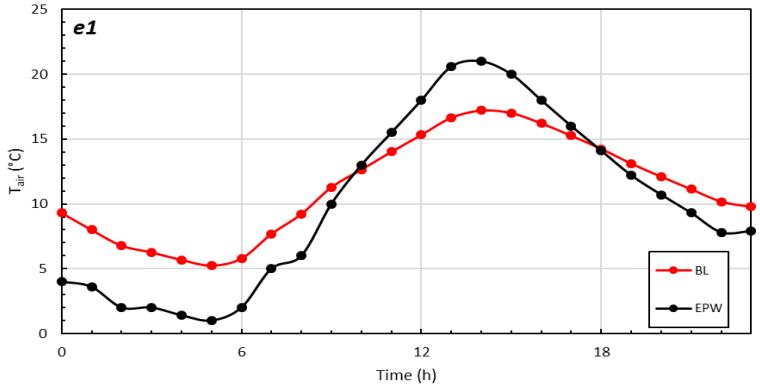 |
| 16th November | 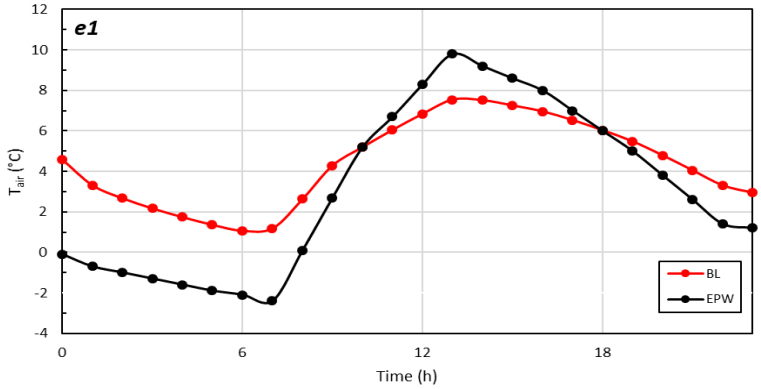 |

| | f1 |
|---|---|
| 21st September | 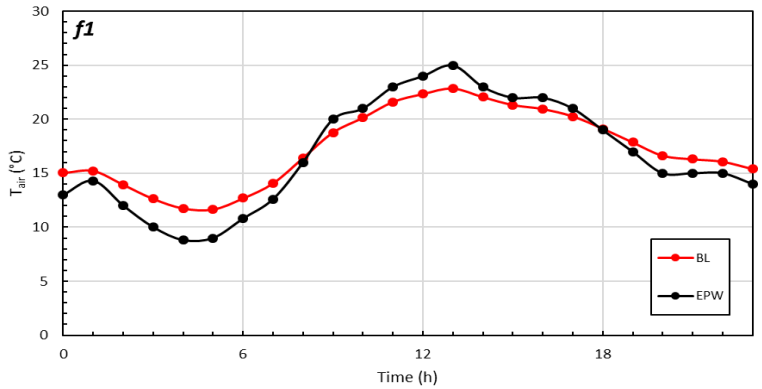 |
| 9th October | 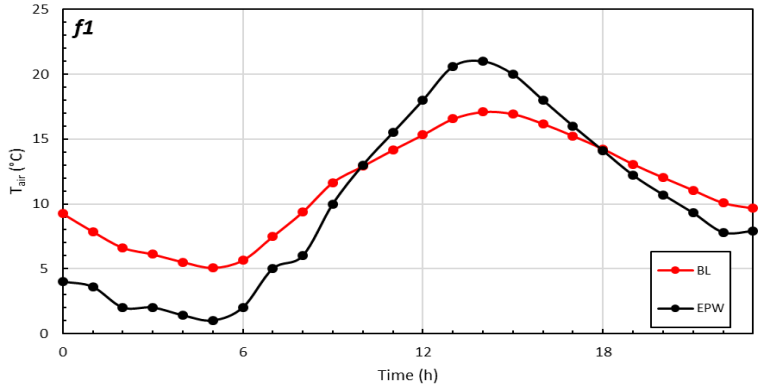 |
| 16th November | 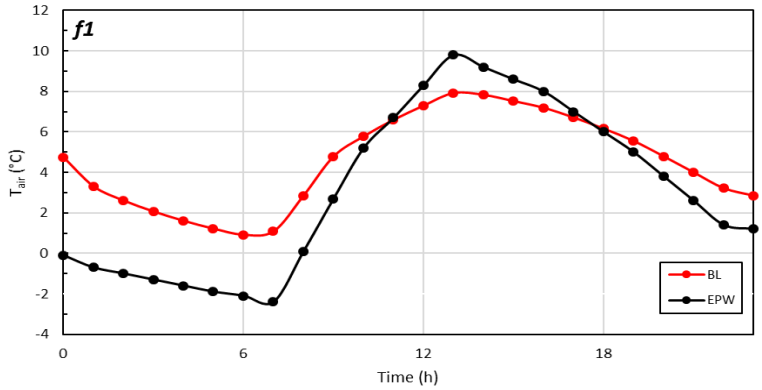 |